UNIVERSITY OF Southampton

University of Southampton Research Repository
ePrints Soton

Copyright © and Moral Rights for this thesis are retained by the author and/or other copyright owners. A copy can be downloaded for personal non-commercial research or study, without prior permission or charge. This thesis cannot be reproduced or quoted extensively from without first obtaining permission in writing from the copyright holder/s. The content must not be changed in any way or sold commercially in any format or medium without the formal permission of the copyright holders.

When referring to this work, full bibliographic details including the author, title, awarding institution and date of the thesis must be given e.g.

AUTHOR (year of submission) "Full thesis title", University of Southampton, name of the University School or Department, PhD Thesis, pagination

http://eprints.soton.ac.uk

UNIVERSITY OF SOUTHAMPTON

FACULTY OF SOCIAL AND HUMAN SCIENCES

Mathematical Sciences

Geometric Foundations of Network Partitioning

by

Maxwell James Fennelly

Thesis for the degree of Doctor of Philosophy

April 2014

UNIVERSITY OF SOUTHAMPTON

ABSTRACT

FACULTY OF SOCIAL AND HUMAN SCIENCES

MATHEMATICAL SCIENCES

Doctorate of Philosophy

GEOMETRIC FOUNDATIONS OF NETWORK PARTITIONING

By Maxwell James Fennelly

We explore and develop various graph-clustering (or partitioning) techniques. Focusing particularly on spectral clustering techniques, which use the spectral properties of the graph Laplacian operator, these spectral partitioning techniques range from the most primitive bi-paritioning techniques (Fiedler's vector method), to cutting edge higher order spectral partitioning techniques most well known within the field of computer science.

The nature of this research is interdisciplinary and we seek to develop strategies to mitigate and manage large area blackouts in electrical networks. This is done by looking for cross overs between these clustering techniques and established electrical engineering techniques such as islanding. We perform simulations on electrical networks throughout to demomstrate the utility of these techniques within the domain of this problem. We develop for the first time hierarchical spectral clustering techniques within this context, whose main advantage over other techniques is that they provide a partitioning scheme indicating which islands should be partitioned and then sub-partitioned and so on.

We develop a discrete version of the Connes metric for its application to weighted graphs. We present an exposition of the different ways that this metric can be represented and show that the computation of this metric can be stated as an optimisation problem, which we resolve for generalised weighted graphs. We show that the optimisation problem can be stated in an alternative way and as a result uncover more about the nature of the metric. We see that this metric is closely related to the resistance metric in its construction and from performing computations on a number of electrical networks we see the metric itself is closely correlated to Thevenin's impedance.

Contents

List of Figures iv

List of Tables vii

1 Introduction **2**

1.1 Literature Review 2

1.1.1 Graph Theoretical Approaches into Blackouts in Power Grids 2

1.1.2 Papers on Blackout Risk Identification 3

1.1.3 Papers on Contingency Frequencies 4

1.1.4 Graph Theory Approaches to Power Network Analysis 4

1.1.5 The Frequency of Blackouts 6

1.1.6 Spectral Islanding Scheme 6

1.1.7 Disconnecting Generators 7

1.1.8 Electricity tracing 7

1.1.9 Preventive Splitting 8

1.1.10 Topological vs Physical methods 9

1.2 An Overview of the Present Work 9

1.3 Assumptions and Contents of the Thesis 10

1.3.1 Chapter 2 11

1.3.2 Chapter 3 12

1.3.3 Chapter 4 12

1.3.4 Chapter 5 12

1.3.5 Chapter 6 13

1.3.6 Chapter 7 13

2 Fiedler's Vector Partitions **14**

2.1 Network splitting 15

2.2 Preliminaries 16

2.3 Fielder's Partition Method 20

2.3.1 The Embedding Partition Method 22

2.3.2 Higher Order Fielder's Partition Method 28

3 Higher Order Cheeger Inequalities **30**

3.1 Preliminaries 31

3.2 Theoretical Framework of Higher Order Spectral Partitioning 32

3.2.1 Higher Order Spectral Partitioning Algorithm 32

3.2.2 Theoretical Framework 38

3.2.3 Functions of Finite Support and Pseudo-Partitions 41

3.3 Theoretical Framework of Higher Order Spectral Partitioning with Dimension Reduction 48

3.4 Implementation of Algorithms 59

3.5 Evolving Set Processes 78

4 Hierarchical Spectral Clustering **82**

4.1 Algorithm and Results 83

4.1.1 Hierarchical Spectral Clustering Algorithm 83

4.1.2 Results 87

4.2 Hierarchical Spectral Clustering with Admittances and Comparisons with Evolutionary Algorithm 88

4.3 Further 89

5 Two-Step Clustering **92**

5.1 Algorithm and Results 93

5.1.1 Two-step Spectral Clustering Algorithm 93

5.1.2 Results of Two-step Spectral Clustering 95

5.1.3 Alternative Two-step Algorithm 96

6 Connes Metric **98**

6.1 Classical Metrics . . . 99

6.2 Operator Framework . . . 103

6.2.1 Spectral Triple . . . 104

6.3 Discrete Connes Metric . . . 106

6.3.1 Davies' Discrete Connes Metric . . . 106

6.3.2 Requardt's Discrete Connes Metric . . . 116

6.3.3 Resistance Metric . . . 124

7 Computation of the Connes Metric **126**

7.1 Convex Optimisation . . . 127

7.1.1 Restatement of the Connes Metric . . . 129

7.1.2 Karush-Kuhn-Tucker Conditions For Convex Problems . . . 130

7.1.3 Application of the Karush-Kuhn-Tucker Conditions . . . 132

7.1.4 Properties of the Optimal Function . . . 133

7.2 Second Lagrangian Approach . . . 137

7.3 Physical interpretation of the Connes metric . . . 145

7.3.1 Connes on Electrical Networks . . . 147

A Appendix **148**

A.1 Mathematics . . . 148

A.1.1 Justification of Spectral Clustering From Perturbation Theory . . . 150

A.2 Graph Theoretic Measures . . . 151

A.3 Electricity . . . 152

A.3.1 Basic electrical Measures . . . 152

A.3.2 Generators . . . 152

A.3.3 Alternating Current . . . 153

A.3.4 DC Approximation of AC Power Flow . . . 156

Bibliography **157**

List of Figures

1-1 This is the IEEE 39-bus test case network. 10

1-2 This is the graph theoretic interpretation of the topological of the IEEE 39-bus test case network. 11

2-1 A graph of 14 vertices, where the power flows are illustrated on the oriented edges. This is a 'DC' Direct current, 'OPF' optimal power flow. 15

2-2 Five-point stencil. 18

3-1 The $\mathcal{S}^2$ is illustrated in blue here with a yellow horizon. 34

3-2 The colouring of the edges indicates the magnitude of direct current in the corresponding line, the colours lie on the spectrum between yellow and blue: yellow for low power flow, green for intermediate power flow and blue for high power flow. 35

3-3 35

3-4 IEEE 39-bus test case system 59

3-5 The upper plot shows the un-normalised embedding, on the lower plot the coordinates have been normalised (points lie on a unit circle) and in both plots the points have been labelled by bus number. 60

3-6 The upper plot shows the normalised-embedding using eigenvalues of the normalised Laplacian, on the lower plot shows the embedding using eigenvalues of the un-normalised Laplacian. The potential cuts along each ray are preserved in both graphs. 62

3-7 The colour assigned to edges indicate the strength of power flow in the line ranging from yellow (weak power flow) to deep blue (strong power flows). 63

3-8 64

3-9 On the left is the application of the method with the d_F metric and on the right with the $\hat{d}_F$ metric. 67

3-10 The lower graph shows the stereographic projection of this with $(-1, 0, 0)$ as the projection point on $\mathcal{S}^2$. 69

3-11 Islands are formed by visual inspection. 70

3-12 73

3-13 The graph on the left hand side below illustrates the three subsets obtained by the higher order Fiedler method and the graph on the right hand side illustrates the partition obtained by the higher order spectral partitioning algorithm with varied ball radiuses. 76

4-1 84

4-2 Dendrogram of the spectral 3 embedding of the system weighted by power flows. 85

4-3 Dendrogram of the spectral 3 embedding of the system weighted by power flows. The Blue, Green, Yellow and Red islands are recovered at height 1, while cutting at height 3 suggests merging the Green and Red islands for a good 3-partition (cf. Fig. 1 and Table II). Long vertical lines in a dendrogram reveal a good clustering at that level. 85

7-1 This is a polynomial function of second order with positive coefficients, for the vector space of $\mathbb{R}$ this function is a convex function. 127

A-1 Current and voltage for a purely capacitive circuit. 154

A-2 Current and voltage for a purely inductive circuit. 155

A-3 Real and reactive power. 155

List of Tables

3.1 Partition into four (or three) Islands 64
3.2 Partition into four Islands 65
3.3 IEEE 39-bus test case for the d_F metric 77
3.4 IEEE 39-bus test case for the $\hat{d}_F$ metric 77
3.5 IEEE 118-bus test case for the d_F metric 77
3.6 IEEE 118-bus test case for the $\hat{d}_F$ metric 78
3.7 GB network for the d_F metric 78
3.8 GB network for the $\hat{d}_F$ metric 78

4.1 Results from systems 88
4.2 Results from systems 89

5.1 Results for Two-step Spectral Clustering of IEEE 39-bus test case . . . 95
5.2 Results for Alternative Two-step Spectral Clustering of IEEE 39-bus test case 96

List of Accompanying Material

1. CD of MATLAB codes . . . . . (inside front cover)

ACKNOWLEDGEMENTS

I would like to thank my supervisor Jacek Brodzki for being with me during this difficult and interesting journey, thank you for your help, patience and persistence, I wouldn't be able to be at this point without it. Also big thanks to Ruben for being inspiring and enthusiastic and always ready to help. Of course, not to forget the wider research team from Durham and Edinburgh, who did make this happen especially Janusz Bialek, Paddy McNabb, Sean Norris and Chris Dent.

Special thanks to my family who believed in me and showed their support during these 4 years. And of course my wife Dasha, who was with me in the hardest moments, and never let me give up.

This research has been supported by an EPSRC grant (grant number EP/G059101/1).

Chapter 1

Introduction

Over the past four year I have been a part of the Preventing Blackouts Project headed by Professor Janusz Bialek and Professor Jacek Brodzki. The objective of this project is to find ways to mitigate the spread of cascading failures through electrical systems, to stop the occurrence of blackouts in large area networks (such as the North American Network of the continental European network). This thesis arises from efforts to create a mathematical understanding of theoretical problems involved in solving this engineering challenge. As we will see, solving the problem of islanding requires an interaction of a number of modern mathematical tools and techniques, from graph theory, through spectral properties of the Laplace operator to the extension of clustering algorithms. As well as bringing mathematical techniques to bear on a subject area which has had underdeveloped ties with the mathematical world, I also endeavoured to develop new mathematics.

1.1 Literature Review

To set the territory for my work I will review the literature of research that has gone before with similar objectives.

1.1.1 Graph Theoretical Approaches into Blackouts in Power Grids

Research that has used graph theoretic methods can be found by B Carreras and V Lynch et al in [7], where two types of network blackouts are characterised. The first type of blackout appears when the limit on total generator capacity is surpassed, the second

type of blackout is due to the power flow limits of the network lines being exceeded. A simulation of a network is carried out where the power demands are increased until the system starts to cascade. After a disturbance in the system, the amount of load shedding of the generators is studied and whether or not the amount of load shedding is continuous or not for example. In [7] the authors are concerned with the probability distribution across all sizes of cascades. In particular it is found that near these critical transitions (where the system is close to failing), the tail of this distribution is not exponential bounded (a so called heavly tailed distribution). Real data collected from 15 years of North American blackouts indicated that, the distribution characterises the system as one that is near critical transition. Thus the authors reach the conclusion that the system is operating near critical transition, suggest that large blackouts maybe more probable than a cruder statistical analysis may suggest (for example Gaussian statistics, [20] also warns of naive statistical analysis being misleading). With models in [8] we have the same findings of distributions of blackouts again but this time the models are constructed in a more dynamical way, where the system is evolving to compensate an increase in demands. In achieving this dynamical model 'economic, regulatory, and political responses to blackouts and increases in load power demand', are taken into consideration. It is claimed that there is one particularly important parameter, which is the ratio of the generator margin capability to the maximum daily fluctuation of the loads'. This they claim is a good indicator of 'the systems ability to absorb fluctuations'. The conclusions include that the ratio should be taken into large consideration, when deciding how to evolution system.

1.1.2 Papers on Blackout Risk Identification

S Ranade and R Kolluru in [50] for any give system states the probability of transition to a new state is analysed it is possible to identify an arbitrarily large set of event trees that lead to catastrophic failures. It is claimed that such identification can enable the development of preventive measures, both at the planning and operation levels, to strengthen a system against inherent vulnerabilities. It is also said "The contributing factors are numerous and complex, structural relationships, hidden failures, operator action (or inaction), and system stability are only some of the major considerations. The level of detail to which these need to be modelled is another concern that must be

explored."

[29] is in very much a similar vein as the [50]. It is concerned with having a database of information that could be utilised to spot states that would lead to a cascade. To identify these critical states, the authors undertake a study of characteristics of blackouts.

1.1.3 Papers on Contingency Frequencies

Q Chen, C Jiang, et al in [11] built a model proposed that tackles the question of "If power systems are weakened due to losses of more than one transmission line, what would be the probability that another transmission line trips?". Herein it is found that the best predictor of the spread of a cascading failure is an exponentially accelerating cascade where there is an acceleration present in the sense that the more failures that occur; the more likely the occurrence of a failure is. With this insight it is proposed that a network is set up so that statistics can be continually collected to help predictions, and in real time give the probability of a blackout occurring.

1.1.4 Graph Theory Approaches to Power Network Analysis

I Petreska and I Tomovski et al in [49] deal more broadly with Vulnerability of complex networks, but does specifically mention electrical networks. Attacks on several segments of the EU power grid are simulated in this work. The authors introduce various quantities associated with the nodes of a network: its degree, its betweenness centrality (this is a measure of how often a vertex occurs in the shortest paths between all pairs of vertices). To enforce a failure of the network, they then proceed to remove nodes preferentially according to these three different factors namely 'vertex ranking', 'modal weight ranking' (this is a spectral measure), and 'betweenness centrality'. The paper then concludes that, from these strategies for enforcing network failures the one that uses the topological measure of node degree is the most efficient strategy.

N Zlatanov and L Kocarev in [69] address the notion of cover time, this is the expectation of the number of steps a random walk would take through a graph before it has visited all vertices in the graph. This value is derived for simple graphs such as: a complete graph, a cycle graph, and a path graph. A method for calculating an accurate approximation for the distribution of these is provided.

Also here the hitting times are calculated; this is the number if steps that a random walk would take in order to reach a certain destination and commute times; this is the number of steps that a walk would take to reach a destination and come back. This kind of analysis is potentially relevant to us when we want to calculate how a failure dissipates through a network.

Certain features of wide area blackouts in networks are of course not restricted to electrical power grids. For example R Carvalho, L Buzna, et al in [10] address the tolerance of the trans-european gas pipe-line network. They achieve this by looking at the topology of the network and its flows, [10] discusses betweenness centrality in this context (as does [49]). It is concluded that, as in the electrical power grid, the degree distribution of the European gas transmission network austensably decays in an exponential manner, the distribution however is not exponentially bounded as degree size diverges, thus the significant feature of a tailed distribution is identified.

M Woolf and Z Huang, et al in [68] networks are build intentionally to brake down via a cascade, various types of topologies and flows are compared to identify the characteristics that bring about cascading failures. As in [7] and [8] two types of cascading blackouts are analysed: one resulting from the total generator capacity being exhausted and the other due to the power flow limits of the network lines being exceeded. It is concluded that network with low levels of heterogeneity in their vertex degrees will be readily susceptible to cascading failures.

I Mishkovski and M Biey in [42] device a vulnerability measure of a network by considering the normalised average edge betweenness and taking the relative difference of this when certain number of nodes and/or edges are removed from the network, they call this the vulnerability index. This vulnerability index is calculated for various types of synthetic graphs as well as some real-world graphs including two electricity grids. The paper concludes that the most robust networks are the Watts-Strogatz small world network model, and the real world human brain network.

L Kocarev, N Zlatanov, et al in [35] investigation into finding a vulnerability rank for a network when this network is considered as a Markov chain. This is interesting work which introduces a measure of the strength of interaction between vertices through a particular adjacency matrix. They assume that an edge (i, j) only exists in their graph when the status of vertex j can be influenced by the status of i, the weight of this

edge (i, j) is the amount of influence that i exerts on j relative to the total amount of influence that j receives from other vertices. It is this graphs that presents the vulnerability index for each edge.

A simulation for the electrical network of the EU is performed, where each node represents a country in the EU. The authors calculate the exports of electricity and the vulnerability index. The calculation of the vulnerability index is done in two different ways: the vertex degree way and the vertex betweenness centrality way. Each method giving a different country as the most vulnerable.

M Szenes , Z Farkas, et al in [62] summarise the setup of a linear model of power flow in a network, with a very simple algorithm of updating the system when a line trips.

1.1.5 The Frequency of Blackouts

B Carreras, D Newman, et al in [6] first give a definition what Self-Organised Criticality is (which the paper refers to). Self-organised criticality (SOC) can be considered as a characteristic state of criticality, which is formed by self-organisation in a long transient period at the border of stability and chaos. A supposition is made that the power system runs similarly to the sand pile system (the archetypal example given of self-organised criticality where grains are added randomly to a sand pile), supported by the fact that there are correlations between the probability distribution of size of blackouts from 15 year of the north American power system and the probability distribution of the size of avalanches of the sand pile. This is not conclusive evidence of course that power systems are have SOC [6] instead concludes the dynamics of SOC systems may play a big part in the global dynamics of black-out in power systems. [6] has influenced the modelling of power systems dynamics from this perspective in [9] and [21].

1.1.6 Spectral Islanding Scheme

R Moreno, M Rios, et al in [44] prepose a security scheme for power systems, consists of two stages. First islanding (which means splitting the system into disconnected components) and secondly frequency load shedding within each Island (which synchronises the generators within each island). The possible scenarios for cascades are calculated off-line and then make up data to support real time contingencies. The load shedding

here is determined by the so-called Under-frequency load shedding (UFLS). An important connection with our work is given by the Fiedler's partitioning scheme, which is the starting point of our more advanced strategies, as we shall see in Chapter 2.

1.1.7 Disconnecting Generators

I Dobson in [19] reviews high level probabilist methods used to ascertain a risk profile for blackout sizes, such as Monte Carlo simulation, or a high level model branching process which assesses the probability of a failure occurring and then the probability of this failure propagating. These methods are designed to complement an engineer's more traditional deterministic approach of detailing retrospectively the chain of events that lead to a blackout. It is argued that there is a critical amount of loading that an electrical system can undergo before the probability distribution of blackout risk transitions from having an exponential tails to having a power law tail (which converges to zeros significantly slower that an exponential tailed distribution). A consequence of this is that the expected blackout size will rise sharply as the load is increase to critical levels. The challenges of utilising these techniques as monitoring tools for blackout risk.

The starting point of [24] by R Fitzmaurice, A Keane, et al is the power law relationship between the size and the frequency of blackouts. A main result of the paper is a discussion of strategies for dealing with the danger of blackouts to the grid. These fall broadly into conservative or non-conservative generator dispatches. The difference between the two approaches lies in the treatment of the stress of the system.

1.1.8 Electricity tracing

The important paper by C Achayuthakan, C Dent, et al [1] establishes a way of calculating the electrical tracing measure between two vertices of an electrical network which is similar to [35] but in an electrical setting. The measure between vertices i and j is of the proportion of electricity that flows through j which comes from i, out of the total of all electricity that flow through j. The subtlety of this calculation is in the fact that this has to be calculated across all paths with exist between vertices i and j, and in [1] the calculation is performed in one step.

C Wang, B Zhang, et al [65] discuss islanding, more specifically they discusses the methods used to minimise the Generation-load unbalance within each island. The

algorithm is carried out by considering the domain of each generator, this domain is derived from using the tracing methodologies on the power flow. Once a line trip occurs the domains of the generator may change and the islanding is performed so that the generators inside an given island are in sync. There are a certain number of nodes which lie at the periphery of two or more domains, in such cases these are assigned in such a way that balances the generation and load of each island.

1.1.9 Preventive Splitting

K Sun, D Zheng, et al in [61] review what is called the OBDD ("Ordered Binary Decision Diagram")-based proper splitting strategies. The Algorithm follows in a very similar way to the one that we are already considering in [44] in section 1.1.6.

Phase 1; simplifies the system (this means excluding edges and combining nodes if possible), and then using the Fiedler vector techniques (see later in Chapter 2) to reduce the searching space significantly.

Phase 2; here we have what was touched upon in [44], about how the synchronous generators have to be grouped together in the same islands, but also constrained so that for the groupings generation and load in each island are balanced after system splitting.

Phase 3; Checks the constraint that all transmission lines and other transmission devices must not be loaded above their transmission capacity limits.

[61] analyses the feasibility of the splitting strategy above for the IEEE 118-bus test case[1], by observing the general disturbance in each island formed. It is proposed that if the analysis is done off-line the contingency can operate more efficiently, it is said that a considerable number of spitting method yield stable islands.

The same authors [60] device the same splitting strategy as in [61] but with modifications, the claim is made that for a IEEE 118-bus test case, the cut set could be found in less than a second, thus making the method more realistic for real time large networks.

X Wang and V Vittal in [66] use a technique similar to the ones discussed in [60], apart from once all the islands are established a method called 'Tuning Trial-Error Iterations' can be performed, this modifies the islands so that they are more balanced.

[1] This is a standard test case of an electrical network consisting of 118 buses.

The 'Aggregated Island Approach', acts on this set of islands after they have been tuned; it determines the set of 'load rich islands', "Consider all those generators in load rich islands as one group, and find out the minimal cut sets for this aggregated group with minimal net flow, which indicates the aggregated islands." The load generation index is then calculated for each island, and hopefully reduced.

M Jin, T Sidhu and K Sun in [32] proposes a new scheme of network splitting, the way that generations will ocsillate within a group cannot be predicted, this method is supposedly much more effective when these oscillations cause complications. This new scheme is based on the unification of techniques with those of emerging stability controls.

1.1.10 Topological vs Physical methods

P Hines, E Cotilla-Sanchez, et al in [31] attempt to quantify the susceptibility of a electrical system to random failures and directed attacks with the use of three different topological measures: characteristic path lengths, connectivity loss and blackout sizes. The paper concludes that topological measures can provide some indication of systems vulnerability they are not strong enough to draw conclusions from in isolation.

1.2 An Overview of the Present Work

A starting point of this thesis is an observation that, while there were attempts to use graph theory to understand blackouts, there is scope for a systematic exploration of the spectral properties of graph Laplacian in this context. Spectral graph theory examines the eigenvalues and eigenvectors of the graph Laplacian or adjacency matrix (the so called spectral information) to establish principal properties and structure of a graph. An excellent starting place to learn spectral graph theory is [14], where the spectral emphasis is placed on the graph in topological and algebraic terms. It should be clear from our discussion of previous efforts to understand blackouts that a good understanding of topological and electrical features of a network is of great importance. Given the islanding mitigation strategy eluded to earlier in [65] and [30] it is intuitive that this topological feature would be a benefit to an electrical network undergoing islanding. It was clear from the beginning of our research that graph theory

alone, without a strong basis of the electrical theory will not be sufficient to solve this problem. A good general source of information on power grid modelling and engineering was [41], the book enabled me to get a basic understanding of: load and generation, quantify demands and requirements, factors that influence demands and different types of generation technology. Chapter 3 of [41] was also useful for its presentation of grid geography and contingencies power surpluses etc. and naturally looking for cross overs of between pure mathematics and electrical engineering S Smale in [55] describes the differential equation that describe the interactions between components of electrical networks.

1.3 Assumptions and Contents of the Thesis

Throughout the thesis there are a number of assumptions that are made when applying graph theoretic techniques to electric networks. The buses and the electrical generators in the network are interpreted as nodes, and the electrical transmission lines are interpreted as edges.

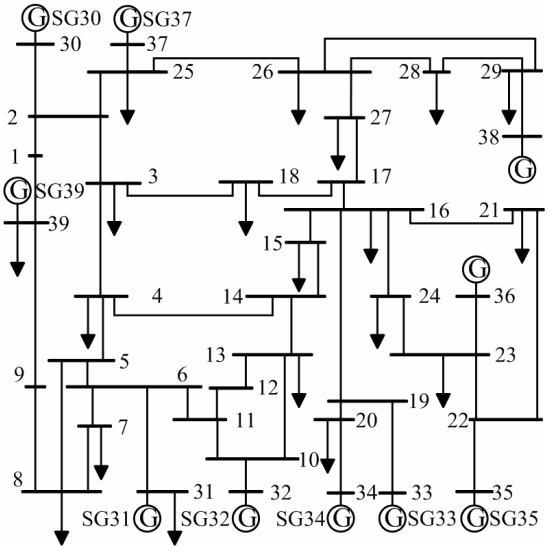

Figure 1-1: This is the IEEE 39-bus test case network.

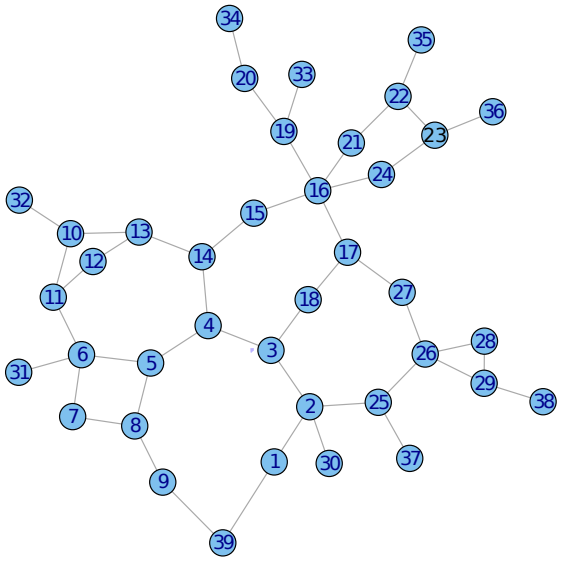

Figure 1-2: This is the graph theoretic interpretation of the topological of the IEEE 39-bus test case network.

The direct current (DC) approximation of alternating current (AC) is an approximation that is made throughout the document (see A.3.4 for more detail), this is a simplification that enables us to apply graph theoretic approaches to problems in AC electrical power networks. We now describe the contents of the thesis in more detail.

1.3.1 Chapter 2

In this chapter we introduce our first spectral partitioning technique based on the results of Fielder, and adapt it to the problems of blackouts. Our main source here is Chung in [14] which shows that the application of the Fiedler partition method will lead to an island with a relatively small boundary compared to it size, thus an good cut that will minimise disturbance to an electrical power system. Our analysis extends that of Chung's in a small but significant details.

In this chapter we also address a significant weakness of the Fiedler method which

allows the partitioning of graphs into any number of islands.

1.3.2 Chapter 3

In this Chapter we review some of the most advanced higher order spectral clustering techniques (which form k islands where k is generalised as any $k \in \mathbb{N}$), specifically those of J Lee, G Oveis, et al in [38]. Here we am able to take these techniques a little farther giving me a number of results.

I have programmed these higher order spectral clustering techniques and then I have implemented them on the IEEE 39 and 118-bus test cases and the GB networks. Certain adjustments are made to this algorithms and their performance is compared to that of a Fiedler method based algorithm from Chapter 2. We find instances where these high order spectral clustering techniques out perform the higher order Fiedler with much reduced computation time.

At the end of the chapter we explain another set of partitioning techniques the *evolving set process* whose techniques are quite different. For one of these *evolving set process* algorithms I have programmed and collected results.

1.3.3 Chapter 4

In this chapter a new spectral clustering technique is introduced, this is unique in that it doesn't just perform partitions of a graph, it presents a complete partitioning scheme which determines how a graph should be split into any number of subsets and how any subset should be farther partitioned. *This work was as a result of collaboration with Dr Rubén J. Sáchez-García.*

1.3.4 Chapter 5

During the course of our research a couple of groups use a similar technique to Fiedler one mentioned before in [44], and also a research group in Manchester. A particular interesting feature by L Ding and F Gonzalez-Longatt, et al presented in [18] is combining dynamics with the spectral methods. In this chapter we explain their approach and I have simulated their technique in the IEEE 39-bus test case and collected results. Also I have devised a similar two-step algorithm to that in [44] the main difference be-

ing that the spectral method employed is the Fiedlers vector method form chapter 2, I find that this does improve results in certain aspects for the IEEE 39-bus test case.

1.3.5 Chapter 6

Embeddings of an electrical networks into metric spaces will be a dominant theme throughout my thesis. In Chapter 6 we explore the previous research into a metric called the discrete Connes metric. Herein two different constructions of the metric are presented, with the objective to eventually calculate this metric for any weighted graph we note how these metrics can be described as an optimisation problems.

1.3.6 Chapter 7

Within this chapter we explore the optimisation problem introduced in Chapter 6. This is an optimisation problem with a linear objective and a quadratic constraint, in an attempt to simplify this problem we use various techniques to convert this into an optimisation problem with a quadratic objective and a linear constraint. Within the course of this conversion we are able to determine certain properties of the Connes metric which we will state. This work was a result of a collaboration with Jörg Fliege. [2]

We find this metric to be well correlation with a more established electrical distance metrics (Thévenin's impedance), as well as this we are able to show that the appearance of this metic is similar to the Resistance metric in certain forms.

[2] I have calculated the Connes metric for the IEEE 39-bus test case and the IEEE 118-bus test case, use a machine learning technique to perform linear regression.

Chapter 2

Fiedler's Vector Partitions

Given a network, it is an interesting and challenging problem to disconnect it into islands, or connected components, by cutting a number of edges. Typically there is an overall criterion that dictates what islands are deemed 'good' or interesting. In electrical engineering, in particular, there are established techniques to divide a power grid into a number of components. In this Chapter we shall adapt a particular isoperimetric problem from graph theory to the problem of islanding of power grids. We will study the so called the Cheeger constant and its relation to spectral properties of a Laplace operator, which as we shall see, encodes both the structure of the network as well as its function. The partioning method described here was based on an observation in [22] that the eigenvectors of the adjacency matrix could be used to create partitions. In the same year, Fiedler has devised such a technique in [23].

The aim of this Chapter is to describe and assess Fiedler's partitioning algorithm and to introduce the theoretical results on which it is based. In particular, we will address the question of quality of a particular decomposition, and will provide various ways to describe it. The original Fiedler algorithm would split a network into two components, but we shall show in this Chapter how to generalise this so that we can create a larger number of islands. This is known as the higher order spectral partitioning and we will investigate it in greater detail in the Chapter that follows.

There are four different varieties to this theorem presented in [13] one of which is shown again in [14, p. 26]. Here we will present a corrected version of the proof.

2.1 Network splitting

In this Chapter we will introduce a network splitting techniques applied to power systems. The original motivation for the development of such techniques was in the advent of parallel computing, where the process speed could be increased by splitting computations into many parts, which could be processing simultaneously and then reassembled. This is performed best when the computation is split into near equal portions and in such a way that these portions can be reassembled easily.

It was G.Kron in the 1950s [36] who developed techniques to solve power flow problems by cutting the edges of a power system and in doing so breaking the problem down into a set of subproblems, which could be solved independently and reassembled. This technique was notably improved by H Happ [28], J Chow [12] and others.

These techniques can also be used to mitigate the spread of a cascading failure in networks so for example in electrical grids. The general principle being that if this is applied to a network partition iteratively a failure can be isolated, so that potential spread of the failure and damage to the system is minimised.

In this Chapter we will be considering DC networks, or the DC approximation of an AC power flow (refer to appendix section A.3.4). The figure below includes all the information that we will need to apply the Fiedler partition strategy, namely the magnitude of the power flow in each edges of a network the orientation of the edges is not in fact needed.

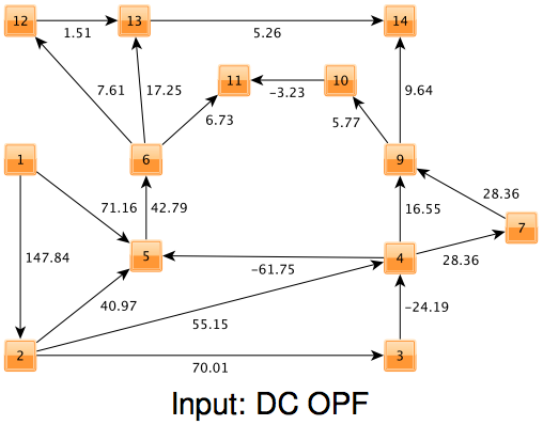

Figure 2-1: A graph of 14 vertices, where the power flows are illustrated on the oriented edges. This is a 'DC' Direct current, 'OPF' optimal power flow.

2.2 Preliminaries

Definition 2.1. ***(Weighted Graph)*** *A weighted graph G consists of a set of vertices V and a set of edges E. For an edge which connects vertices $u \in V$ to $v \in V$ is denoted as $(u, v) = e \in E$ the edge with reversed orientation $\overline{e} = (v, u) \in E$ there will be an associated weight, $b(e) = b(\bar{e}) \in \mathbb{R}$.*

Definition 2.2. ***(Degree)*** *The degree of a vertex is given by the sum of the weights of the edges that are adjacent to it. For $v \in V$ the degree is given by*

$$d(v) = \sum_{v \sim w} b(v, w),$$

where $\sum_{v \sim w}$ is the sum of all vertices that are adjacent to v.

Definition 2.3. ***(Volume)*** *For a graph G the volume of a subset $S \subseteq V$ is the sum of the degrees of all vertices in S*

$$Vol(S) = \sum_{\forall v \in S} d_v.$$

Definition 2.4. ***(Boundary of subset S)*** *The boundary of a subset $S \subset V$ is the set of edges that connect the subset S to its complement $V \backslash S = \bar{S}$*

$$\delta(S) = \{\{u, v\} \in E : u \in S \text{ and } v \in \bar{S}\}$$

where $\{u, v\}$ is an unordered pair of vertices.

Definition 2.5. ***(Cheeger constant of $S \subseteq V$)***

$$h(S) = \frac{\sum_{e \in \delta(S)} |b(e)|}{\min\left(Vol(S), Vol(\bar{S})\right)}. \tag{2.1}$$

Remark 2.6. *The Cheeger constant of a subsets $S \subseteq V$ is equal to the Cheeger constant of its compliment,*

$$h(S) = h(\bar{S}).$$

Remark 2.7. *The Cheeger constant is an isoperimetric ratio of subset S, of which there are other forms, for example the sparsest cut ratio in [45].*

Definition 2.8. ***(Cheeger constant of** G**)*** *The Cheeger constant of a graph G is,*

$$h_G = \min_{\forall S \subset V} \{h_G(S)\}. \tag{2.2}$$

We will now define the weighted Laplacian operator for finite networks of $n \in \mathbb{N}$ vertices.

Definition 2.9. ***(Weighted Laplacian operator)*** *The weighted Laplacian will be given as an $n \times n$ matrix, where A_w is the adjacency matrix,*

$$A_w(v_i, v_j) = \begin{cases} b(e) & \text{if } e = (v_i, v_j) \in E, \\ 0 & \text{otherwise.} \end{cases} \tag{2.3}$$

The weighted Laplacian is,

$$\mathcal{L} = diag\{d(v_1), d(v_2), \ldots, d(v_n)\} - A_w.$$

Remark 2.10. *We will refer to the spectrum of eigenvalues of the Laplacian operator as $0 = \lambda_1 \leq \lambda_2 \leq \cdots \leq \lambda_n$ and the corresponding eigenvectors $\underline{y_1}, \underline{y_2}, \ldots, \underline{y_n}$ where $\underline{y_1}$ is a constant vector.*

Definition 2.11. ***(Normalised Laplacian)*** *The normalised Laplacian operator $\mathscr{L}$ is*

$$\mathscr{L}(v_i, v_j) = \begin{cases} \frac{-w(v_i,v_j)}{\sqrt{d_i \cdot d_j}} & \text{if } e = (v_i, v_j) \in E, \\ 0 & \text{if } e = (v_i, v_j) \notin E, \\ 1 & \text{if } i = j. \end{cases} \tag{2.4}$$

Remark 2.12. *In this Chapter and the following chaper we will refer to $\lambda_1, \ldots, \lambda_n$ as the eigenvalues (in ascending order) of the normalised Laplacian $\mathscr{L}$ and $\underline{x_1}, \ldots, \underline{x_n}$ as the corresponding set of eigenvectors. The transformation from the unnormalised to the normalised Laplacian is given by the conjugation by a diagonal matrix $D^{-1/2}$ whose nonzero entry $D^{-1/2}(i,i)$ is the inverse square root of the degree of vertex v_i. We will mostly consider eigenvectors of the normalised Laplacian but for the simplification of some expressions we will consider also the eigenvectors of the unnormalised Laplacian*

which we will denote $\underline{y_1}, \ldots, \underline{y_n}$ *where for all* $i \in \{1, \ldots, n\}$ *we have*

$$\underline{y_i} = D^{-1/2}\underline{x_i}. \tag{2.5}$$

The Laplacian is of course a classical operator, a continuous Laplacian operator on $\mathbb{R}^n$ is given by $\partial^2/\partial x_1^2 + \cdots + \partial^2/\partial x_n^2$. When using the finite difference method to describe the continuous Laplacian an analog of the discrete Lapcian operator is also found. To demonstrate this we will show that for the continuous Laplacian operator on function $f : \mathbb{R}^2 \to \mathbb{C}$ coinsides with the discrete Lapacian operator when taking finite differences on a five point stencil.

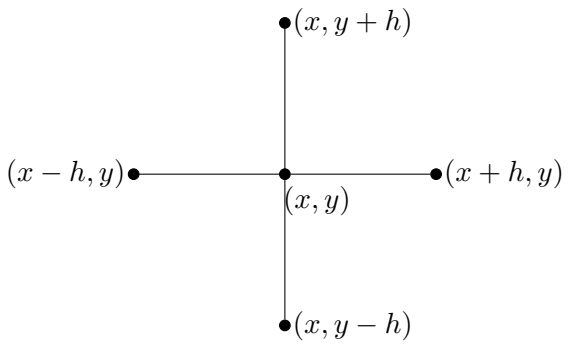

Figure 2-2: Five-point stencil.

Where

$$D_1^-(f)(x,y) = \frac{f(x,y) - f(x-h,y)}{h}, D_1^+(f)(x,y) = \frac{f(x+h,y) - f(x,y)}{h},$$
$$D_2^-(f)(x,y) = \frac{f(x,y) - f(x,y-h)}{h} \text{ and } D_2^+(f)(x,y) = \frac{f(x,y+h) - f(x,y)}{h}$$

(taking limits of these as $h \to 0$ will give the partial derivatives).

The continuous Laplacian operator of $f(x,y)$ is

$$\begin{aligned}\Delta(f)(x,y) &= \lim_{h\to 0}\left(D_1^+D_1^-(f)(x,y) + D_2^+D_2^-(f)(x,y)\right)\\ &= \lim_{h\to 0}\left(D_1^+\frac{f(x,y)-f(x-h,y)}{h} + D_2^+\frac{f(x,y)-f(x,y-h)}{h}\right)\\ &= \lim_{h\to 0}\left(\frac{1}{h}\left(\frac{f(x+h,y)-f(x,y)}{h} - \frac{f(x,y)-f(x-h,y)}{h}\right)\right)\\ &\quad + \lim_{h\to 0}\left(\frac{1}{h}\left(\frac{f(x,y+h)-f(x,y)}{h} - \frac{f(x,y)-f(x,y-h)}{h}\right)\right)\\ &= \lim_{h\to 0}\frac{f(x+h,y)+f(x-h,y)+f(x,y+h)+f(x,y-h)-4f(x,y)}{h^2}.\end{aligned} \tag{2.6}$$

If we were to interpret figure 2-2 as a discrete graph containing nodes and edges so that: the set of vertices $V = \{(x-h,y),(x,y-h),(x,y),(x,y-h),(x,y+h)\}$, the weight of each edge is $1/h^2$ and $f : V \to \mathbb{C}$, we would find the the same results as (2.6),

$$\mathcal{L}(f)(x,y) = \frac{f(x+h,y)+f(x-h,y)+f(x,y+h)+f(x,y-h)-4f(x,y)}{h^2}.$$

The Rayleigh Quotient

The Rayleigh quotient of $\underline{x} \in \mathbb{R}^n$ with respect to the normalised Laplacian $\mathscr{L}$ is given as follows,

$$\mathscr{R}(\underline{x}) = \frac{\langle \mathscr{L}\underline{x}, \underline{x}\rangle}{\|\underline{x}\|^2} = \frac{\langle \mathcal{L}D^{-1/2}\underline{x}, D^{-1/2}\underline{x}\rangle}{\sum_{i=1}^n \underline{x}_i^2}. \tag{2.7}$$

We will introduce an alternative inner product space, which will allow our to state (2.7) as a Rayleigh quotient of $\underline{y}$. First note that functions of the form $f : V \to \mathbb{R}$ we will consider to be interchangeable with $\underline{f} \in \mathbb{R}^n$ where $\underline{f}_i = f(v_i)$.

Definition 2.13. ***(Alternative Inner Product Space)*** *For any two functions $f, g \in \ell^2(V, d_v)$ we have the inner product,*

$$\langle \underline{f}, \underline{g}\rangle_{\ell^2(V,d_v)} = \sum_{i=1}^n \underline{f}_i\overline{\underline{g}}_i d_i.$$

As with the eigenvalues in (2.5) say $\underline{y} = D^{-1/2}\underline{x}$ we then have ($\sum_{u\sim v}$ is the sum

over all unordered adjacent pairs),

$$\mathscr{R}(\underline{x}) = \frac{\langle \mathcal{L}\underline{y}, \underline{y}\rangle}{\sum_{i=1}^{n} d_i \underline{y}_i^2} = \frac{\sum_{i\sim j} b(v_i, v_j)(\underline{y}_i - \underline{y}_j)^2}{\sum_{i=1}^{n} d_i \underline{y}_i^2}.$$

We can then have the following alternative Rayleigh quotient of the normalise Laplacian ($\mathscr{L}$) but in the alternative inner production space defined in 2.13,

$$\mathcal{R}(\underline{y}) = \frac{\langle \mathscr{L}\underline{y}, \underline{y}\rangle_{\ell(V,d_v)}}{\|\underline{y}\|_{\ell(V,d_v)}} = \frac{\sum_{i\sim j} b(v_i, v_j)(\underline{y}_i - \underline{y}_j)^2}{\sum_{i=1}^{n} d_i \underline{y}_i^2}. \tag{2.8}$$

Remark 2.14. *Note that value of the $\mathcal{R}$ on an eigenvector $\underline{y_i}$ corresponds to the i^{th} eigenvalue λ_i.*

2.3 Fielder's Partition Method

The Fiedler partition method is a way of finding an island (subset) of a network which has a small Cheeger constant. However, there is no guarantee that the island resulting from the application of the Fiedler's method will have an optimally small Cheeger constant (there are 2^{n-1} possible cuts that can be taken). In fact, the work by S Guattery and G Miller, in [26] presents several examples of graphs for which there is no optimal solution. The purpose of the application of Fiedler's partition method is however to find an island which can be proved to have a small Cheeger constant. In the method the Cheeger constant of n islands is assessed, dramatically deducing the computational complexity which would be involved in assessing the Cheeger constant of all possible bi-partitions, as there are 2^{n-1} possible ways to group the vertices into two separate groups.

In the context of power grids if we take the edges of a graph to be weighted by the absolute value of the power flow, the Cheeger constant is the amount of power which will have to be redistributed as a result of a cut, this is given by the numerator in (2.1) which is divided by the size of the island formed by a cut. If the objective was to form an island with just the electrical disruption minimised, a trivial island of one isolated vertex would most likely be formed. To take a simple example if we were to find an island with the size of the boundary minimised for the graph below (in which we take the edges weights to be one), it could be any isolated vertex as this is a regular graph

this would give a Cheeger constant of 3.

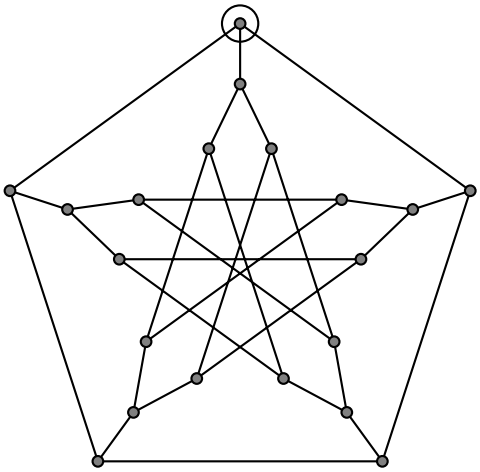

It is justifiable to want to reduce the Cheeger constant parameter of a cut as the total disruption to the power's flow is small and a network will be split approximately in half, meaning that the cut will be nontrivial. The island that will gives the Cheeger constant for the graph below is illustrated here.

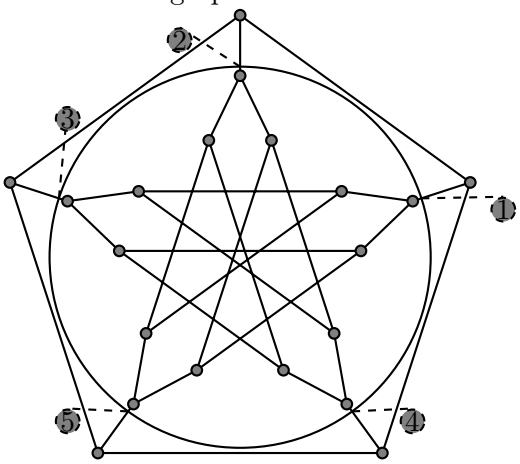

This give a Cheeger constant of one, for such a problem we could use an algorithm as in [59].

As well as the total power disruption being minimised, it is also desirable to minimise the total energy imbalance of each island. Once a partition is taken, one of the islands will have a power surplus, and its complement will have an equal but opposite power deficit. If we look at one of the islands of a partition, the power disruption of the cut which forms the island can be expressed as the power throughput of that island Throughput $= P_{\text{in}} + P_{\text{out}}$ where P_{in} is the power flowing into the island and P_{out} is the power flowing out of the island. The power imbalance of the island is then give as Power balance $= P_{\text{in}} - P_{\text{out}}$. It is preferable to minimise the power throughput of the

island and the power imbalance takes a lesser importance as it can be dealt with after the cut has been taken by load shedding.

Next we will go through the steps of the method algorithmically.

2.3.1 The Embedding Partition Method

The first step: of the Fielder partition method is to take a vector $\underline{f} = \underline{y_2} \in \mathbb{R}^n$ (the eigenvector associated with the first nonzero eigenvalue of the normalised Laplacian). We will also consider the *embedding partition method* outside of the implementation of *Fiedler's partition method* in which case we will consider $\underline{f}$ generalised vector in $\mathbb{R}^n$.

We relabel the vertices $\{v_1, v_2, \ldots, v_n\}$ where there is some standard numbering (of $i \in \mathbb{N}$ for v_i) so that the entries of this vector are in ascending order.

$$\underline{f} = \begin{bmatrix} f(v_1) \\ f(v_2) \\ \vdots \\ f(v_n) \end{bmatrix},$$

$f(v_1) \leq f(v_2) \leq \cdots \leq f(v_n)$ as $f(v_i) \in \mathbb{R}$ for each $i \in \{1, 2, \ldots, n\}$ this is essentially an embedding of the vertices labeled $\{v_1, v_2, \ldots, v_n\}$ into the real line where v_i is in position $f(v_i)$, ordering of the vertices in the network, and in doing so will, present $n-1$ possible partitions.

The second step: in this step the Cheeger constants of all of the $n-1$ possible islands are computed and the smallest taken. The cuts are taken on an ever increasing coordinate on the real line, so the the sequence of groupings follow the order given by values of f are $\{v_1\}$, $\{v_1, v_2\}$, $\{v_1, v_2, v_3\}$, etc. We will label the smallest Cheeger constant of the $n-1$ cuts as $\alpha_G(\underline{x})$.

Theorem 2.15. *If we apply the embedding partition method with vector of function $f : V \to \mathbb{R}^n$ which is such that $\sum_{\forall v \in V} f(v) = 0$,*

$$\mathcal{R}(f) \geq \frac{\alpha_G^2(f)}{2}. \tag{2.9}$$

Proof. Applying the embedding partition method we will take f to be an embedding of G into the real line and relabel the vertices such that $f(v_i) < f(v_{i+1})$ for all $i \in$

$\{1, \ldots, n-1\}$. We will take S_0 to be an empty set and for $i \in \{1, \ldots, n-1\}$,

$$S_i = \{v_1, \ldots, v_i\}$$

and

$$\alpha_G = \min_i h_G(S_i). \tag{2.10}$$

Noting that $Vol(S_i)$ is an increasing sequence in i, we will now go through a route for the selection of a vertex v_r. If there does not exist an $i \in \{1, 2, \ldots n\}$ such that $S_i = Vol(V)/2$, then we take $r \in \mathbb{N}$ to be the largest integer such that $Vol(S_{r-1}) < Vol(V)/2$, else if there does exist an $i \in \{1, 2, \ldots n\}$ such that $S_i = Vol(V)/2$ then we take $r \in \mathbb{N}$ to be such that $S_r = Vol(V)/2$. This selection procedure is the main distinguishing feature for Chung's proof in [13, p.26] and allows for there to be truly no loss in generality for (2.16) see later.

$\underline{f}$ can be adjusted by the addition of a constant vector which will mean that the following inequality holds, and most significantly will not effect the numerator of $\mathcal{R}(f)$. So without loss of generality we can assume that,

$$\sum_{v \in V} f^2(v) d_v \leq \sum_{v \in V} (f(v) - f(v_r))^2 d_v. \tag{2.11}$$

This can easily be seen once we expand the righthand side,

$$\sum_{v \in V} (f(v) - f(v_r))^2 d_v = \sum_{v \in V} f(v)^2 d_v - 2f(v_r) \cdot \underbrace{\sum_{v \in V} f(v)}_{=0} + \underbrace{f(v_r)^2 \cdot \sum_{v \in V} d_v}_{>0}.$$

If we separate the positive from the negative parts of f to give the following functions can be formed,

$$f_+(v) = \begin{cases} f(v) - f(v_r) & \text{if } \underline{f}(v) - \underline{f}(v_r) > 0, \\ 0 & \text{otherwise.} \end{cases} \tag{2.12}$$

and

$$f_-(v) = \begin{cases} |f(v) - f(v_r)| & \text{if } f(v) - f(v_r) < 0 \\ 0 & \text{otherwise.} \end{cases} \tag{2.13}$$

If we take the $\mathcal{R}(f) = \lambda_G$ note that $\sum_{u \sim v}$ is the sum over all ordered pair of adjacent

vertices,

$$\begin{aligned}
\lambda_G &= \frac{\sum_{u\sim v} b(u,v)(f(u)-f(v))^2}{\sum_{\forall v} f^2(v)d_v} \\
&\geq \frac{\sum_{u\sim v} b(u,v)(f(u)-f(v))^2}{\sum_{\forall v}(f(v)-f(v_r))^2 d_v} \\
&\geq \frac{\sum_{u\sim v} b(u,v)(f_+(u)-f_+(v))^2+(f_-(u)-f_-(v))^2}{\sum_{\forall u\sim v} b(u,v)(f_-(v)+f_+(v))^2} \qquad (2.14) \\
&= \frac{\sum_{u\sim v} b(u,v)(f_+(u)-f_+(v))^2+\sum_{u\sim v} b(u,v)(f_-(u)-f_-(v))^2}{\sum_{\forall v} f_-^2(v)d_v+\sum_{\forall v} d_v f_+^2(v)d_v} \qquad (2.15)
\end{aligned}$$

In (2.15) the numerator is the addition of numerators of $\mathcal{R}(f_+)$ and $\mathcal{R}(f_-)$ and the denominator is the addition of denominators of $\mathcal{R}(f_+)$ and $\mathcal{R}(f_-)$. Thus using $\frac{a+b}{c+d} \geq \min\{\frac{a}{c},\frac{b}{d}\}$ assuming that we can imply that $\mathcal{R}(f_+) \leq \mathcal{R}(f_-)$ we have $\lambda_G \geq \mathcal{R}(f_+)$.

There is no loss in generality to say

$$\mathcal{R}(f_+) \leq \mathcal{R}(f_-) \qquad (2.16)$$

because if (2.16) doesn't hold the steps of the proof could be repeated with the function $-f = g$ instead of f. For the embedding g we would have a reversed order hence $g(v_{i+1}) \leq g(v_i)$, as $\mathcal{R}(f) = \mathcal{R}(g)$ and $\alpha_G(f) = \alpha_G(g)$ this would be just as valid a proof of the theorem. Using $g = -f$ and following the steps of the proof up to this point we would find $\mathcal{R}(g_+) = \mathcal{R}(f_-)$ and $\mathcal{R}(g_-) = \mathcal{R}(f_+)$, thus there is a loss of generality when stating that $\mathcal{R}(f_+) \leq \mathcal{R}(f_-)$ as in this way f_+ and f_- are interchangeable.

To simplify exposition, let us denote

$$\widetilde{Vol}(S) = \min\{Vol(S), Vol(G) - Vol(S)\}.$$

Referring back to (2.10) and the definition of (2.1), we have for any subset S_i,

$$\sum_{e\in\delta(S_i)} |b(e)| \geq \alpha_G \widetilde{Vol}(S_i). \qquad (2.17)$$

To process with the proof two Lemmas need to be introduced.

Lemma 2.16. $\sum_{u\sim v} b(u,v)(f_+(u)+f_+(v))^2 \leq 2\sum_{\forall v} f_+^2(u)d_v$.

Proof.

$$\begin{aligned}\sum_{u\sim v} b(u,v)(f_+(u)+f_+(v))^2 &= \sum_{u\sim v} b(u,v)(f_+^2(u)+2f_+(u)\cdot f_+(v)+f_+^2(v)) \\ &= \sum_{u\sim v} b(u,v)(f_+^2(u)+f_+^2(v)) + 2\sum_{u\sim v} b(u,v)f_+(u)\cdot f_+(v) \\ &= \sum_{\forall v} f_+^2(v)d_v + 2\sum_{u\sim v} b(u,v)f_+(u)\cdot f_+(v). \qquad (2.18)\end{aligned}$$

The inequality required will result from the following calculation,

$$0 \leq \sum_{u\sim v} b(u,v)(f_+(u)-f_+(v))^2 = \sum_{u\sim v} b(u,v)(f_+^2(u)+f_+^2(v)) - 2\sum_{u\sim v} b(u,v)f_+(u)\cdot f_+(v)$$

$$\implies 2\sum_{u\sim v} b(u,v)f_+(u)\cdot f_+(v) \leq \sum_{u\sim v} b(u,v)(f_+^2(u)+f_+^2(v))$$

$$\implies 2\sum_{u\sim v} b(u,v)f_+(u)\cdot f_+(v) \leq \sum_{\forall v} f_+^2(v)d_v.$$

Substituting this back into (2.18) we have,

$$\sum_{u\sim v} b(u,v)(f_+(u)+f_+(v))^2 \leq 2\sum_{\forall v} f_+^2(v)d_v.$$

□

Lemma 2.17.

$$\sum_{u\sim v} b(u,v)|(f_+^2(u)-f_+^2(v))| = \sum_{i=1}^{n-1} |(f_+^2(v_i)-f_+^2(v_{i+1}))| \sum_{e\in\delta(S_i)} |b(e)|. \qquad (2.19)$$

This holds as we take any individual edge $(v_k, v_l) \in E$ where $k < l$ will contribute $b(v_k, v_l)$ to every $\sum_{e\in\delta(S_i)} |b(e)|$ where $i \in [k, l-1]$ and thus contribute to this term $b(v_k,v_l)(\underline{f}_+^2(v_k) - \underline{f}_+^2(v_{k+1}) + f_+^2(v_{k+1}) - \cdots - \underline{f}_+^2(v_{l-1}) + \underline{f}_+^2(v_{l-1}) - \underline{f}_+^2(v_l)) = b(v_k,v_l)(\underline{f}_+^2(v_k) - \underline{f}_+^2(v_l))$ after the cancellation of all intermediate terms. This does assume that $v_l, v_k \in S_r$, if $\{v_l, v_k\} \in \delta(S_r)$ there will be a $-\underline{f}_+^2(r)\cdot b(v_k,v_l)$ term that had not appeared in $\sum_{u\sim v}$ hence the inequality.

Now we are able to complete the proof and show that $\lambda_G \geq \alpha_G^2/2$ (note here that

$\sum_{\forall v}$ is the summation through all vertices $v \in V$,

$$\begin{aligned}
\lambda_G \geq \mathcal{R}(f_+) &= \frac{\sum_{u\sim v} b(u,v)(f_+(u)-f_+(v))^2}{\sum_{\forall v} f_+^2(v)d_v} \\
&= \frac{(\sum_{u\sim v} b(u,v)(f_+(u)-f_+(v))^2)(\sum_{u\sim v} b(u,v)(f_+(u)+f_+(v))^2))}{(\sum_{\forall v} f_+^2(v)d_v)\sum_{u\sim v} b(u,v)(f_+(u)+f_+(v))^2} \\
&\geq \frac{\left(\sum_{u\sim v} b(u,v)|(f_+^2(u)-f_+^2(v))|\right)^2}{(\sum_{\forall v} f_+^2(v)d_v)\sum_{u\sim v} b(u,v)(f_+(u)+f_+(v))^2} \qquad (2.20)
\end{aligned}$$

$$\begin{aligned}
&\geq \frac{\left(\sum_{u\sim v} b(u,v)|(f_+^2(u)-f_+^2(v))|\right)^2}{2\left(\sum_{\forall v} f_+^2(v)d_v\right)^2} \qquad (2.21) \\
&= \frac{\left(\sum_{i=1}^{n-1}\left(|(f_+^2(v_i)-f_+^2(v_{i+1}))|\sum_{e\in\delta(S_i)}|b(e)|\right)\right)^2}{2\left(\sum_{\forall v} f_+^2(u)d_u\right)^2} \qquad (2.22) \\
&= \frac{\left(\sum_{i=r+1}^{n-1}\left(|(f_+^2(v_i)-f_+^2(v_{i+1}))|\sum_{e\in\delta(S_i)}|b(e)|\right)\right)^2}{2\left(\sum_{\forall v} f_+^2(u)d_u\right)^2} \qquad (2.23) \\
&\geq \frac{\left(\sum_{i=1}^{n-1}|(f_+^2(v_i)-f_+^2(v_{i+1}))|\cdot|\widetilde{Vol}(S_i)|\alpha_G\right)^2}{2\left(\sum_{\forall v} f_+^2(v)d_v\right)^2} \qquad (2.24) \\
&= \frac{\left(\sum_{i=1}^{n}|(f_+^2(v_i))|\cdot|\widetilde{Vol}(S_i)-\widetilde{Vol}(S_{i-1})|\alpha_G\right)^2}{2\left(\sum_{\forall v} f_+^2(v)d_v\right)^2} \\
&= \frac{\left(\sum_{i=1}^{n}|(f_+^2(v_i))|d_i\cdot\alpha_G\right)^2}{2\left(\sum_{\forall v} f_+^2(u)d_u\right)^2} \qquad (2.25) \\
&= \frac{\alpha_G^2}{2}\frac{\left(\sum_{i=1}^{n}|(f_+^2(v_i))|d_i\right)^2}{\left(\sum_{\forall v} f_+^2(v)d_v\right)^2} \\
&= \frac{\alpha_G^2}{2}.
\end{aligned}$$

The second inequality (2.20) is a result of the application of Cauchy-Schwarz inequality. (2.21) is an application of Lemma 2.16, and equality (2.22) is an application of Lemma (2.17).

□

Remark 2.18. *This is a very similar proof to that in [13, p.26] a notable difference is the selection procedure for $r \in \{1, 2, \ldots, n\}$, which leads onto different constructions of f_- and f_+ in (2.12) and in (2.13).*

The correction here allows and there to be truly no loss of generality between $\mathcal{R}(f_+)$ and $\mathcal{R}(f_-)$ in the statement (2.16). This can be shown by repeating the steps of the proof up to (2.16) but with $g = -f$ as an exchanged version of f. When using Chungs approach and repeating the steps of the proof up to the claim of (2.16) with $g = -f$ as an exchanged version of f, we do not find necessarily that $\mathcal{R}(f_+) = \mathcal{R}(g_-)$ and $\mathcal{R}(f_-) = \mathcal{R}(g_+)$ (as in our proof). This is because the selection set of vertex v_r will not necessarily be the same both times, in fact we will only find this with Chung's approach when there exists an $r \in \{1, 2, \ldots, n\}$ where $S_r = Vol(V)/2$. With our approach for f and then for $g = -f$ as an exchanged version of f, the selection of vertex v_r will be the same both times this leads functions f_+, f_- and g_+, g_- where $f_+ = g_-$ and $f_+ = g_-$ which allows for there to be no loss in generality in the statement $\mathcal{R}(f_+) \leq \mathcal{R}(f_-)$ implying that (2.16) is w.l.o.g.

Also Chung's proof in [13] only applies to unweighted graphs this theorem is generalised to include weighted graphs.

Corollary 2.19. *The following estimate holds:*

$$\lambda_2 > \frac{\alpha_G^2(\underline{y_2})}{2}. \tag{2.26}$$

Proof. If we take $\underline{f} = \underline{y_2}$ in Theorem 2.15 , then the estimate follows since $\mathcal{R}(\underline{y_2}) = \lambda_2$. □

There also and upper bound to the Rayleigh quotient this can be seen in [14, p. 25].

Lemma 2.20.

$$\lambda_2 \leq 2h_G \tag{2.27}$$

Proof. Let S be any subset of V, and let us define a function $f : V \to \mathbb{R}$ by:

$$f(v) = \begin{cases} \frac{1}{Vol(S)} & \text{if } v \in S, \\ -\frac{1}{Vol(\overline{S})} & \text{otherwise.} \end{cases}$$

The Raleigh quotient associated with the function f is then:

$$\begin{aligned}
\mathcal{R}(f) =& \frac{\sum_{\{u,v\}\in\delta(S)} b(u,v)(1/Vol(S) + 1/Vol(\bar{S}))^2}{\sum_{v\in S} d_v/Vol(S)^2 + \sum_{v\in\bar{S}} d_v/Vol(\bar{S})^2} \\
=& \frac{\sum_{\{u,v\}\in\delta(S)} b(u,v)(1/Vol(S) + 1/Vol(\bar{S}))^2}{1/Vol(S) + 1/Vol(\bar{S})} \\
=& \sum_{\{u,v\}\in\delta(S)} b(u,v)(1/Vol(S) + 1/Vol(\bar{S})) \\
=& |\delta(S)|(1/Vol(S) + 1/Vol(\bar{S}) \\
&\leq 2|\delta(S)|(1/\min(Vol(S), Vol(\bar{S}))) \\
&= 2h_G(S).
\end{aligned}$$

As $\sum_{v\in V} f(v) = 0$ meaning that $\underline{f}$ is thus perpendicular to the constant function that has eigenvalue zero, so $\mathcal{R}(f) \in [\lambda_2, \lambda_n]$.

$$\lambda_2 \leq 2h_G(S).$$

Say that S is chosen to minimise $h_G(S)$ this will imply that,

$$\lambda_2 \leq 2h_G$$

completing the proof. □

Remark 2.21. *Similar analysis is carried out in [34] but with the $\mathscr{R}$ Rayleigh quotient given in (2.7).*

2.3.2 Higher Order Fielder's Partition Method

We will now investigate an extension of this method so that it will create k subsets instead of two. We first need to define an higher order Cheeger constant for a $k-$way partition.

Definition 2.22. ***(Higher Order Cheeger Constants of k-way Partition)*** *The higher order Cheeger constant of a partitions resulting in the formation of k disjoint*

subsets where $S_1 \cup S_2 \cup \cdots \cup S_k = V$ *is given as follows,*

$$h^{(k)}(S_1 \cup S_2 \cup \cdots \cup S_k) = \min_{\substack{S_1,S_2,\ldots,S_k \subseteq V \\ S_1 \cup S_2 \cup \cdots \cup S_k = V}} \max\{h_G(S_i) \big| \forall i = 1, 2, \ldots, k\}. \tag{2.28}$$

With $k = 2$ this is the Fiedler partition method shown in the *Embedding Partition Method* in section 2.3.1 where f is taken as the first non trivial eigenfunction. After the embedding in *The first step* all $n-1$ cuts are explored in *The second step* of the algorithm and the cut with giving a partition with the lowest Cheeger constant is taken. So for an analogous method with $k \in \mathbb{N}$ will explore all C_{k-1}^{n-1} possible combinations of $k-1$ cuts in its second step and take the one that results in a partition with the lowest higher order Cheeger constant. A clear problem arises with the computation time needed for the execution of such an algorithm as $C_{k-1}^{n-1} = \mathrm{O}(n^k)$, thus this algorithm would soon become impractical for large network when looking for many subsets. Nevertheless as we will be developing techniques for decomposing the network into higher number of islands, it will be useful to compare this simple minded approach with the strategies developed in what follows.

For such an algorithm we will have the same first two steps as shown in *The embedding partition method*, and we will take $S_i = \{v_1, \ldots v_i\}$. The $k-1$ cut points will be represented as $i_1 < i_2 < \cdots < i_{k-1}$ and will result in the following k subsets $S_{i_1}, S_{i_2} \backslash S_{i_1}, \ldots, S_{i_{k-1}} \backslash S_{i_{k-2}}, V \backslash S_{i_{k-1}}$, if we use the following notation $T_1 = S_{i_1}$, for $j \in \{2, 3, \ldots, k-2\}$ $T_j = S_{i_j} \backslash S_{i_{j-1}}$ and $T_k = S_{i_{k-1}}$,

$$\alpha_G^{(k)} = \min_{\substack{\forall i_1, i_2, \ldots, i_{k-1} \\ i_1 < i_2 < \cdots < i_{k-1}}} h^{(k)}(T_1 \cup T_2 \cup \cdots \cup T_k). \tag{2.29}$$

Remark 2.23. *It is possible to prove a result similar to Theorem 2.15 that would establish an estimate for* $\alpha_G^{(k)}$ *when considering* k *way partitions. Some of the steps in the proof would follow analogously, we would however not be able to apply step (2.24) and the elegance of the theorem would break down.*

Chapter 3

Higher Order Cheeger Inequalities

We have already met the Cheeger constant in the previous chapter our discussion of Fiedler's partition method, where a partition is taken with the objective of minimising the Cheeger constant. In this Chapter, we will investigate higher dimensional analogues of this procedure. A new tool will be required in the form of spectral partitioning, described in [38], among others. As shown in the previous chapter (refer to Corollary 2.19) the Cheeger constant of the subset resulting from the Fiedler partition method can be proved to have an upper bound depending in λ_2 (the first non-trivial eigenvalue of the unnormalised Laplacian), the smaller this eigenvalue the better the method can be proved to be. In an analogous way the theory expounded in this chapter that supports higher order Cheeger inequalities is based around the observation that if the first k nontrivial eigenvalues of the Laplacian are close to zero, then there will exist a partition that results in k islands each of which have a small Cheeger constants.

These spectral clustering techniques have a vast literature and are used across many fields of research such as statistics, computer science, bioinformatics and to the social sciences and psychology. The techniques can be used to analyse data whenever one wishes to identify groups that are similar, in our case that will be identifying nodes in electrical network using a notion of similarity relevant to the problem.

U Luxburg in [64] presents a accessible review of the most basic spectral clustering algorithms. Similar techniques exist in [54] and [46] for example but utilise algorithms

which cannot be supported by a rigorous mathematical framework.

The techniques in [38] are perhaps the most sophisticated spectral partitioning algorithm that there are and belong in the realm computer science where the focus is on how to cluster systems where the size tends to infinity. There is much research showing bounds on the higher order Cheeger constant in this context such as [3], [25], [39], [47], [57] etc. [38] has the advantage of providing constructive proofs this means that they can be interpreted algorithmically and thus the claims of a theorem will be true for the resulting partitions of the algorithm in the proof. As well as this it is said in [38] that their algorithms give more satisfactory bounds for low values of k when compared to [3], [25], [47] and [57]. In this chapter we will be extending some of the results of [38] and testing the application of their algorithms by implementing them on the IEEE 39 and 118-bus test cases and the GB network.

3.1 Preliminaries

Higher Order Cheeger Constant

In definition 2.22 we met the Higher Order Cheeger Constant of a given k-way partition, the higher order Cheeger constant of a graph G, will be the minimum of this for all possible $k-$way partitions of the graph. This is defined as follows.

Definition 3.1. ***(Higher Order Cheeger Constant)*** *The higher order Cheeger constant of a graph G is the minimum of higher order Cheeger constant over all possible $k-$way partitions of V. The $k-$way partition below is represented as the k subsets $S_1, S_2, \ldots, S_k \subset V$ where all subsets and disjoint and $S_1 \cup S_2 \cup \cdots \cup S_k = V$,*

$$h_G{}^{(k)} = \min_{\substack{S_1,S_2,\ldots,S_k \subset V \\ S_1 \cup S_2 \cup \cdots \cup S_k = V}} \{h^{(k)}(S_1, S_2, \ldots, S_k)\}. \tag{3.1}$$

Vectors, Matrices and Functions

Note here that as in the previous chapter vectors $\underline{x} \in \mathbb{R}^n$ will be considered interchangeably with functions of the form $x : V \to \mathbb{R}$ where $x(v_i) = \underline{x}(i))$ and in a similar way matrices $\mathbf{F} \in \mathbb{R}^{n \times k}$ will be considered interchangeably with functions $F : V \to \mathbb{R}^k$ where $F(v_i) = (\mathbf{F}_{i1}, \mathbf{F}_{i2}, \ldots, \mathbf{F}_{ik})$.

Note also that in this chapter the norm $\|\cdot\|$ will be taken to be equal to the ℓ^2 norm and the $\langle\cdot,\cdot\rangle$ is the standard inner product on $\ell^2(V)$.

Rayleigh Quotient

Remark 3.2. *Let $\boldsymbol{F}$ be the $n \times k$ matrix composed of the eigenvectors of the Laplace operator $\mathcal{L}$, and let $\tilde{\boldsymbol{F}}$ be the corresponding matrix composed of the eigenvectors of the normalised Laplace operator $\mathscr{L}$. Here we will define a similar measure to the Rayleigh quotient $\mathscr{R}$ but one which can be applied to matrices such as $\boldsymbol{F} = [\underline{x_1}, \underline{x_2}, \ldots, \underline{x_k}]$ and $\tilde{\boldsymbol{F}} = D^{-1/2}\boldsymbol{F} = [\underline{y_1}, \underline{y_2}, \ldots, \underline{y_k}]$,*

$$\mathscr{R}'(\boldsymbol{F}) = \frac{\langle \boldsymbol{F}, \mathscr{L}\boldsymbol{F}\rangle}{\sum_{l=1}^{k} \|\underline{x_l}\|^2} = \frac{\langle D^{-1/2}F, \mathcal{L}D^{-1/2}F\rangle}{\sum_{l=1}^{k}\sum_{v_i\in V} {y_l}^2(v_i)d_{v_i}} = \frac{\sum_{(v_i,v_j)\in E} b(v_i,v_j)\left\|\tilde{F}(v_i) - \tilde{F}(v_j)\right\|}{\sum_{v_i\in V}\langle \tilde{F}(v_i), \tilde{F}(v_i)\rangle d_{v_i}}$$

where d_{v_i} is the degree of vertex v_i and where $F(v_i) = (\underline{x_1}(i), \underline{x_2}(i), \ldots, \underline{x_k}(i)) \in \mathbb{R}^k$.

Another similar operator to the Rayleigh quotient is defined here, analogous to $\mathcal{R}'$ in the previous chapter but operates on matrices such that $\mathscr{R}'(F) = \mathcal{R}'(\tilde{F})$, so we have,

$$\mathcal{R}'(\tilde{F}) = \frac{\sum_{l=1}^{k}\sum_{(v_i,v_j)\in E}\left(\underline{y_l}(i) - \underline{y_l}(j)\right)^2}{\sum_{l=1}^{k}\sum_{v_i\in V} {y_i}^2(v_i)d_{v_i}}. \tag{3.2}$$

3.2 Theoretical Framework of Higher Order Spectral Partitioning

We will now present an algorithm for higher order spectral partitioning.

3.2.1 Higher Order Spectral Partitioning Algorithm

There will be two possible initial steps (Step 0's) for the higher order spectral partitioning algorithm, because Step 0 is the formation of the metric space which G will be embedded into, and we have is two different metrics which will be called d_F and $\hat{d}_F$.

Embedding and Metrics: Algorithm Step 0

The first step of higher order spectral partitioning algorithms is to take the first k nontrivial eigenvalues of the normalised Laplacian operator line these up to form the

columns of a $n \times k$ matrix thus we would have,

$$\mathbf{F} = [\underline{x_1}, \underline{x_2}, \ldots, \underline{x_k}]. \tag{3.3}$$

This represents an embedding of the vertex set V into $\mathbb{R}^k$. If $V = \{v_1, v_2, \ldots, v_n\}$ then we have $\mathbf{F}(v_i) = (\underline{x_1}(i), \underline{x_2}(i), \ldots, \underline{x_k}(i))$, so that the i^{th} row of the $\mathbf{F}$ matrix in (3.3), is the coordinate in $\mathbb{R}^k$ where v_i is embedded.

For this spectral clustering algorithm we will not be using the Euclidean distance in $\mathbb{R}^k$ between vertices v_i and v_j which is $\|F(v_i) - F(v_j)\|$, but instead the pseudo metric (all of these norms are ℓ^2 norms).

$$d_F(v_i, v_j) = \Big\| \frac{F(v_j)}{\|F(v_j)\|} - \frac{F(v_i)}{\|F(v_i)\|} \Big\|, \tag{3.4}$$

this is the radial projection distance and effectively turns the spectral embedding in $\mathbb{R}^k$ into an embedding into $\mathcal{S}^{k-1}$ (the unit sphere in $\mathbb{R}^k$).

The justification of using the spherical embedding can be appreciated when referring to the trivial case of a network that is already partitioned into k subsets, for such a network we would obviously want our algorithm to identify the k subsets as clusters, the first k eigenvectors of the Laplacian will be trivial eigenvectors where each eigenvector relates to each one of the subsets in that the only nonzero entries of the eigenvector are those entries that correspond to the vertices of the subset, using these eigenvector to embed the network may not necessarily result in vertices from different subset being a large Euclidean distance from one another and that an algorithm may struggle to identify the subsets, however when using the radial projection distance vertices of the same subset will be embedding into the same point in $\mathbb{R}^k$ and all vertices of different subsets will be a distance of $\sqrt{2}$ from each other thus a partitioning algorithm will readily identify the k subsets.

This is a pseudo metric because if $F(v_i)$ were a zero vertex the metric would be infinite, so we have a rule to deal with this: if $F(v_i) = \underline{\mathbf{0}}$ then $d_F(v_i, v_j) = \Big\| \frac{F(v_j)}{\|F(v_j)\|} \Big\|$, if $F(v_j) = \underline{\mathbf{0}}$ then $d_F(v_i, v_j) = \Big\| \frac{F(v_i)}{\|F(v_i)\|} \Big\|$ and if both $F(v_i)$ and $F(v_j)$ are equal to $\underline{\mathbf{0}}$ then $d_F(v_i, v_j) = 0$.

The figure below illustrates an embedding in $\mathcal{S}^2$ of the IEEE 39-bus test case. The IEEE 39-bus test case is a standard test system for electrical network simulations, where

the 39 buses are represented as nodes which are intersection point of transmission lines in the network which are represented as edges.

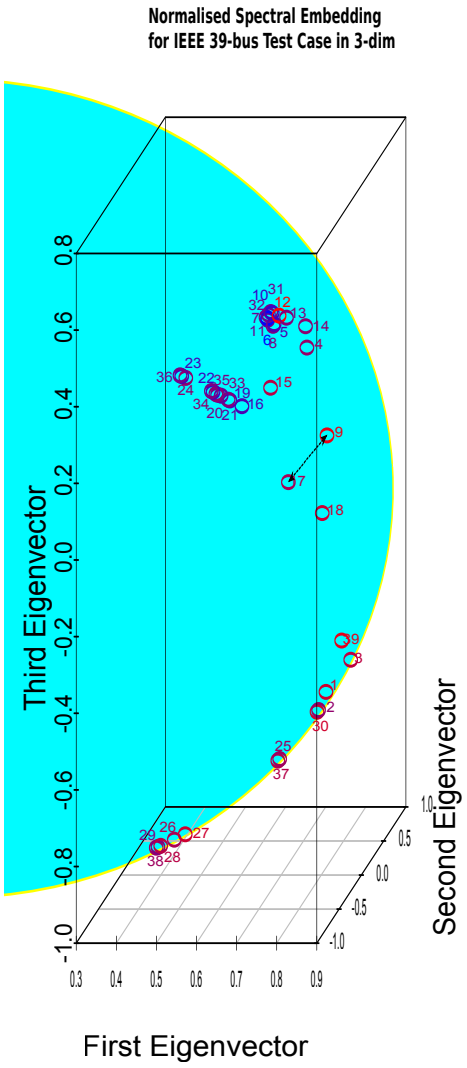

Figure 3-1: The $\mathcal{S}^2$ is illustrated in blue here with a yellow horizon.

The distance between buses will be given by the Euclidean distance for this embedding, illustrated in figure 3-1 for buses 17 and 9 given as the length of the dashed line.

There is an alternative metric that we can impose on the vertices once this embedding is complete. The Euclidean metric induced on the image of the embedding does not take into account the topology of the graph. Retaining this information is potentially useful, and can be encoded metrically as follows. We first declare the length

of an edge in the original graph to be $d_F(v_i, v_j)$ and then define $\hat{d}_F(v_i, v_j)$ to be the shortest path distance.

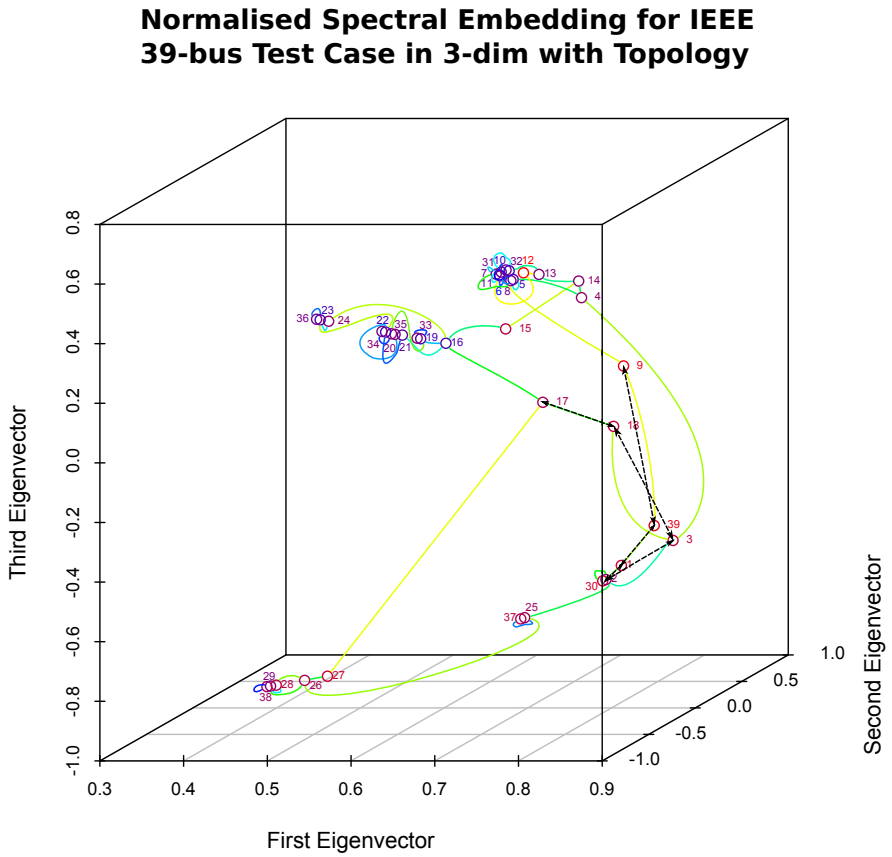

Figure 3-2: The colouring of the edges indicates the magnitude of direct current in the corresponding line, the colours lie on the spectrum between yellow and blue: yellow for low power flow, green for intermediate power flow and blue for high power flow.

Figure 3-3:

The metric is illustrated here between buses 17 and 9 (which are labeled in figure 3-3) given as the total length of all the dashed lines on a path between them.

Remark 3.3. *Notice here that in figure 3-1 and figure 3-3 we have only points on the right hand side of the sphere, with positive x-coordinates, this is because the trivial eigenvector for the normalised Laplacian is $(\sqrt{d_1}, \sqrt{d_2}, \ldots, \sqrt{d_n})^T$ thus the first coordinate is positive at every entry.*

Definition 3.4. ***(Diameter)*** *The diameter of a subset $S \subset V$ for a metric d is,*

$$diam(S, d) = \max_{u \in S \text{ and } v \in S} \{d(u, v)\}.$$

Forming Pseudo-Partitions: Algorithm Step 1 and Step 2

Step 1 Spherical Embedding: In this step k disjoint subsets will be formed $S_1, S_2, \ldots, S_k \subseteq V$, note here that this does not necessarily encompass the whole of V, thus is not necessarily a partition and will be referred to as a pseudo-partition.

This pseudo-partition will be selected in a stochastic manner. We will introduce the terminology of this random process here. We will denote any one selection of a partition as $P = S_1 \cup S_2 \cup \cdots \cup S_k \subseteq V$ and take $\mathcal{P}$ to be a distribution of any possible partition so that this assigns a probability measure for the occurrence of any partitions $P \in \mathcal{P}$. There will be just one constraint for the distribution $\mathcal{P}$ which is that $\forall P \in \mathcal{P}$, where $P = S_1 \cup S_2 \cup \cdots \cup S_k$ and $\forall i \in \{1, 2, \ldots, k\}$ we must have $\text{diam}(S_i, d_F) \leq \Delta$ (we will call such a $\mathcal{P}$ $\Delta-$bounded)[1]. As shown in Step 0 the distance measure could be taken as the d_F metric or the $\hat{d}_F$ metric.

Forming partitions: Algorithm Final Step

This is the final step were the random partition is formed, we take the k subsets of the pseudo partition $S_1 \cup S_2 \cup \cdots \cup S_k$ and relabel them so that the volumes of the subsets are in ascending order $vol(S_1) \leq vol(S_2) \leq \cdots \leq vol(S_k)$. The largest subset S_k is then replaces by $S'_k = V \backslash (S_1 \cup S_2 \cup \cdots \cup S_{k-1})$, the partition is now complete and given by $S_1, S_2, \ldots, S_{k-1}, S'_k$.

The Trivial Case

To understand the approach of the partitioning algorithm, it is easiest to start by looking at the system that is already partitioned into k clusters or islands. It is known that the number of connected components of a graph is equal to the number of trivial eigenvalues of the graph Laplacian. Say that for a graph G there is k trivial eigenvalues $\lambda_1 = \lambda_2 = \cdots = \lambda_k = 0$ the graph is thus composed of k connected components $\{S_1, \ldots, S_k\}$, each subset $S_i = (V_i, E_i)$ where V_i are vertices contained in the subset

[1] We will assume that for any distribution Δ will be taken as large as possible.

and E_i are edges contained in the subset. In the most straightforward way the first k eigenvectors will provide us with the internal structure of the graph, they will tell us what each connected component is and the degree of every one of its vertices. Each of the trivial eigenvectors will relate to one of the k connected components S_i by only having non-zero entries at coordinates where the corresponding vertex is in the component. If we consider the Rayleigh quotient type operator (as defined in (3.2)) of $\tilde{\mathbf{F}}_T$ where $\tilde{\mathbf{F}}_T$ is as in (3.3), we have

$$\mathcal{R}'(\tilde{\mathbf{F}}_T) = \frac{\sum_{(v_i,v_j)\in E} b(v_i,v_j) \left\| \tilde{F}_T(v_i) - \tilde{F}_T(v_j) \right\|^2}{\sum_{v_i\in V} \langle \tilde{F}_T(v_i), \tilde{F}_T(v_i)\rangle d_i}. \tag{3.5}$$

As any given vertex will only lies in one of the subsets, thus its corresponding coordinate will only be non-zero at one trivial eigenvector, a consequence of this is that the rows of $\tilde{\mathbf{F}}_T$ will only have one non-zero entry. The equation above can be broken into the addition of k components one for each one of the islands S_i (3.5) is given by,

$$= \frac{\sum_{l=1}^{k} \sum_{\forall(v_i,v_j)\in E_l} b(v_i,v_j) \left\| y_l(v_i) - y_l(v_j) \right\|^2}{\sum_{l=1}^{k} \sum_{v_i\in V} y_\ell^2(v_i) d_i}.$$

using $\frac{a+b}{c+d} \leq \max\{\frac{a}{c}, \frac{b}{d}\}$ and that fact that for all $l \in \{1, \dots k\}$

$$0 = \lambda_l = \mathcal{R}(y_l) = \frac{\sum_{\forall(v_i,v_j)\in E_l} b(v_i,v_j) \left\| y_l(v_i) - y_l(v_j) \right\|^2}{\sum_{v_i\in V} y_\ell^2(v_i) d_i}$$

tells us that $\mathcal{R}'(\tilde{\mathbf{F}}_T) = 0$.

Philosophy of the Algorithm

The general idea of the algorithm is that if we have a system that has k eigenvalues that are close to zero, then we will be able to take a partition into k islands using the information of the first k eigenvectors of the normalised Laplacian which will result in a small disturbance. In the same way that we will be able to find a partition that will result in a small disturbance, we can say that the system is a small perturbation from the *Trivial Case*. To minimise the disturbance resulting from a partition we will cut edges so that the new Rayleigh quotient type operator of $\mathbf{F}$ to be as close as possible to zeros as in the *Trivial Case*. The theorems will be based around making all the

Rayleigh quotients (one for each island) small.

The algorithm will take a partition into k subsets, when we consider this in the embedded space this means k regions of $\mathcal{S}^{k-1}$ are selected which in total captures all of the vertices and the vertices within each region form the subsets. This will be done in such a way that all regions capture a large portion of the $\ell^2(V,d)$ mass of $\tilde{\mathbf{F}}$ or $\ell^2(V)$ mass of $\mathbf{F}$, this will be done in a optimal way when the mass of each region $\sum_{\forall v \in S_i} \|F(v)\|^2$ are approximately the same across all regions.

Remark 3.5. *As well as capturing a large portion of the $\ell^2(\mathbb{R}^k)$ mass with each region, we can also make the* localisation *smooth by cutting edges that contribute to the numerator of (3.2) to the largest degree, remembering our objective to minimise the Rayleigh quotient type operators.*

3.2.2 Theoretical Framework

Random Partitions

Here we introduce the notion of splitting the sphere up into regions (and thus taking a partitions of V) in a stochastic way. From this approach we have a distribution of possible partitions $\mathcal{P}$ every partition P within the distribution has a certain probability of occurring. Distributions can have certain characteristics as we see in the following definition.

Definition 3.6. ***($\Delta-$bounded $\mathcal{P}$)*** *A distribution of partitions $\mathcal{P}$ is Δ bounded when $\forall P \in \mathcal{P}$ and for every subset $S \subset P$ we have diam$(S,d) \leq \Delta$.*

The two definitions 3.7 and 3.8 are different properties that a distribution of partitions $\mathcal{P}$ can have and the definition 3.9 is a property that an embedding F can have. For a partition $P \in \mathcal{P}$ and for $x \in V$ we will take $P(x)$ to be equal to the unique subset of partition P that contains the vertex x. In the following definitions $\mathbb{P}$ will mean the probability over $\mathcal{P}$ and $B_d(x,L)$ will be a ball of radius L centred at x (where the distance is measured with the metric d).

Definition 3.7. ***((Δ,α,δ)-padded)*** *A distribution $\mathcal{P}$ is (Δ,α,δ)-padded if it is $\Delta-$bounded, and for every $v \in V$, we have*

$$\mathbb{P}[B_d(v,\Delta/\alpha) \subseteq P(v)] \geq \delta.$$

To put this into words; if we select any vertex v and take a random partition of the vertices (which is from a distribution of (Δ, α, δ)-padded partitions) the probability that a ball centred at v and with radius Δ/α lies within the subsets that v has been partitioned into $(P(v))$ is greater or equal to δ.

Definition 3.8. ***((Δ, L)-Lipschitz)*** *A distribution $\mathcal{P}$ is (Δ, L)-Lipschitz if $\mathcal{P}$ is $\Delta-$bounded, and for every pair $x, y \in V$, we have*

$$\mathbb{P}[P(x) \neq P(y)] \leq L \cdot \frac{d(x,y)}{\Delta}.$$

To put this into words; if we select any pair of vertices x and y and take a random partition of the vertices (which is from a distribution of (Δ, L)-Lipschitz and $\Delta-$bounded partitions) the probability that vertices x and y will be partitioned into different subsets $(P(x) \neq P(y))$ is less than or equal to $L \cdot \frac{d(x,y)}{\Delta}$. This is intuitive for the point of view that a random partition will more likely separate vertices that are further apart.

Definition 3.8 can be loosely related to the classical definition a Lipschitz continuous function where for two metric spaces (X, d_X) and (Y, d_Y) a function $f : X \to Y$ can be said to be Lipschitz continuous, if for all x and $y \in X$ there exists a constant $K \geq 0$ such that

$$d_Y(f(x), f(y)) \leq K d_X(x, y).$$

If we take K in the classical definition to be equivalent to L/Δ in definition 3.8, $d_X(x, y)$ to be equivalent to $d(x, y)$ and $d_Y(f(x_1), f(x_2))$ to be equivalent to $\mathbb{P}[P(x) \neq P(y)]$. $d_Y(f(x), f(y))$ being equivalent to $\mathbb{P}[P(x) \neq P(y)]$ this where the abstraction of this notion of equivalence lies, that being said the probability of x and y lying in different subsets is lower the smaller $d(x, y)$ and higher the larger $d(x, y)$ is, so $\mathbb{P}[P(x) \neq P(y)]$ is not dissimilar to a metric from this point of view, as for $d_Y(f(x), f(y))$ this is also not dissimilar from the metric $d_X(x, y)$ given that the function f is Lipschitz continuous.

Definition 3.9. ***((Δ, η)-spreading)*** *An embedding $\boldsymbol{F}$ is $(\Delta, \eta)-$spreading (with respect to G) if for every $S \subseteq V$,*

$$diam(S, d_F) \leq \Delta \implies \sum_{v \in S} d(v)\|F(v)\|^2 \leq \eta \sum_{v \in V} d(v)\|F(v)\|^2.$$

We will only be using this property when the metric d_F determines the diameter.

The first two of the following lemmas 3.11 and 3.12 are relevant to any embedding of the vertices but the properties that can be inferred from these lemmas are not precise hence the $O(\cdot)$ notation.

Definition 3.10. *($O(\cdot)$ **notation**) Let f and g be functions of real variable. We say that*

$$f(k) = O(g(k)),$$

if and only if there exist $M \in \mathbb{R}^+$ such that

$$\lim_{k\to\infty} \frac{f(k)}{g(k)} = M.$$

Lemma 3.11. *For any embedding of V in $\mathbb{R}^k$, for every $\Delta > 0$ and $\delta > 0$, the embedding admits a $(\Delta, O(k/\delta), 1-\delta)-$padded random partition.*

Lemma 3.12. *For any embedding of V in $\mathbb{R}^k$, and for every $\Delta > 0$, the embedding admits a $(\Delta, O(\sqrt{k}))-$Lipschitz random partition.*

Theorem 2.3 in [27] is essentially the same as the above Lemma 3.11 but for $\delta = 1/2$ and $\alpha \geq 64k$, the proof of this can be changed in a very simple way to generalise for all δ, this will give the following lemma.

Lemma 3.13. *For any embedding of V in $\mathbb{R}^k$, for every $\Delta > 0$ and $\delta > 0$, the embedding admits a $(\Delta, \alpha, 1-\delta)-$padded random partition when $\alpha \geq 32k/\delta$.*

With this lemma we now have absolute padding properties as opposed to lemma 3.11.

An equivalent version of the following Lemma is given in Lemma 3.16 of [37].

Lemma 3.14. *For any embedding of V in $\mathbb{R}^k$, and for every $\Delta > 0$, the embedding admits a $(\Delta, L)-$Lipschitz random partition where $L \geq \sqrt{k}$.*

From this lemma we can now infer absolute Lipschitz properties as opposed to lemma 3.12.

The following lemma will be useful for us as we will be embedding with a set of orthonormal vectors.

Lemma 3.15. *For a set of k orthonormal functions $f_1, f_2, \ldots, f_k : V \to \mathbb{R}$ where $\forall i \in \{1, 2, \ldots, k\}$ $f_i \in \ell^2(V)$ let $F : V \to \mathbb{R}^k$ be the embedding which sends each $v_i \in V$ to the point $F(v_i) = (f_1(i), f_2(i), \ldots, f_k(i)) \in \mathbb{R}^k$. For any $\Delta > 0$, F is $\left(\Delta, \frac{1}{k(1-\Delta^2)}\right)-$ spreading for the graph G where the metric d_F is used.*

This is proven using the fact that $\forall x \in \mathcal{S}^{k-1}$,

$$\sum_{\forall v \in V} \langle x, F(v) \rangle = 1,$$

which intuitively conveys that the embedding is well spread through the space $\mathbb{R}^k$.

Geometric Considerations

The expectation isoparametric ratio of a subset formed through the application of the algorithm (section 3.2.1) can be improved by the added topological information that comes with the use of the $\hat{d}_F$ metric. Geometric considerations have to be taken into account to make these improvements; if we are able to exclude K_h (the complete graph over h vertices) as a graph minor (see appendix definition A.12) and the other consideration is the graph genus g.

Remark 3.16. ***Graph Genus*** *If graph G is embedded into the surface of a sphere, the genus of the graph will be the smallest possible number of handles that are attached to the surface of the sphere that will enable no two edges from crossing on the surface.*

Lemma 3.17. *If we use the $\hat{d}_F$ metric for our embedded set of vertices V, excluding K_h as a graph minor of G, then $\forall\ \Delta > 0$ and $\forall\ \delta > 0$, our embedding admits a $\Delta-$bounded distribution $\mathcal{P}$ which is $(\Delta, O(h^2/\delta), 1-\delta)-$padded and $(\Delta, O(h^2))-$ Lipschitz.*

Lemma 3.18. *If we use the $\hat{d}_F$ metric for our embedded set of vertices V, the graph G has genus g, then $\forall \Delta > 0$ and $\forall\ \delta > 0$, our embedding admits a $\Delta-$bounded distribution $\mathcal{P}$ is $(\Delta, O((\log g)/\delta), 1-\delta)-$padded, and $(\Delta, O(\log g))-$Lipschitz.*

3.2.3 Functions of Finite Support and Pseudo-Partitions

Finding a pseudo-partition $S_1, S_2, \ldots, S_k$ and finding a set of k functions which have disjoint supports in V $\psi_1, \psi_2, \ldots, \psi_k$ are similar, in that they both find k disjoint subsets in the latter case these subset finitely support k the functions.

In this section we will be pursuing the analysis of the partitioning algorithms which finds k subsets by observing the properties of k disjoint finitely supported functions on V.

Lemma 3.19. *For a function on the Hilbert space $\ell^2(V)$ given by $\psi : V \to \mathcal{H}$, there exists a subset $S \subseteq supp(\psi)$ with*

$$h_G(S) \leq \sqrt{2\mathcal{R}_G(\psi)}.$$

Our aim in this section is not to find a set of subsets $\{S_1, \ldots, S_h\}$ which can be thought of as our pseudo-partitions, but equivalently to finding a set of h disjointly supported functions $\psi_1, \psi_2, \ldots, \psi_h$ each of which is of the form $\psi_i : V \to \mathbb{R}^h$, and we will show that the Rayleigh quotient of each of these functions can have an upper bound. Thus when lemma 3.19 is applied this in turn will give a bound for Cheeger constant of each subset S_i.

In the next lemma we are able to show that when given a set of disjoint subsets of a graph G, which have a lower bound for the distance between individual subsets (definition 3.20) and a lower bound for the $\ell^2(V)$ mass of each $\mathbf{F}$ which it contains, then we are able to bound the Rayleigh quotient of a set functions whose finite supports are equal to the set of subsets of V.

Definition 3.20. ***(Distance between subsets)*** *The distance between two subsets $S_1,\ S_2 \subset V$ denoted*

$$d(S_1, S_2) = \min_{v \in S_1 \text{ and } u \in S_2} \{d(u, v)\}.$$

Lemma 3.21. *For an embedding of the vertices $F : V \to \mathbb{R}^h$ suppose that for some $\beta,\ \delta > 0$ and $r \in \mathbb{N}$, there exists r disjoint subsets $T_1, T_2, \ldots, T_r \subseteq V$ such that $\hat{d}_F(T_i, T_j) \geq \beta$ when $i \neq j$ and $\forall\ i \in \{1, 2, \ldots, r\}$, we have*

$$\sum_{v \in T_i} d(v)\|F(v)\|^2 \geq \delta \sum_{v \in V} d(v)\|F(v)\|^2. \tag{3.6}$$

Then there will exist a set of disjointly supported functions $\psi_1, \psi_2, \ldots, \psi_r : V \to \mathbb{R}$ such that for $i \in \{1, 2, ..., r\}$, we have

$$\mathcal{R}_G(\psi_i) \leq \frac{2}{\delta(r - i + 1)} \left(1 + \frac{\beta}{4}\right) \mathcal{R}'_G(\boldsymbol{F}). \tag{3.7}$$

Remark 3.22. *Note that the function will be labelled such that the Rayleigh quotients are as follows* $\mathcal{R}(\psi_1) \leq \mathcal{R}(\psi_2) \leq \cdots \leq \mathcal{R}(\psi_r)$.

What Lemma 3.21 says is that the larger the proportion of the $\ell^2(V)$ mass of $\mathbf{F}$ contained in every subset and the farther apart each of the subsets are from one another the better bounds we are able to put on the Rayleigh quotients of a functions that are supported by the particular subsets $T_1, T_2, \ldots, T_r \subseteq V$. This resonates with the philosophy of the algorithm if we form h function supports by only deleting edges that have a distance of a least β between them and only form supports with at lease δ of the ℓ^2 mass of F, this is respectively make the numerator of the Rayleigh quotient small and the denomination large. Once we have shown that the Rayleigh quotient of a function is small we can then use lemma 3.19 to bound the Cheeger constant, this is what this analysis is working towards.

Applications of Random Partitioning

Remember that eventually we will aim to use Lemma 3.21 the conditions of which, a set of subset $T_1, T_2, \ldots, T_r \subseteq V$ will be well separated and each subset contains a large fraction of the $\ell^2(V)$ mass of F.

The following Lemma is equivalent to Lemma 3.5 in [38].

Lemma 3.23. *For a given* r *and* $k \in \mathbb{N}$ *where* $k/2 \leq r \leq k$ *and the embedding of the vertices* $F : V \to \mathbb{R}^h$ *is* $(\Delta, \frac{1}{k} + \frac{k-r+1}{8rk})-$*spreading for some* $\Delta > 0$. *If a random partition* $P \in \mathcal{P}$ *has the following two properties*

1. *For every* $S \in P$, $diam(S, \hat{d}_F) \leq \Delta$, *and*
2. *For every* $v \in V$, $\mathbb{P}[B_{\hat{d}_F}(v, \Delta/\alpha) \subseteq P(v)] \geq 1 - \frac{k-r+1}{4r}$,

then there exists r *disjoint subsets* $T_1, T_2, \ldots, T_r \subseteq V$ *and when* $i \neq j$, *we have* $\hat{d}_F(T_i, T_j) \geq 2\Delta/\alpha$, *and for all* $i \in \{1, 2, \ldots, r\}$ *this holds*

$$\sum_{v \in T_i} \|F(v)\|^2 \geq \frac{1}{2k} \sum_{v \in V} \|F(v)\|^2. \tag{3.8}$$

The two lemmas above 3.21 and 3.23 then yield the following Corollary because with a suitable choice of δ and β in 3.23, we can apply Lemma 3.21. The analysis

differs here from what James R. Lee did in [38], therein an estimate of the order of $\mathcal{R}_G(\psi_i)$ is made, whereas we make an absolute estimate.

Corollary 3.24. *For any $k \in \mathbb{N}$ and $\delta \in (0,1)$, suppose the embedding of the vertices $F : V \to \mathbb{R}^k$ is a $(\Delta, \frac{1}{k} + \frac{k-r+1}{8rk})-$spreading for some $\Delta > 0$, and there is a distribution of random partitions $\mathcal{P}$ with the properties that if $P \in \mathcal{P}$,*

1. *For all $S \in P$, $diam(S, d_F) \leq \Delta$ and*
2. *And for all $v \in V$, $\mathbb{P}[B_{\hat{d}_F}(v, \Delta/\alpha) \subseteq P(v)] \geq 1 - \frac{k-r+1}{4r}$.*

Then there are at least $r \geq \lceil (1-\delta)k \rceil$ disjointly supported functions $\psi_1, \psi_2, \ldots, \psi_r : V \to \mathbb{R}$ such that for all $i \in \{1, \ldots, r\}$

$$\mathcal{R}_G(\psi_i) \leq \frac{2}{\delta(r-i+1)} \left(1 + \frac{2\alpha}{\Delta}\right)^2 \mathcal{R}'_G(\boldsymbol{F}).$$

Proof. Applying lemma 3.23 we have that there exist $r = \lceil (1-\delta/2)k \rceil$ disjoint subsets $T_1, T_2, \ldots, T_r \subseteq V$ and when $i \neq j$, we have $\hat{d}_F(T_i, T_j) \geq 2\Delta/\alpha$, and for all $i \in \{1, 2, \ldots, k\}$ this holds

$$\sum_{v \in T_i} \|F(v)\|^2 \geq \frac{1}{2k} \sum_{v \in V} \|F(v)\|^2.$$

Now we have the conditions to apply lemma 3.21 where $\delta = \frac{1}{2k}$, $\beta = \frac{2\Delta}{\alpha}$ and $r = \lceil (1-\delta)k \rceil$. This gives us,

$$\mathcal{R}_G(\psi_i) \leq \frac{2}{\delta(r-i+1)} \left(1 + \frac{2\alpha}{\Delta}\right)^2 \mathcal{R}'_G(\mathbf{F}).$$

□

As a result of this analysis, we have now is a Rayleigh quotients for r functions whose support is given by a set of disjoint subsets who have two specific conditions, these conditions happen to resemble padded properties for a distribution $\mathcal{P}$.

Higher Order Cheeger Inequalities

The following theorem uses similar techniques to theorem 3.7 in [38] but here we give more precise bounds here are more precise and we are able to have a definite bound in (3.9) as opposed to in with $O(\cdot)$ (where k is considered large).

Theorem 3.25. *For a given $\delta \in (0,1)$, and a weighted graph $G = (V, E, w)$, there exists $r \geq \lceil (1-\delta)k \rceil$ many disjointly supported real-valued functions $\psi_1, \psi_2, \ldots, \psi_r$ on the set V such that*

$$\mathcal{R}_G(\psi_i) \leq \frac{2}{\delta(r-i+1)} \left(1 + \frac{8rk(k+7r+1)^{1/2}}{(k-r+1)^{3/2}}\right)^2 \mathcal{R}'_G(\boldsymbol{F}). \tag{3.9}$$

If G excludes K_h as a minor (refer to Appendix A.12), then following could be an improved bound

$$\mathcal{R}_G(\psi_i) \leq \frac{2}{\delta(r-i+1)} \left(1 + O\left(\frac{8rh^2(k+7r+1)^{1/2}}{(k-r+1)^{3/2}}\right)\right)^2 \mathcal{R}'_G(\boldsymbol{F}) \tag{3.10}$$

and if G has genus $g \geq 1$ (refer to Appendix 3.16), then we have

$$\mathcal{R}_G(\psi_i) \leq \frac{2}{\delta(r-i+1)} \left(1 + O\left(\frac{8r\log(g+1)(k+7r+1)^{1/2}}{(k-r+1)^{3/2}}\right)\right)^2 \mathcal{R}'_G(\boldsymbol{F}). \tag{3.11}$$

Proof. Here we use the fact that our particular construction of embedding $F : V \to \mathbb{R}^k$, uses a set of orthonormal eigenvectors, thus we can use lemma 3.15 to say that the embedding is $\left(\Delta, \frac{1}{k(1-\Delta^2)}\right)-$ spreading. Recalling that $\frac{1}{k(1-\Delta^2)}$ is in fact an upper bound (from definition 3.9) we will be able to claim F to be a $(\Delta, \frac{1}{k} + \frac{k-r+1}{8rk})-$ spreading when

$$\Delta \leq \sqrt{\frac{k-r+1}{k+7r+1}},$$

which ensures that $\frac{1}{k(1-\Delta^2)} \leq \frac{1}{k} + \frac{k-r+1}{8rk}$.

Now we will infer some padded properties using Lemma 3.13 where for any embedding in $\mathbb{R}^k$, $\Delta > 0$ and $\delta'' > 0$ we have an $(\Delta, 32k/\delta'', 1-\delta'')-$ padded embedding. We will set $\delta'' = 8\frac{k-r+1}{r}$, and we can now apply corollary 3.24 with $\alpha = 32k/\delta'' = \frac{4rk}{k-r+1}$ noting that if property 2) holds for d_F this implies that property 2) will hold for $\hat{d}_F$, as a ball formed using the $\hat{d}_F$ will always be a subset of a ball with the same radius formed using the d_F metric,

$$\mathcal{R}_G(\psi_i) \leq \frac{2}{\delta(r-i+1)} \left(1 + \frac{8rk(k+7r+1)^{1/2}}{(k-r+1)^{3/2}}\right)^2 \mathcal{R}'_G(\mathbf{F}).$$

For (3.10) and (3.11) we apply Lemma 3.17 and Lemma 3.18 respectively if we

are able to establish the geometric considerations, these theorems can be used to infer spreading properties instead of Lemma 3.11. Lemma 3.17 and 3.18 give $\alpha = O(h^2/\delta'')$ and $\alpha = O(\log(g+1)/\delta'')$ respectively then when we apply corollary 3.24 we have,

$$\mathcal{R}_G(\psi_i) \leq \frac{2}{\delta(r-i+1)}\left(1+O\left(\frac{8rh^2(k+7r+1)^{1/2}}{(k-r+1)^{3/2}}\right)\right)^2 \mathcal{R}'_G(\mathbf{F})$$

and

$$\mathcal{R}_G(\psi_i) \leq \frac{2}{\delta(r-i+1)}\left(1+O\left(\frac{8r\log(g+1)(k+7r+1)^{1/2}}{(k-r+1)^{3/2}}\right)\right)^2 \mathcal{R}'_G(\mathbf{F}).$$

□

Remark 3.26. *Note that by restricting to the leading terms, the inequalities of (3.10) and (3.11) are simplified to be,*

$$\mathcal{R}_G(\psi_i) \leq O\left(\frac{h^4}{\delta^4}\lambda_k\right)$$

and

$$\mathcal{R}_G(\psi_i) \leq O\left(\frac{\log(g+1)}{\delta^4}\lambda_k\right)$$

respectively, which recovers the estimates given in [38]

We have the absolute estimate (3.9) in theorem 3.25 because we use Lemma 3.13 to infer absolute spreading properties as opposed to using Lemma 3.11 with $O(\cdot)$ spreading properties. The estimates above have the same information as (3.10) and (3.11), but we held onto the precision to show that as with (3.9) if we are able to infer absolute padded properties (with alternative theorems) then we will obtain similar absolute estimates for G when K_h is excluded as a minor and G of genus $g \geq 1$.

We believe that these alternative theorems exist but didn't have time to pursue this here. Were we to pursue this there would be three streams of analysis leading up to an absolute estimate for the higher order Cheeger constant (in Theorem 3.27): one for general graphs, one for graphs where K_h is excluded as a minor and ones for graphs of genus $g \geq 1$. Here however we just pursue a theorem for the estimates of higher order Cheeger constants for general graphs. There is a constructive algorithms which gives the estimates of the higher order Cheeger constants for graphs where K_h is excluded as

a minor and for graphs of genus $g \geq 1$ (this is where the $\hat{d}_F$ metric is used). We will collect experimental results for this algorithm.

Theorem 3.27. ***(Non-expanding k-partition)*** *For a weighted graph $G = (V, E, w)$, there exists a $k-$way partition $P = \{S_1, S_2, \ldots, S_k\}$ where $V = S_1 \cup S_2 \cup \cdots \cup S_k$ such that*

$$h^{(k)}(P) \leq 2k^{1/2}(k-1)(\mathcal{R}'_G(\boldsymbol{F}))^{1/2} \left(\sum_{i=1}^{k-1} (k-i+1)^{-1/2} \right) (1 + 8k^2(8k+1)^{1/2}). \quad (3.12)$$

Proof. Applying theorem 3.25 with $\delta < \frac{1}{k}$ we will have $r = k$ and thus have k functions $\psi_1, \psi_2, \ldots, \psi_k$ of the form $\psi : V \to \mathbb{R}$ whose supports are disjoint and for which equation (3.9) holds where the labelling is such that $\mathcal{R}(\psi_1) \geq \mathcal{R}(\psi_2) \geq \cdots \geq \mathcal{R}(\psi_k)$. We now apply lemma 3.19 we can convert these bounds on the Rayleigh quotients of a function ψ, to bounds on the Cheeger constant of subset contained in the support of ψ. We have that there exists k subsets $S_1, S_2, \ldots, S_k$ and $\forall i \in \{1, 2, \ldots, k\}$ $S_i \subseteq \text{supp}(\psi_i)$. So there exists k disjoint subsets $S_1, S_2, \ldots S_k$ where $\forall i \in \{1, 2, \ldots, k\}$ and from equation (3.9) we have,

$$h_G(S_i) < \left(\frac{4k}{(k-i+1)} \mathcal{R}'_G(\mathbf{F}) \right)^{1/2} \left(1 + 8k^2(8k+1)^{1/2} \right).$$

Notice here that there is a strict inequality unlike Theorem 3.25, this is still essentially an application of that theorem but this strict inequality results from the strict inequality in the condition $\delta < \frac{1}{k}$.

Note that $S_1, S_2, \ldots, S_k$ is not necessarily a partition so there is one more step required in this proof. If all the subsets are relabelled so that the volumes of the k sets are in ascending order $\text{w}(S_1) \leq \text{w}(S_2) \leq \cdots \leq \text{w}(S_k)$, we will take the largest set and amend so that it is equal to an even larger set $S'_k = V \backslash (S_1 \cup S_2 \cup \cdots \cup S_{k-1})$, this way

$S_1, S_2, \ldots, S_{k-1}, S'_k$ forms a partition, and

$$\begin{aligned} h_G(S'_k) =& \frac{w(E(S'_k, \overline{S'_k}))}{\min(w(S'_k), w(\overline{S'_k}))} \\ \leq& \sum_{i=1}^{k-1} \frac{w(E(S_i, \overline{S_i}))}{\min(w(S'_k), w(\overline{S'_k}))} \\ \leq& \sum_{i=1}^{k-1} h_G(S_i) \\ <& 2k^{1/2}(k-1)\mathcal{R}_G^{1/2}(\mathbf{F}) \left(\sum_{i=1}^{k-1} (k-i+1)^{-1/2} \right) (1 + 8k^2(8k+1)^{1/2}). \end{aligned}$$

Which completes the proof for (3.12).

□

Remark 3.28. *The above results can be seen as a constructive procedure for carrying out Step 1. Indeed, for any partition $P \in \mathcal{P}$ which is $\sqrt{\frac{1}{8k+1}}-$bounded, we can randomly select k subsets from any $P \in \mathcal{P}$ to be our pseudo partition $S_1, S_2, \ldots, S_k$ this gives us a way of constructing Step 1. And then after carrying out the final step to give P the expectation of $h^{(k)}(P)$ will satisfy the estimate for $h^{(k)}(P)$ in (3.12).*

3.3 Theoretical Framework of Higher Order Spectral Partitioning with Dimension Reduction

As with the last section we will first go through an algorithm which once the theoretical framework is introduced, will lead to a constructive proof of the expected quality of resulting partitions.

Step 0 is the same for the dimension reduction algorithm as it is for the higher order spectral partitioning algorithm, $F : V \to \mathbb{R}^{\tilde{k}}$ is formed from the first $\tilde{k}$ eigenvalues of the normalised Laplacian. As well as inputing $\tilde{k}$ into this algorithm we also input any $\delta \in (0, 1]$.

Dimension reduction: Algorithm Step 1

In this step we take the configuration of the V given by the embedding $\mathbf{F} \in \mathbb{R}^{n \times \tilde{k}}$ and perform a random projection from $\mathbb{R}^{\tilde{k}}$ into $\mathbb{R}^h$ (this is done with a mapping $\Gamma_{\tilde{k},h}$). The

random projection is a map $\Gamma_{\tilde{k},h} : \mathbb{R}^{\tilde{k}} \to \mathbb{R}^h$ which is defined by generating $\tilde{k} \cdot h$ random numbers from the normal distribution with mean 0 and standard deviation 1 ($N(0,1)$). The numbers generated from the normal distribution will be used to construct h vector $g_1, g_2, \ldots, g_h \in \mathbb{R}^{\tilde{k}}$ so all entries of these vectors are randomly generated numbers. Then for $x \in \mathbb{R}^{\tilde{k}}$,

$$\Gamma_{\tilde{k},h}(x) = h^{-1/2}(\langle g_1, x\rangle, \langle g_2, x\rangle, \ldots, \langle g_h, x\rangle)^T.$$

$F^* : V \to \mathbb{R}^h$ where $F^* = \Gamma_{\tilde{k},h} \circ F$.

Initial Partition: Algorithm Step 2

We now perform a partition of V by taking subsets S_i's in the space $\mathbb{R}^h$ which a $\text{diam}(S_i, d_{F^*}) \leq \Delta$, where we define d_{F^*} in the same way that d_F was defined in (3.4). This is done until we have $S_1 \cup S_2 \cup \cdots \cup S_m = V$.

Forming Partition of r' Subsets: Algorithm Step 3

We take a measure of the m subsets $\mathcal{E}(S_i) = \sum_{v \in S_i} d(v)\|F^*(v)\|^2$. We then proceed by taking disjoint unions of these m sets to form T_i's which are such that

$$\frac{\mathcal{E}(V)}{2\tilde{k}} \leq \mathcal{E}(T_i) \leq \frac{\mathcal{E}(V)}{\tilde{k}}\left(1 + \frac{\delta}{4}\right)$$

the theory tells us that there exists r' such sets where $r' \geq \lceil (1-\delta)\tilde{k} \rceil$.

Multi-way Partitioning: Algorithm Step 4

For each of the r' subsets T_i we will choose a value τ is chosen uniformly from the interval $(0, M)$ where $M = \max\{\|F^*(v)\|^2 : v \in V\}$, the set

$$\hat{T}_i = \{v \in S_i : \|F^*(v)\| \geq \tau\}.$$

Out of the r' sets $\hat{T}_1, \hat{T}_2, \ldots, \hat{T}_{r'}$ the r with the smallest boundaries are chosen where $r = \lceil (1-\delta)\tilde{k} \rceil$. This gives us our pseudo-partition.

The **final step** is the same for this algorithm with dimension reduction as without dimension reduction.

Remark 3.29. *Note here for the algorithm to work, h and Δ must satisfy constraints.*

Dimension Reduction

There is a way to improve some of these bounds further. Notice that in (3.9), (3.10) and (3.11) there is a factor on the right hand side that depends on k (the number of dimensions that we embed V into) if we could reduce k this factor could be reduced and the bound improved.

This has to be done in a way such that, all of the analysis required to obtain the results (3.9) is unaffected. To do this the Rayleigh quotient must be the same and the spreading properties must be the same.

The following properties hold for such an embedding $\Gamma_{\tilde{k},h} : \mathbb{R}^{\tilde{k}} \to \mathbb{R}^h$ for all $x \in \mathbb{R}^{\tilde{k}}$, ($\mathbb{E}$ means the expectation here and the norms are ℓ^2 norms in h and $\tilde{k}$ dimensions)

$$\mathbb{E}\left(\|\Gamma_{\tilde{k},h}(x)\|^2\right) = \|x\|^2, \tag{3.13}$$

the derivation of this can be seen in Lemma A.13 the appendix.

For all $\delta \in (0, \frac{1}{2}]$,

$$\mathbb{P}\left[\|\Gamma_{k,h}(x)\|^2 \notin [(1-\delta)\|x\|^2, (1+\delta)\|x\|^2]\right] \leq 2e^{-\lambda h/12}, \tag{3.14}$$

and for every $\lambda \leq 2$. The derivation of this bound can be see in

$$\mathbb{P}\left[\|\Gamma_{k,h}(x)\|^2 \geq \lambda\|x\|^2\right] \leq e^{-\lambda h/12}. \tag{3.15}$$

The derivation of these results can be seen in [40].

We are able now to construct a relation between the original embedding and its spreading properties, to the dimension reduction embedding and its spreading properties. Also we are able to bound the Rayleigh quotient of the dimension reduced embedding by the Rayleigh quotient of the original embedding.

The following Lemma is similar to Lemma 4.3 in [38].

Lemma 3.30. *For a weighted graph $G = (V, E, w)$. For any $\tilde{k} \in \mathbb{N}$, $\Delta \in [0, 1]$ and $\eta \geq 1/\tilde{k}$, we have the following. For an embedding $F : V \to \mathbb{R}^{\tilde{k}}$ which is $(\Delta, \eta)-$spreading. Then for some value h such that for $\delta = \Delta/16$ we have,*

$$2\exp(-\delta^2 h/12) \leq \delta k^{-3}/128 \tag{3.16}$$

then with a probability of at least $1/2$ *that the map* $\Gamma_{\tilde{k},h}$ *will satisfy the following two conditions:*

1. $\mathcal{R}_G(\Gamma_{\tilde{k},h} \circ F) \leq 8 \cdot \mathcal{R}_G(F)$, *and*

2. $\Gamma_{\tilde{k},h} \circ F$ *is* $(\Delta/4, (1+\Delta)\eta)-$*spreading with respect to* G.

The proof of this is very long and it is made up of numerous stages, the analysis therein is not complex, it is a series of applications of Markov inequalities and use of properties (3.13) - (3.15).

In theorem 3.25 we initiated our analysis of our first algorithm (in section 3.2) by getting estimates for $\mathcal{R}_G(\psi_i)$, we were able to do this by inferring spreading properties for the embedding F. Lemma 3.30 can now be used to inference spreading properties for a dimension reduced space, so our analysis can now proceed in a similar way that theorem 3.25 proceeded for our first algorithm (in section 3.2). This can result in a bettter estimate than (3.9).

The following theorem uses similar techniques to theorem 4.6 in [38] but here we give an absolute estimate.

Theorem 3.31. *For a weighted graph* $G = (V, E)$ *and for any* $\delta > 0$ *the following holds, that for all* $\tilde{k} \in \mathbb{N}$, *there exists* $\psi_1, \psi_2, \ldots, \psi_r : V \to \mathbb{R}$ *disjointly supported functions, where* $r \geq \lceil (1 - \delta/2)\tilde{k} \rceil$, *these function are such that*

$$\mathcal{R}_G(\psi_i) \leq \frac{2}{\delta(r-i+1)} \left(1 + \frac{256rh}{\Delta(r,\tilde{k})(\tilde{k}-r+1)}\right)^2 \mathcal{R}_G(F). \tag{3.17}$$

Where $\Delta(r,\tilde{k}) = -2 + \sqrt{4 + \frac{\tilde{k}+1-r}{\tilde{k}+7r+1}}$ *and* h *must satisfy,*

$$h \geq \frac{-192}{\Delta(\tilde{k},r)}(10\log(2) + \log(\Delta(\tilde{k},r)) - 3\log(k)).$$

Proof. We form the embedding F in accordance with Step 0, thus take $x_1, x_2, \ldots, x_{\tilde{k}} : V \to \mathbb{R}$ be an $\ell^2(V,d)-$orthonormal system of eigenfunctions corresponding to the first $\tilde{k}$ eigenvalues of $\mathscr{L}_G$, and define $F : V \to \mathbb{R}^{\tilde{k}}$ by $F(v_i) = (x_1(v_i), x_2(v_i), \ldots, x_{\tilde{k}}(v_i))$. Using Lemma 3.15 to we have that this embedding F is $\left(4\Delta, \frac{1}{\tilde{k}(1-16\Delta^2)}\right) -$ spreading.

If we now apply lemma 3.30 to this embedding we have an embedding $\Gamma_{\tilde{k},h}(F) :$

$V \to \mathbb{R}^h$ but to do this we need to satisfy condition (3.16) which means,

$$h \geq \frac{-192}{\Delta(\tilde{k}, r)}(10\log(2) + \log(\Delta(\tilde{k}, r)) - 3\log(\tilde{k})) \tag{3.18}$$

and for these spreading properties to make sense we must have $(1-16\Delta^2) > 0 \implies \Delta < 1/4$. This gives us with a probability of at lease $1/2$ a $(\Delta, (\tilde{k}(1-16\Delta^2))^{-1}(1+4\Delta))-$ spreading embedding and setting Δ to ensure that $(\tilde{k}(1-16\Delta^2))^{-1}(1+4\Delta) \leq \frac{1}{\tilde{k}} + \frac{\tilde{k}-r+1}{8\tilde{k}r}$ gives the following bound for Δ,

$$\Delta \leq -2 + \sqrt{4 + \frac{\tilde{k}+1-r}{\tilde{k}+7r+1}}. \tag{3.19}$$

Substituting (3.19) into the previous condition for h (3.18) we can derive an explicit bound for h, (this will be checked in simulations)

$$\Delta(r, \tilde{k}) = -2 + \sqrt{4 + \frac{\tilde{k}+1-r}{\tilde{k}+7r+1}}.$$

We can infer padding properties from Lemma 3.13 to the embedding in $\mathbb{R}^h$ which are that for any $\delta' > 0$, this is a $(\Delta, 32h/\delta', 1-\delta')-$ padded embeddding.

Setting $\delta' = \frac{\tilde{k}-r+1}{4r}$ will give $\alpha = 128\frac{rh}{\tilde{k}-r+1}$, these padding properties imply that property 2) holds in 3.24. We also have the spreading properties necessary for applying corollary 3.24.

Applying this corollary we have a set of functions $\psi_1, \psi_2, \ldots, \psi_r$ with disjoint support where,

$$\mathcal{R}_G(\psi_i) \leq \frac{2}{\delta(r-i+1)}\left(1 + \frac{256rh}{\Delta(r,\tilde{k})(\tilde{k}-r+1)}\right)^2 \mathcal{R}_G(F).$$

□

Remark 3.32. *Theorem 3.31 is in fact an aside from the implementation of the algorithm. What we have in this theorem is similar to (3.9) in lemma 3.25 and this could be taken farther as previously in lemma 3.25 which lead to theorem 3.27. In this way this could lead to an algorithm the same as in section 3.2.1 only with some additional dimension reduction step. However this is not pursued here.*

The following lemma is similar to Lemma 4.7 in [38] but give an absolute estimate. Here $M = \max\{\|F(v)\|^2 : v \in V\}$ and τ is chosen uniformly in the interval $(0, M)$ we have for a subset $S \subseteq V$,

$$\hat{S} = \{v \in S : \|F(v)\|^2 \geq \tau\}. \tag{3.20}$$

Note that $w(\cdot)$ is the sum of the weights of edges if its argument is a set of edges.

Lemma 3.33. *For all $\Delta > 0$ there exists a partition $S_1, S_2, \ldots, S_m$ of a graph G where for all $i \in \{1, 2, \ldots, m\}$ we have diam$(S, d_F) \leq \Delta$, and*

$$\frac{\mathbb{E}\left[w(E(\hat{S}_1, \overline{\hat{S}_1})) + w(E(\hat{S}_2, \overline{\hat{S}_2})) + \cdots + w(E(\hat{S}_m, \overline{\hat{S}_m}))\right]}{\mathbb{E}\left[w(\hat{S}_1) + \cdots + w(\hat{S}_m)\right]} \leq \left(\frac{2\sqrt{h}}{\Delta} + 1\right)\sqrt{\mathcal{R}_G(F)}.$$

Proof. In this proof we will consider $M = 1$ (this can be achieved by transforming $\|F(v)\|$ by dividing through by a factor of $\max\{\|F(v)\|^2 : v \in V\}$), this means that the probability of a vertex $v \in S$ being in $\hat{S}$ (for (3.20)) is $\|F(v)\|^2$. Using Theorem 3.14 we can infer that the embedding has Lipschitz properties for a $\Delta-$bounded random partition $P \in \mathcal{P}$ satisfying, for every $u, v \in V$,

$$\mathbb{P}(P(u) \neq P(v)) \leq \Big(\frac{\sqrt{h}}{\Delta} \cdot d_F(u, v)\Big). \tag{3.21}$$

Let $P = S_1 \cup S_2 \cup \cdots \cup S_m$.

We will have that, $\mathbb{E}[w(\hat{S}_i)] = \sum_{v \in S_i} w(v)\|F(v)\|^2$ thus,

$$\mathbb{E}\left[w(\hat{S}_1) + \cdots + w(\hat{S}_m)\right] = \sum_{v \in V} w(v)\|F(v)\|^2. \tag{3.22}$$

We will now measure the expectation that an edge $\{u, v\} \in E$ with $\|F(u)\|^2 \leq \|F(v)\|^2$ will lie on the boundary of this multi-way partition (we have indicated different uniform

selections of τ for subset S by a subscript of a vertex in S e.g. τ_u),

$$\begin{aligned}
&\mathbb{P}\Big[\{u,v\} \in E(\hat{S}_1, \overline{\hat{S}_1}) \cup \cdots \cup E(\hat{S}_m, \overline{\hat{S}_m})\Big] \\
&\qquad \leq \mathbb{P}\Big[P(u) \neq P(v)\Big] \cdot \mathbb{P}\Big[\|F(u)\|^2 \geq \tau_u \text{ or } \|F(v)\|^2 \geq \tau_v \big| P(u) \neq P(v)\Big] \\
&\qquad\qquad + \mathbb{P}\Big[\tau \in [\|F(u)\|^2, \|F(v)\|^2] \big| \mathcal{P}(u) = \mathcal{P}(v)\Big] \cdot (1 - \mathbb{P}[P(u) \neq P(v)]) \\
&\qquad \leq \Big(\frac{\sqrt{h}}{\Delta} \cdot d_F(u,v)\Big)\Big(\|F(u)\|^2 + \|F(v)\|^2 - \|F(v)\|^2 + \|F(u)\|^2\Big) + \|F(v)\|^2 - \|F(u)\| \qquad (3.23) \\
&\qquad = \Big(\|F(u)\| + \|F(v)\|\Big)\left(\frac{\sqrt{h}}{\Delta} \cdot d_F(u,v) \frac{2\|F(u)\|^2}{\|F(u)\| + \|F(v)\|} + \|F(v)\| - \|F(u)\|\right) \\
&\qquad \leq (\|F(u)\| + \|F(v)\|)\left(\frac{\sqrt{h}}{\Delta}\|F(u)\| \cdot d_F(u,v) + \|F(v)\| - \|F(u)\|\right) \\
&\qquad \leq (\|F(u)\| + \|F(v)\|)\left(\frac{2\sqrt{h}}{\Delta}\|F(u) - F(v)\| + \|F(v)\| - \|F(u)\|\right) \qquad (3.24) \\
&\qquad \leq (\|F(u)\| + \|F(v)\|)\left(\frac{2\sqrt{h}}{\Delta} + 1\right)\|F(u) - F(v)\|.
\end{aligned}$$

Here we use (3.21) in (3.23) and lemma A.10 from the appendix, which gives that for any $u, v \in V$, we have $\|F(u)\| d_F(u,v) \leq 2\|F(u) - F(v)\|$ in (3.24).

So using the Cauchy-Schwartz inequality we are able to perform the following,

$$\begin{aligned}
&\mathbb{E}\Big[E(\hat{S}_1, \overline{\hat{S}_1}) \cup \cdots \cup E(\hat{S}_m, \overline{\hat{S}_m})\Big] \\
&\qquad \leq \sum_{u \sim v} w(u,v)\left(\big(\|F(u)\| + \|F(v)\|\big) \cdot \left(\frac{2\sqrt{h}}{\Delta} + 1\right)\|F(u) - F(v)\|\right) \\
&\qquad \leq \left(\frac{2\sqrt{h}}{\Delta} + 1\right)\sqrt{\sum_{u \sim v} w(u,v)(\|F(u)\| + \|F(v)\|)^2}\sqrt{\sum_{u \sim v} w(u,v)\|F(u) - F(v)\|^2} \\
&\qquad \leq \left(\frac{2\sqrt{h}}{\Delta} + 1\right)\sqrt{\sum_{v \in V} w(v)(\|F(v)\|)^2}\sqrt{\sum_{u \sim v} w(u,v)\|F(u) - F(v)\|^2}.
\end{aligned}$$

Combining this with (3.22) we have,

$$\frac{\mathbb{E}_{\mathcal{P}}\mathbb{E}\left[w((\hat{S}_1,\overline{\hat{S}_1}))\cup\cdots\cup w(E(\hat{S}_m,\overline{\hat{S}_m}))\right]}{\mathbb{E}\left[w((\hat{S}_1))\cup\cdots\cup w(E(\hat{S}_m))\right]}\leq\frac{\left(\frac{2\sqrt{h}}{\Delta}+1\right)\sqrt{\sum_{u\sim v}w(u,v)\|F(u)-F(v)\|^2}}{\sqrt{\sum_{v\in V}w(v)(\|F(v)\|)^2}},$$

where we use $\mathbb{E}_{\mathcal{P}}$ to denote expectation over the random choice of $P\in\mathcal{P}$.

□

The following lemma is proven using lemma 3.12 to infer a Lipschitz property of the embedding $F:V\to\mathbb{R}^h$.

Lemma 3.34. *Let $G=(V,E,w)$ be a weighted graph, $\tilde{k}\in\mathbb{N}$ and $\delta\in(0,1)$. If we have embedding $F^*:V\to\mathbb{R}^h$ is $(\Delta,\frac{1}{\tilde{k}}+\frac{\delta}{4\tilde{k}})-$ spreading, then there exists $r=\lceil(1-\delta)\tilde{k}\rceil$ disjoint sets which are formed through **step 3** of the algorithm $T_1,T_2,\ldots,T_r$,*

$$h_G(T_i)\leq\frac{2}{(1-\delta)}\cdot\left(\frac{2\sqrt{h}}{\Delta}+1\right)\cdot\sqrt{\mathcal{R}_G(F)}.$$

Proof. First of all the partition guaranteed by lemma 3.33 for an embedding $F^*:V\to\mathbb{R}^h$ is $S_1,S_2,\ldots,S_m$ where for all $i\in\{1,2,\ldots,m\}$, $\operatorname{diam}(S_i,d_{F^*})\leq\Delta$. Say that we have $\mathcal{E}:=\sum_{v\in V}w(v)\|F(v)\|^2$. We now carry out **step 3** of the algorithm to form the sets $T_1,T_2,\ldots T_{r'}$ which are disjoint unions of S_i's these must also be formed in such a way that,

$$\frac{\mathcal{E}(V)}{2\tilde{k}}\leq\mathcal{E}(T_i)\leq\frac{\mathcal{E}(V)}{\tilde{k}}\left(1+\frac{\delta}{4}\right).\tag{3.25}$$

Taking $r=\lceil(1-\delta)\tilde{k}\rceil$ from the r' we will take the first r with the smallest boundaries. If we relabel so that $w(E(\hat{T}_1,\overline{\hat{T}_1})\leq w(E(\hat{T}_2,\overline{\hat{T}_2})\leq\cdots\leq w(E(\hat{T}_{r'},\overline{\hat{T}_{r'}})$ and take the first $w(E(\hat{T}_i,\overline{\hat{T}_i}))$ for $i=\{1,2,\ldots,r\}$,

$$\begin{aligned}\mathbb{E}\Big[w(E(\hat{T}_i,\overline{\hat{T}_i}))\Big]\leq&\frac{1}{(1-\delta)\tilde{k}}\mathbb{E}\Big[\sum_{j=1}^{m}w(E(\hat{S}_j,\overline{\hat{S}_j}))\Big]&(3.26)\\ \leq&\frac{1}{(1-\delta)\tilde{k}}\cdot\left(\frac{2\sqrt{h}}{\Delta}+1\right)\cdot\sqrt{\mathcal{R}_G(F)}\cdot\mathbb{E}\Big[\sum_{j=1}^{m}w(\hat{S}_j)\Big]&(3.27)\\ =&\frac{1}{(1-\delta)\tilde{k}}\cdot\left(\frac{2\sqrt{h}}{\Delta}+1\right)\cdot\sqrt{\mathcal{R}_G(F)}\cdot\mathcal{E}.&(3.28)\end{aligned}$$

The inequality in (3.26) is due to the fact that we would expect there to be fewer cut

edges in total after taking unions of subsets and the (3.27) inequality holds by the application of lemma 3.33.

Using the fist inequality in (3.25) and (3.28) we have that,

$$\frac{\mathbb{E}\Big[w(E(\hat{T}_i,\overline{\hat{T}_i}))\Big]}{\mathbb{E}[w(\hat{T}_i)]} \leq \frac{2}{(1-\delta)} \cdot \left(\frac{2\sqrt{h}}{\Delta}+1\right) \cdot \sqrt{\mathcal{R}_G(F)}.$$

For $\hat{T}_i = T_i^*$ we have completed the proof.

□

Theorem 3.35. *Let be a weighted graph of $G = (V, E, w)$ embedding dimension $\tilde{k} \in \{1, 2, \ldots, n\}$ and $\delta \in (0, 1)$. Suppose that $x_1, x_2, \ldots, x_{\tilde{k}} : V \to \mathbb{R}$ are the first $\tilde{k}$ eigenfunctions of the normalised Laplacian. Then there exist $r = \lceil (1-\delta)\tilde{k} \rceil$ disjoint sets $T_1, T_2, \ldots, T_r \subseteq V$ with*

$$h_G(T_i) \leq \frac{2}{(1-\delta)} \cdot \left(\frac{2\sqrt{h}}{\Delta}+1\right) \cdot \sqrt{8\mathcal{R}_G(F)}.$$

For $\Delta(r,\tilde{k}) = -\frac{1}{2\delta} + \sqrt{(\frac{1}{2\delta})^2 + \frac{1}{16}}$, h must satisfy,

$$h \geq \frac{-192}{\Delta(\tilde{k},r)}(10\log(2) + \log(\Delta(k,r)) - 3\log(\tilde{k})).$$

Proof. $\Delta(r,\tilde{k}) = -\frac{1}{2\delta} + \sqrt{(\frac{1}{2\delta})^2 + \frac{1}{16}}$, this will guarantee that $(1-16\Delta^2)^{-1}(1+4\Delta) \leq 1 - \frac{\delta}{4}$, so that when we apply lemma 3.15 for this embedding we can show $F^* : V \to \mathbb{R}^{\tilde{k}}$ is a $\left(4\Delta, \frac{1}{\tilde{k}(1-16\Delta^2)}\right)-$ spreading embedding. We then applying Lemma 3.30 we will have a dimension reduced embedding $F^* : V \to \mathbb{R}^h$ (where the condition for h in (3.18) must hold), which is $(\Delta, \frac{1}{\tilde{k}} - \frac{\delta}{4\tilde{k}})-$ spreading. Also we have from Lemma 3.30 that $\mathcal{R}(F^*) \leq 8 \cdot \mathcal{R}(F)$.

If we now apply lemma 3.34 we have $r = \lceil (1-\delta)\tilde{k} \rceil$ disjoint subsets $T_1, T_2, \ldots, T_r$,

$$h_G(T_i) \leq \frac{2}{(1-\delta)} \cdot \left(\frac{2\sqrt{h}}{\Delta}+1\right) \cdot \sqrt{\mathcal{R}_G(F^*)} \leq \frac{2}{(1-\delta)} \cdot \left(\frac{2\sqrt{h}}{\Delta}+1\right) \cdot \sqrt{8\mathcal{R}_G(F)}.$$

□

Remark 3.36. *Theorem 3.35 embodies the application of the algorithm for spectral*

embedding with dimension reduction and all steps are present apart from the final step which transforms the pseudo-partition into a partition of V.

Theorem 3.37. ***(Non-expanding $k-$partition with dimension reduction)*** *Let any weighted graph $G = (V, E, w)$ with embedding dimension $\tilde{k}$ and $\delta \in (0, 1)$ be given. Suppose that $x_1, x_2, \ldots, x_{\tilde{k}} : V \to \mathbb{R}$ are the first $\tilde{k}$ eigenfunctions of the normalised Laplacian. Then there exists a partition $T_1, T_2, \ldots, T_r \subseteq V$ (where $r = \lceil (1-\delta)\tilde{k} \rceil$) with*

$$h_G(T_i) \leq \frac{k-1}{(1-\delta)\tilde{k}} \cdot \left(\frac{2\sqrt{h}}{\Delta} + 1 \right) \cdot \sqrt{8\mathcal{R}_G(F)}.$$

For $\Delta(r, \tilde{k}) = -\frac{1}{2\delta} + \sqrt{(\frac{1}{2\delta})^2 + \frac{1}{16}}$, h must be such that,

$$\tilde{k} > h \geq \frac{-192}{\Delta(\tilde{k}, r)}(10\log(2) + \log(\Delta(\tilde{k}, r)) - 3\log(\tilde{k})). \tag{3.29}$$

Proof. Applying Theorem 3.35 to the graph $G = (V, E, w)$ and if condition (3.29) holds for a selected h (this indicates that we are able to perform dimension reduction) we have $r = \lceil (1-\delta)\tilde{k} \rceil$ disjoint subsets $T_1, T_2, \ldots, T_r \subseteq V$ for which,

$$h_G(T_i) \leq \frac{2}{(1-\delta)\tilde{k}} \cdot \left(\frac{2\sqrt{h}}{\Delta} + 1 \right) \cdot \sqrt{8\mathcal{R}_G(F)}.$$

Where $\Delta(r, \tilde{k}) = -\frac{1}{2\delta} + \sqrt{(\frac{1}{2\delta})^2 + \frac{1}{16}}$. We take the k least expanding of these r sets, these will be called $T_1, T_2, \ldots T_k$ this can be achieved by relabelling. We now as in the proof of Theorem 3.27 relabel the subsets of the pseudo-partition so that the volumes of the r sets are in ascending order $w(T_1) \leq w(T_2) \leq \cdots \leq w(T_r)$, we will take the largest set and amend so that it is equal to an even larger set $T'_k = V \backslash (T_1 \cup T_2 \cup \cdots \cup T_{k-1})$,

this way $T_1, T_2, \ldots, T_{k-1}, T'_k$ forms a partition, and

$$\begin{aligned} h_G(T'_r) =& \frac{w(E(T'_k, \overline{T'_k}))}{\min(w(T'_k), w(\overline{T'_k}))} \\ &\leq \sum_{i=1}^{k-1} \frac{w(E(T_i, \overline{T_i}))}{\min(w(T'_k), w(\overline{T'_k}))} \\ &\leq \sum_{i=1}^{k-1} h_G(T_i) \\ &\leq \frac{k-1}{(1-\delta/2)\tilde{k}} \cdot \left(\frac{2\sqrt{h}}{\Delta} + 1 \right) \cdot \sqrt{8\mathcal{R}_G(F)} \end{aligned}$$

□

3.4 Implementation of Algorithms

In section 3.2.1 we devised the metric d_F (3.4) and $\hat{d}_F$ on the initial embedding of the graph. This initial embedding was constructed using the first $k \in \mathbb{N}$ eigenvectors of the graph Laplacian and embedded the graph into $\mathbb{R}^k$. When these coordinates in $\mathbb{R}^k$ are normalised this embedding is now in $\mathcal{S}^{k-1}$, the metric d_F is essentially the euclidean metric of this embedding. $\hat{d}_F$ is the shortest path metric when the distance between two adjacent vertices $u, v \in V$ is $d_F(u, v)$.

We will be performing higher order spectral partitioning with both d_F and $\hat{d}_F$ metrics, these simulations will be on the IEEE 39-bus test case where edges are weighted with power flows.

Figure 3-4: IEEE 39-bus test case system

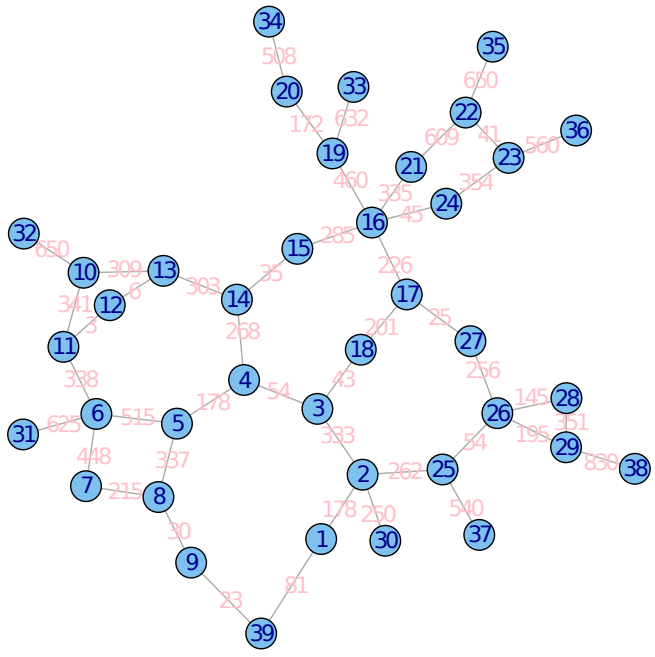

Step zero of both of these algorithms is to spectral embedded (this was outlined in **Embedding and Metrics** section earlier in this chapter), for illustrative purposes we will show this below in two dimensions for the IEEE 39-bus test case.

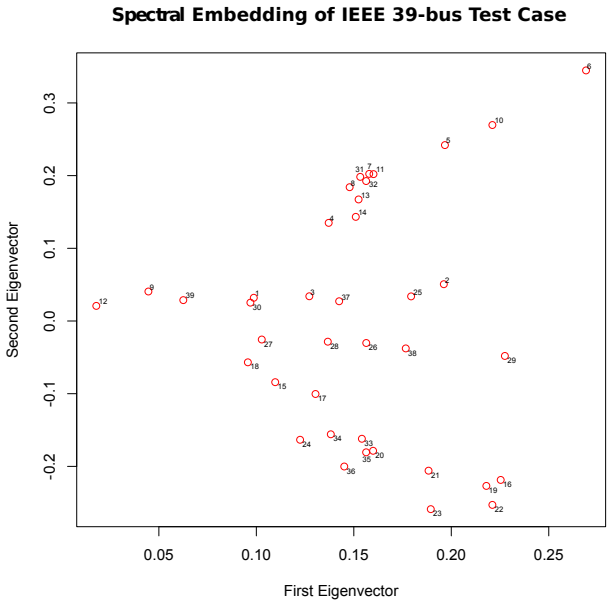

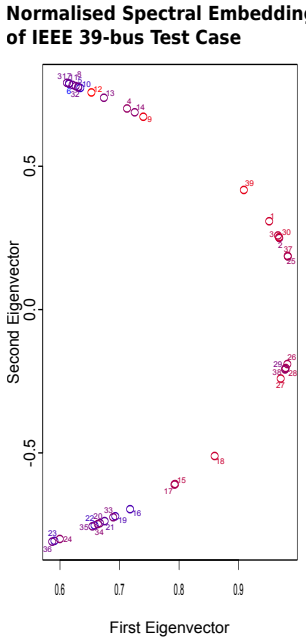

Figure 3-5: The upper plot shows the un-normalised embedding, on the lower plot the coordinates have been normalised (points lie on a unit circle) and in both plots the points have been labelled by bus number.

Remark 3.38. *Notice in Figure 3-5 that the points on the right-hand plot take on a range of different colours, these are an indication of the magnitude of the point's*

coordinates before normalisation, these colours range from red for points with small magnitude such 12 and 9 through to blue for points with high magnitude such as 6 and 22. Although these magnitudes are ignored in the higher order spectral partitioning, this however is information which will not be discarded when dimension reduction is included, it will be used in the Cheeger sweep *step (see* ***Algorithms*** *section earlier in this chapter).*

Remark 3.39. *When applying the higher order spectral partitioning methods we take partitions of the graph embedded in the surface of $\mathcal{S}^{k-1}$, when $k = 2$ using Fiedler's partition method to create cuts will give essentially the same results. The potential cuts created by the higher order spectral partitioning methods are represented as rays from the origin of a sphere on upper graph in figure 3-6 and the cuts which are assessed in the Fiedler partitioning method are represented by the horizontal lines in the graph on the lower graph in figure 3-6. If we perform the transition using $D^{-1/2}$ to the eigenvectors of the normalised Laplacian $\underline{x_1}, \underline{x_2}$, these eigenvectors will become the eigenvectors of the unnormalised Laplacian $\underline{y_1}, \underline{y_2}$ where $\underline{y_1} \propto \underline{1}$, points are thus transformed by moving along radial lines, consequentially the potential cut resulting from both methods are the same, as illustrated but the seven potential cut lines below*[2].

Spectral Embedding of IEEE 39-bus Test Case

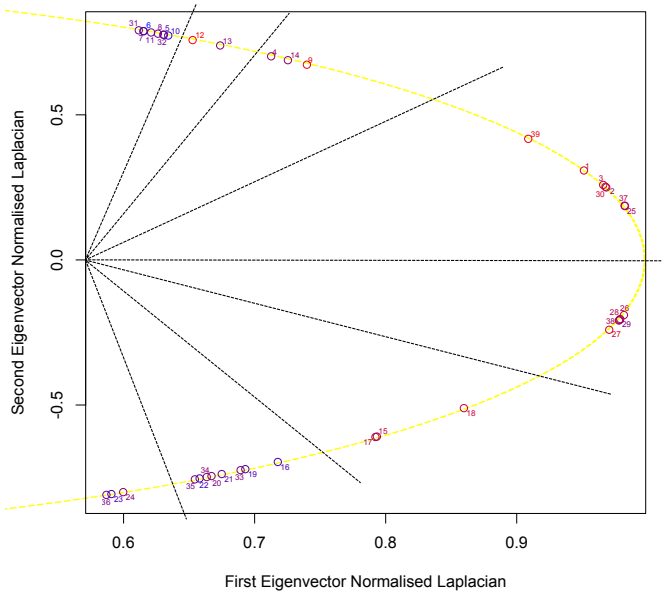

[2]Note that the scaling of the x and y axises in the figure below are different making the yellow line which is in fact circle like figure 3-5 but appears elliptical. This scaling is done to show distribution of nodes more clearly.

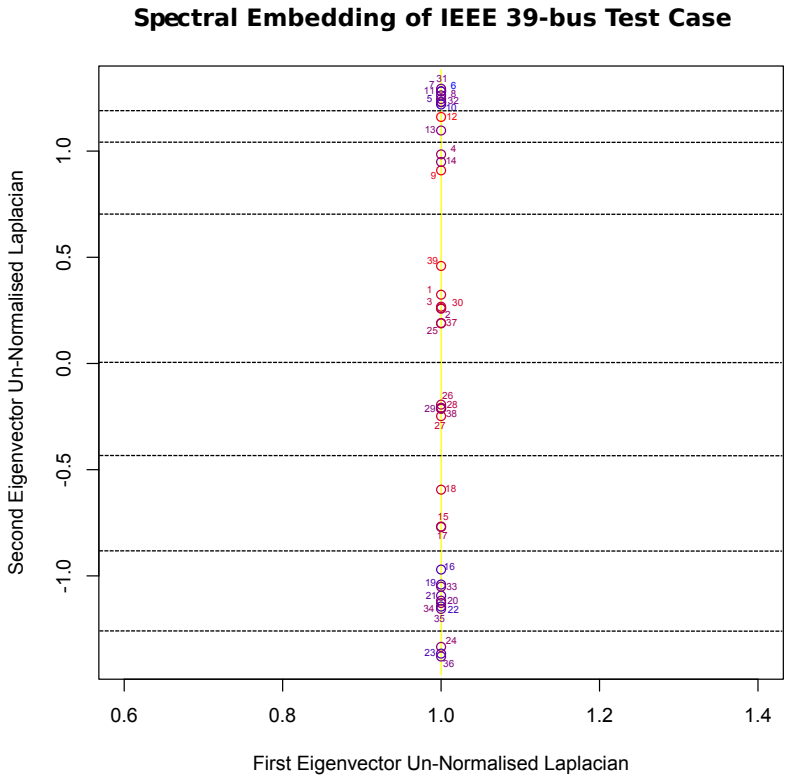

Figure 3-6: The upper plot shows the normalised-embedding using eigenvalues of the normalised Laplacian, on the lower plot shows the embedding using eigenvalues of the un-normalised Laplacian. The potential cuts along each ray are preserved in both graphs.

To give an intuition for what the spectral embedding does, we have included edges in the following figure where the magnitude of power flow determines the colour of an edge. These colours range from deep blue indicate a large power flow such as between buses 29 and 38 with a power flow of 830.00 units, through to yellow which indicates a low power flow such as between buses 9 and 39 with a power flow of 23.25 units.

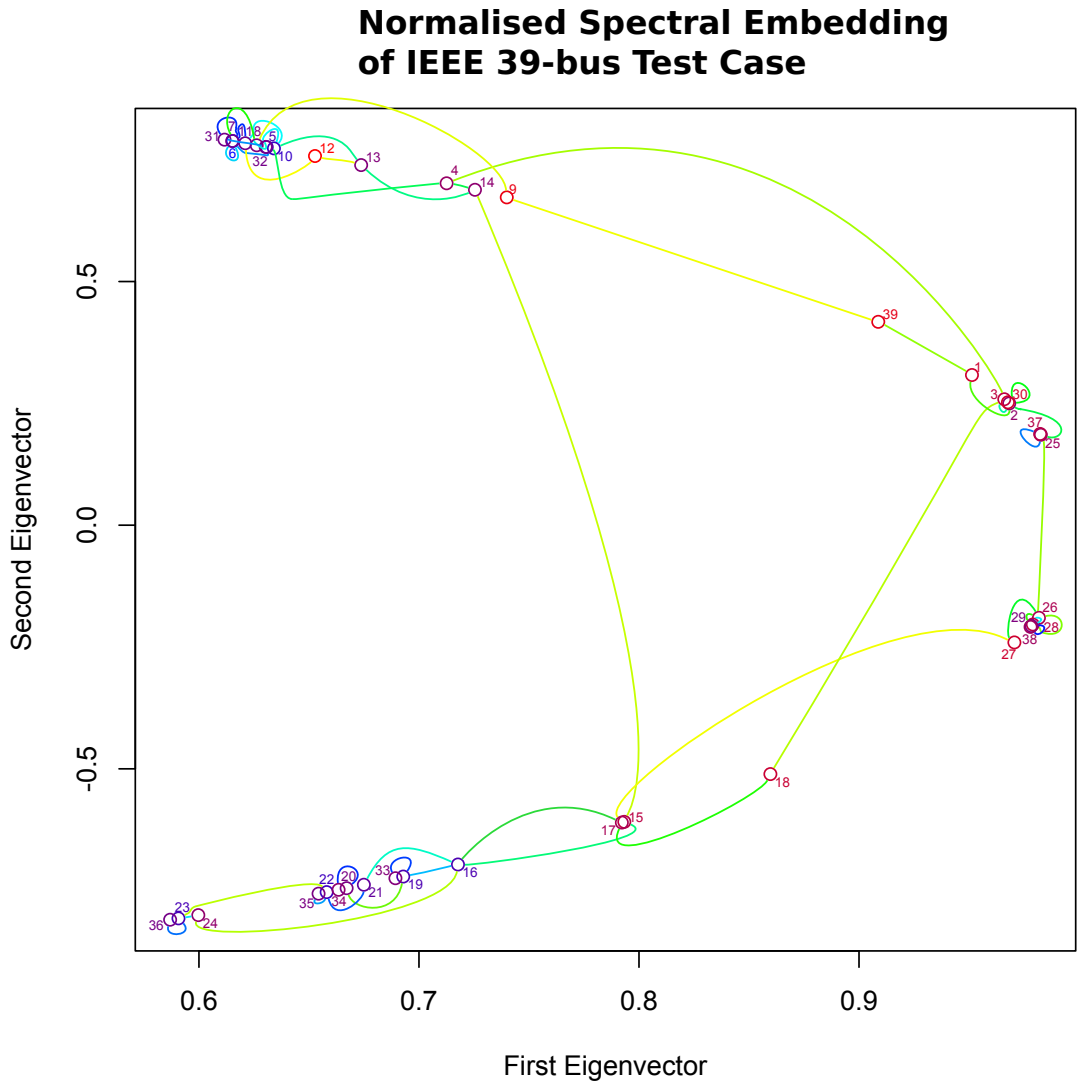

Figure 3-7: The colour assigned to edges indicate the strength of power flow in the line ranging from yellow (weak power flow) to deep blue (strong power flows).

It can be clearly seen that there is a strong negative correlation between the strength of power flows between buses and the geometric distance between those buses in the embedding, for example the strongest power flow is between buses 29 and 38 are embedded in approximately the same position and the edges that are stretched to a large extent in the embedding are yellow or light green (indicating weak power flows). The embedding forms clusters with high levels of interconnectivity of power and relatively low levels of power connectivity between clusters. We can by visual inspection identify

three or four cluster (or islands) as shown in the figure below.

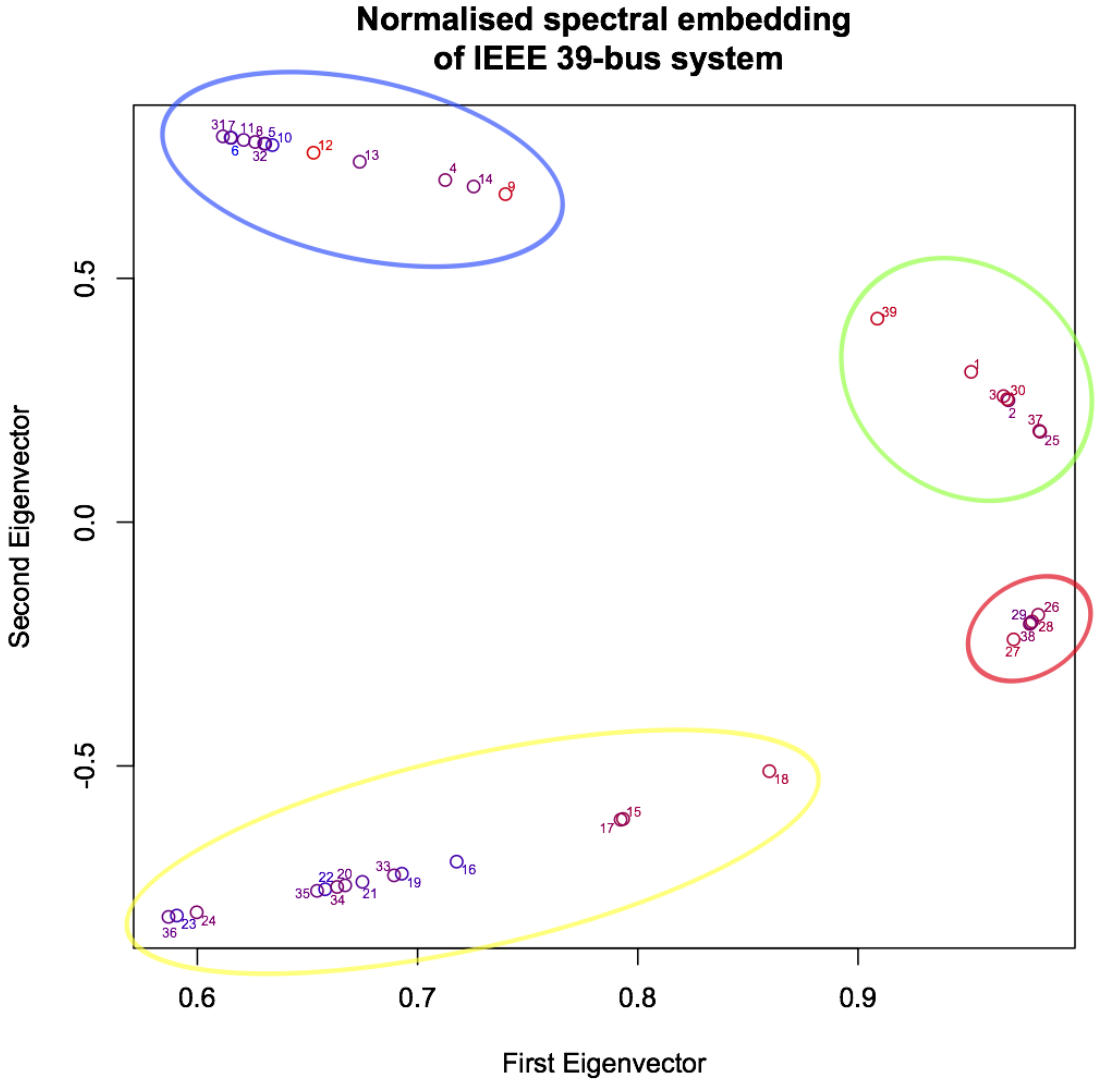

Figure 3-8:

Table 3.1: Partition into four (or three) Islands

Island	Buses	Boundary	Isoparametric Ratio
Blue	4-14,31-32	112.4	1.22%
Green	1-3,25,30,37,39	174.3	5.03%
Red	26-29,38	79.5	2.19%
Yellow	15-24,33-36	103.0	1.00%
Green + Red	1-3,25-30, 37-39	145.3	2.05%

Remark 3.40. *With the partition indicated in Figure 3-8, we take* $\rho_G(4) = 0.0503$ *(notice here that this is not an optimal solution as in defined (3.1) but this is taken as a possible candidate for* $\rho_G(4)$*), but in fact there exists a better set of cuts which will minimise* $\rho_G(4)$*. Here Blue and Green are not partitioned and are taken as one subset and Yellow split in two pieces, here* $\rho_G(4) = 0.0451$*.*

Table 3.2: Partition into four Islands

Island	Buses	Boundary	Isoparametric Ratio
Blue+Green	1-14,25,30-32,37,39	112.4	1.04%
Red	26-29,38	79.5	2.19%
Yellow one	15-22,33-35	174.3	2.27%
Yellow two	23-24,36	103.0	4.51%

Partitions that gives $\rho_G(3) = 0.0205$ and $\rho_G(4) = 0.0451$ can be found using the higher order Fiedler's partition method see in section 2.3.2.

The general ethos of these spectral partitioning methods is that they will find partitions with small ${h_G}^{(k)}$ when embedded into k dimensions, so it will be interesting later to compare other techniques that embed in higher dimensions with higher order Fiedler partition method as this method only embeds in 2-dimensions.

We will now outline the first step of our stochastic higher order spectral partitioning methods. We outlines the general notion of taking random partitions earlier in *Forming Pseudo-Partitions: Algorithm Step 1 and Step 2* a subsection of 3.2.1, but didn't specify a way this could be done.

Implementation of the Step 1

We will implement algorithms giving partitions where Theorem 3.27 is applicable, this algorithm is given in section 3.2.1 on page 36, however details of Step 1 are not specified.

To devise Step 1 after spectral embedding (Step 0) we need to take a partition, and do this in a probabilistic way so that the partition will essentially be a sample from a distribution of possible partitions $\mathcal{P}$. There is just one condition for every partition in the distribution, this is that the diameter of each subset from any partition has a bound of $\text{diam}(S, d_F) \leq \Delta$ where $\Delta = \sqrt{\frac{k-r+1}{k+7r+1}}$ (satisfying lemma 3.25). In our

implementations this will be simplified farther as we will take $k = r$ and thus $\delta < \frac{1}{k}$ and $\Delta = \sqrt{\frac{1}{8k+1}}$.

As mentioned earlier this step is where the pseudo-partition is taken and disjoint subsets $S_1, \ldots, S_k \subset V$ are selected in a stochastic manner. Note that this is not necessarily a partition of V, meaning that it is possible for $S_1 \cup \cdots \cup S_k \neq V$. This partition is carried out by selecting k balls on the surface of $\mathcal{S}^{k-1}$ and thus separating the vertices in k subsets.

Firstly we will select a vertex randomly with a uniformly probability distribution which is in accordance with the vertices degree's, so that the probability of a vertex's selection is weighted by the vertex's degree. If $v_1 \in V$ is selected first the vertex v_1 will then be the centre of one of these balls on the surface of $\mathcal{S}^{k-1}$ with radius $\Delta/2$, all vertices which lie in this ball $B(v_1, \Delta/2)$ will constitute the first subset S_1 (the metric used to establish this metric is d_F).

We will choose a vertex to be a centre preferentially in according with the degree because, as can be observer in Figure 3-7 vertices with high degree tend to lie in the centre of clusters whereas vertices of lesser degree lie on the periphery of clusters.

We can now introduce an iterated step for $i = 2$ to k, we select again uniformly in accordance with the vertex degrees, but we exclude from our selection vertices which have a distance of less than $\Delta/2$, from vertices which have already been selected to be part of a subset (thus allowing disjoint subsets to form). We then take S_i to be all vertices which lie in $B(v_i, \Delta/2)$ on the surface of $\mathcal{S}^{k-1}$, this gives us $S_1, \ldots, S_k$ disjoint subsets of V.

If this is not possible for the given value of Δ then try and smaller value.

Implementation of the Step 2

Now as in the proof of Theorem 3.27 we reorder the sets labels so that $w(S_1) \leq w(S_2) \leq \cdots \leq w(S_k)$, we then replace S_k with the larger set $S'_k = V \backslash (S_1 \cup S_2 \cup \cdots \cup S_{k-1})$ we now have a partition $S_1, \ldots, S_{k-1}, S'_k$.

Remark 3.41. *When the algorithm is constructed in a way that will satisfy the application of Theorem 3.27 it yields poor results. This is due to the bound that has to be placed on the radius of the balls being too low. When the constraint of the diameter of the balls is lifted we see good heuristic results however sacrifice the theoretical*

framework.

In the analysis that follows a heuristic approach where the constraint is lifted will be presented first and then the results of an application where Theorem 3.27 can be applied will be presented.

Analysis of Higher Order Spectral Partitioning $\rho_G(2)$ for the IEEE 39-bus Test Case

Below we have a plot of the probability of finding a *possible* optimal partition giving $\rho_G(2)$ (meaning the partition of the "Yellow" subsets illustrated in Figure 3-8), with the application of the algorithm with differing radiuses, for the d_F metric on the left and the $\hat{d}_F$ metric on the right. These probabilities have been obtained through calculation and not simulation.

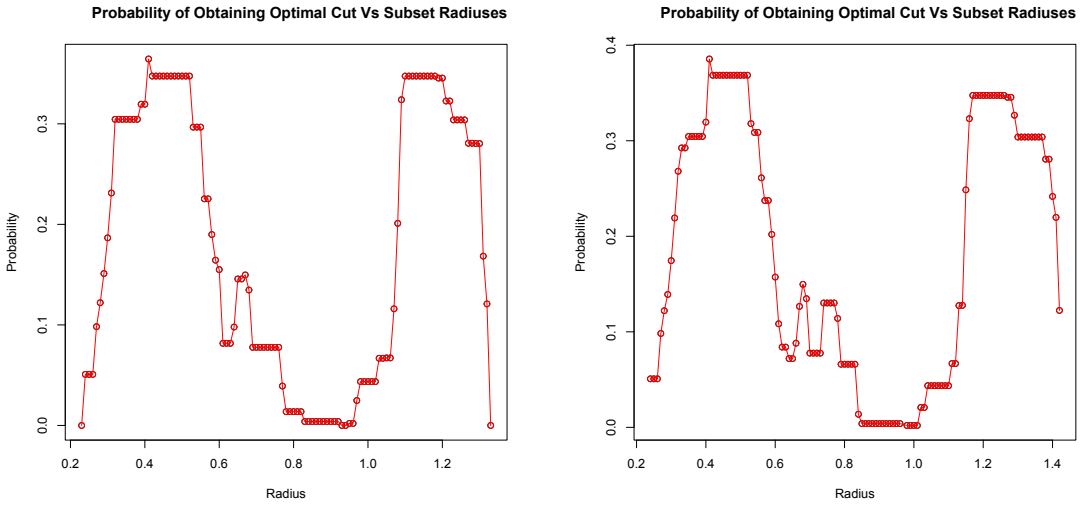

Figure 3-9: On the left is the application of the method with the d_F metric and on the right with the $\hat{d}_F$ metric.

Analysis of Higher Order Spectral Partitioning $\rho_G(3)$ for the 39-bus IEEE Test Case

When spectral embedding in 3 dimension we are of course including more information than spectral embedding in 2 dimensions (which can be thought of as equivalent to Fiedler partition method). The spectral embedding in three dimensions is illustrated

in the upper graph of figure 3-13 and to make the clusters more clear we have perform stereographic projection on the lower graph of figure 3-13.

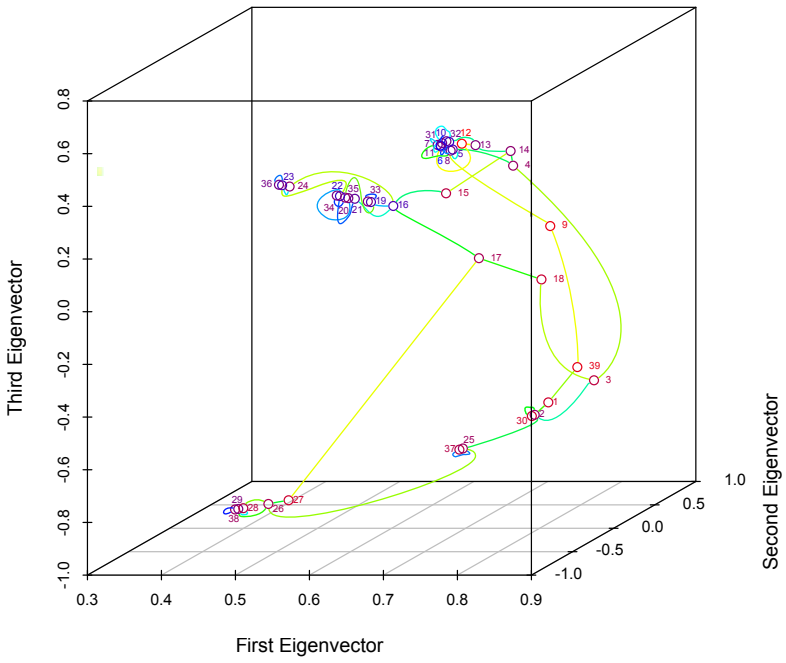

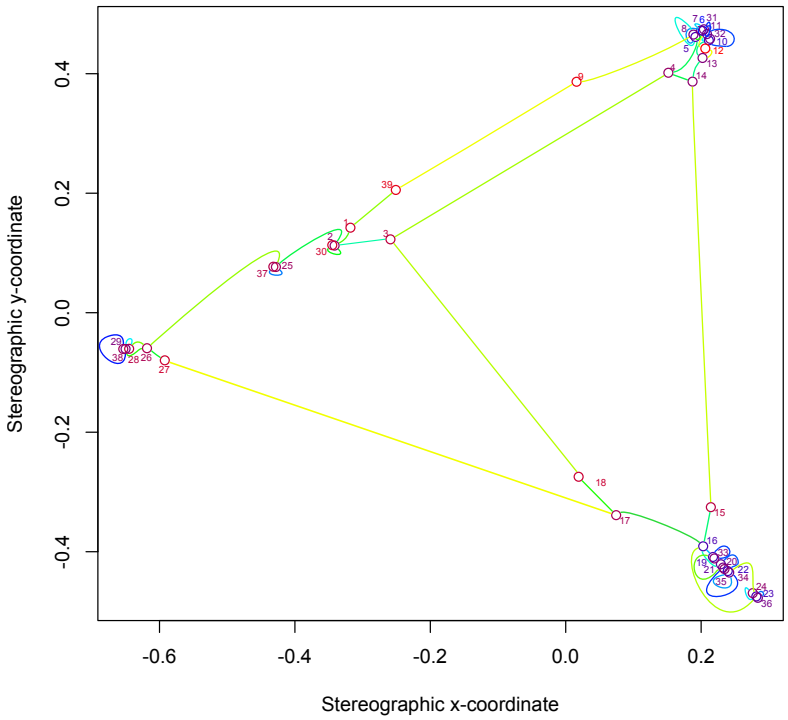

Figure 3-10: The lower graph shows the stereographic projection of this with $(-1, 0, 0)$ as the projection point on $\mathcal{S}^2$.

If we cluster this by visual inspection the same three or four clusters seem to prevail.

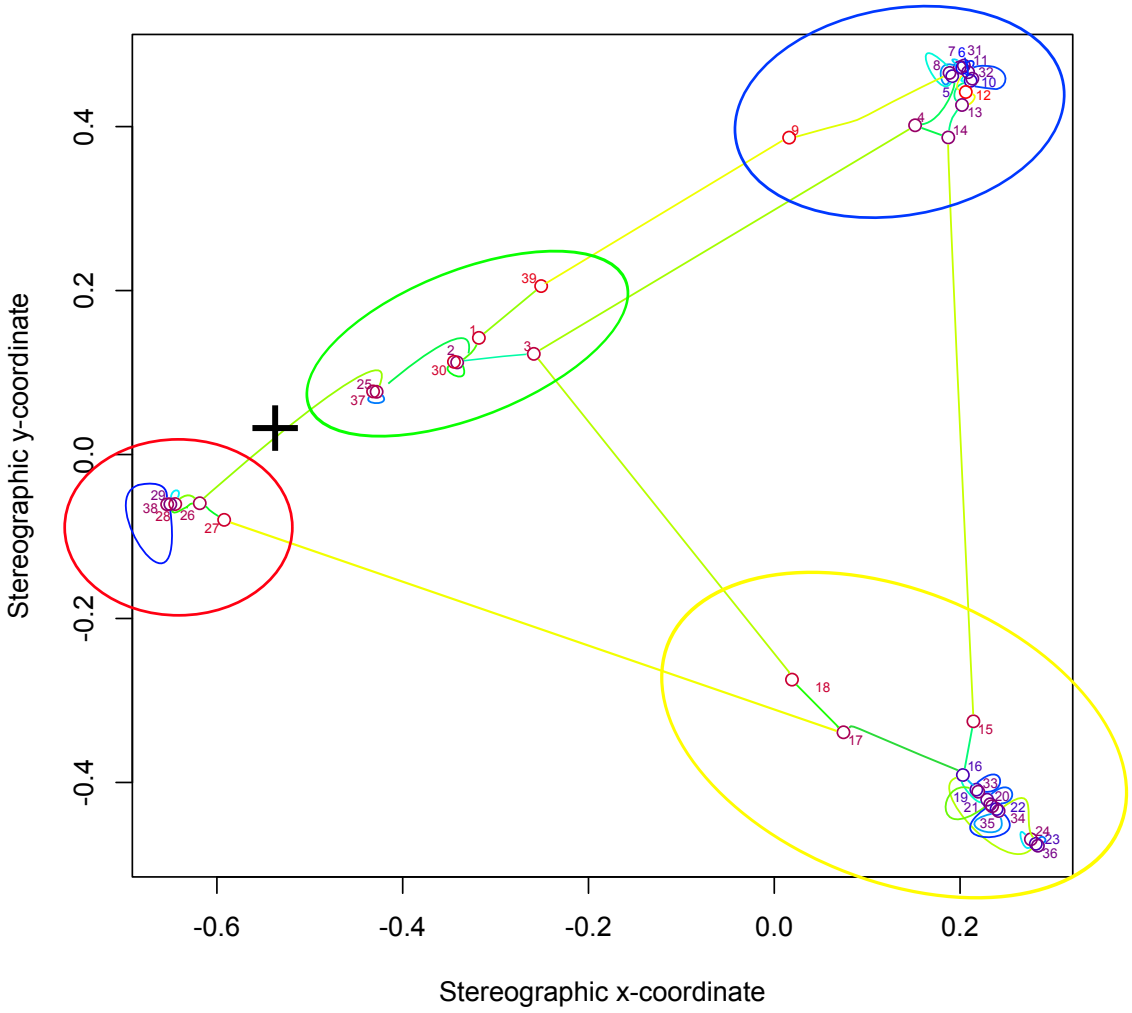

Figure 3-11: Islands are formed by visual inspection.

Below we have a plotting of the probability of finding a *possible* optimal partition giving $\rho_G(3)$ (meaning the partition in to the "Yellow", "Blue" and "Green + Red" subsets as illustrated in figure 3-11), with the application of the algorithm with differing radiuses, for the d_F metric on the left and the $\hat{d}_F$ metric on the right. Again these probabilities have been obtained through calculation and not simulation.

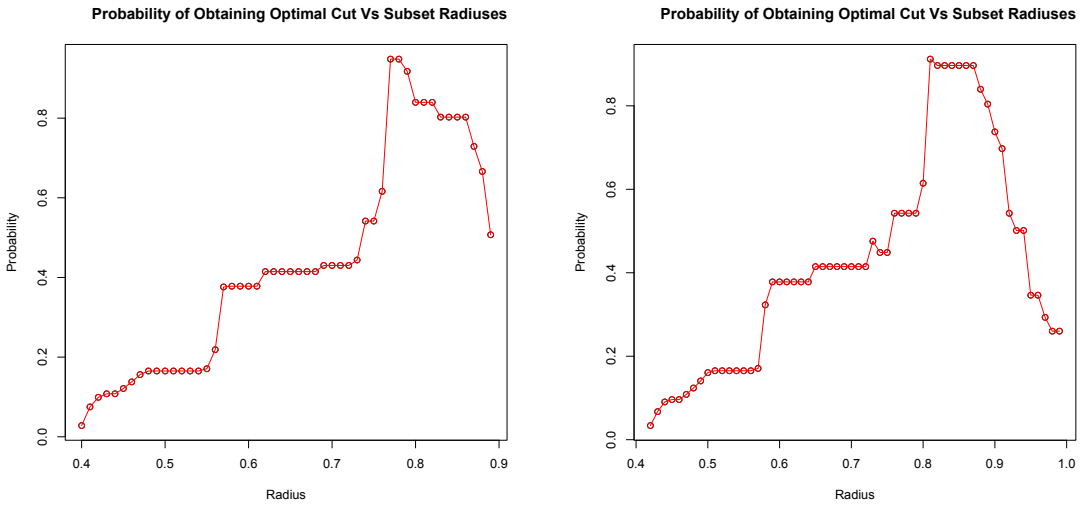

Analysis of Higher Order Spectral Partitioning $\rho_G(4)$ for the IEEE 39-bus Test Case

Here we will consider a *possible* optimal partition to be that found by the higher order Fielder partition method this is given in Table 3.2. The algorithm here is unable to find this cut for both the d_F metric and the $\hat{d}_F$ metric. The reason for this can be found when we look at the *possible* optimal cut and observe the ranges of ball radiuses that are capable of capturing each one of these subsets are $(0.0112 - 0.0861), (0.2007 - 0.2723), (0.0327 - 0.3432)$ and $(0.4775 - 1.0487)$ for d_F, there is no one radius that is capable of capturing three of the four subsets, thus it is clear that after Step 1 the optimal cut cannot be obtained. Similarly for the $\hat{d}_F$ metric these ranges are $(0.029 - 0.4259), (0.4355 - 0.8000), (0.1661 - 1.4342)$ and $(1.0531 - 1.6311)$ again no one radius lies in three of these four ranges.

Analysis of Higher Order Spectral Partitioning $\rho(2)$ for the IEEE 118-bus Test Case

What we take to be a *possible* optimal partition giving $\rho(2) = 0.0138$ this is the partition obtained by the Fiedler's method, one of the subsets of this partition is $34 - 71, 73 - 112, 116, 118$. Again below we have the probability of obtaining this partition with the application of our algorithm with varying radiuses using the d_F metric on the left and the $\hat{d}_F$ metric on the right.

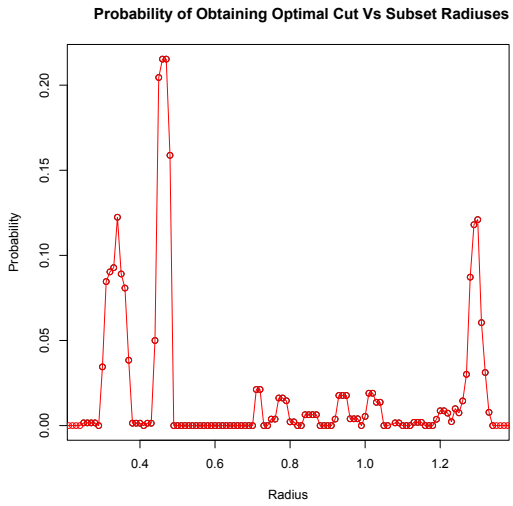

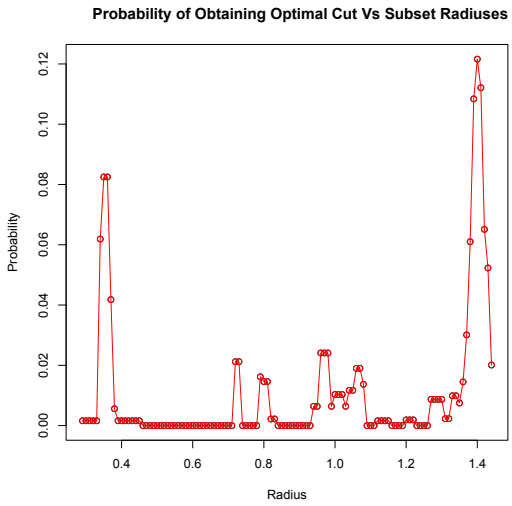

Analysis of Higher Order Spectral Partitioning $\rho_G(3)$ for the IEEE 118-bus Test Case

What we will take to be the optimal cut giving $\rho_G(3) = 0.0216$ is found using the higher order Fiedler method and gives a partition of subsets $(82-96, 99-112), (34-71, 73-81, 97-98, 116, 118)$ and $(1-33, 72, 113-115, 117)$. For the d_F metric it is not possible to obtain this partition, the ranges of radiuses needed to to capture the three optimal subsets are $(0.2022-0.5216), (0.7138-0.8758)$ and $(0.4934-1.2019)$. If we set the radius to be in $(0.4934-0.5216)$ it is possible to capture two out of three of these subsets S_1, S_2 in **step1**, but for the algorithm to then obtain the partition in the final step S_3 must have the largest volume of the three subsets, which isn't possible. It is possible however to obtain this cut with the $\hat{d}_F$ metric, where the ranges of radiuses needed are $(0.6722-0.9824), (0.5549-1.2629)$ and $(0.5792-0.8672)$, below is a plot of the probabilities of obtaining this optimal cut when applying the higher order spectral partitioning algorithm.

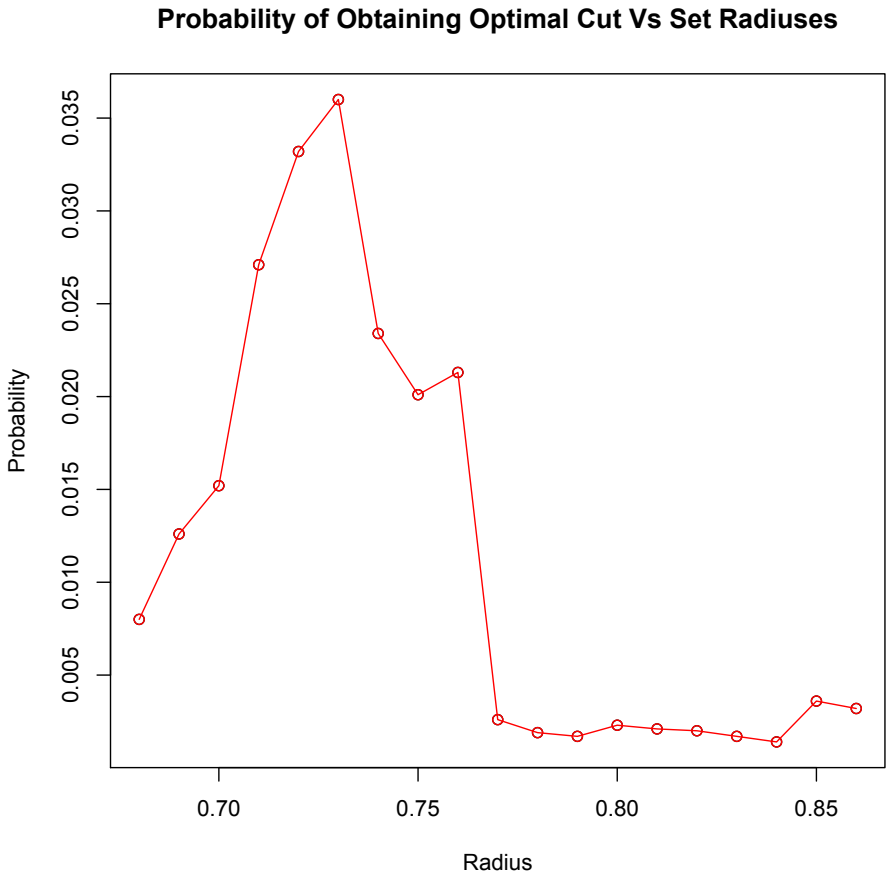

Figure 3-12:

Analysis of Higher Order Spectral Partitioning $\rho(4)$ for the IEEE 118-bus Test Case

Again we will consider our optimal solution to be that obtained by the higher order Fiedler partition method which gives $\rho_G(4) = 0.0451$, for the d_F metric the range of radiuses needed to capture the four subsets $(0.1111 - 0.2497), (0.9189 - 1.0030), (0.5475 - 1.0782)$ and $(0.1553 - 0.7237)$, here we don't have three ranges that any one radius would lie in, thus it would be impossible to find this partition with the application of our method. Similarly for the $\hat{d}_F$ metric the ranges of radiuses are $(0.1312 - 0.2637), (1.1969 - 1.3169), (0.7118 - 1.2071)$ and $(0.1817 - 0.8381)$ so again there is no one radius that lies in three of the four islands.

Analysis of Higher Order Spectral Partitioning $\rho(2)$ for GB Network

We take to be a *possible* optimal partition giving $\rho(2) = 0.0099$ is the partition obtained by the Fiedler's method. Again below we have the probability of obtaining this partition with the application of our algorithm with the d_F metric on the left and the $\hat{d}_F$ metric on the right.

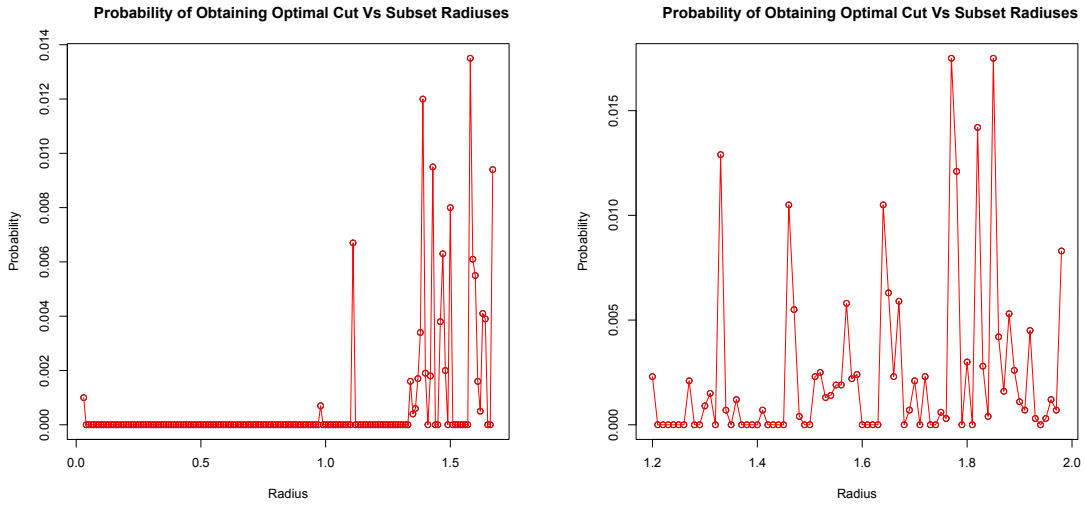

Alternative Algorithm

We can clearly see some shortcomings of the algorithm as it is being consistently out performed by the higher order Fiedler partition method. The nature of these shortcomings have been made clear when we observe the ranges of radiuses needed in Step 1 to capture the subsets obtained by the higher order Fiedler partition method, this being that the radiuses can't vary.

In the alternative algorithm the radius will not be a set quantity but be allowed to vary. In this alternative algorithm's Step 1 for each iteration where a ball is selected a function will generate the radius, this function will take as input: the sum of all radiuses of balls previous selected ($SumPre$), the number of previous balls selected ($NoPre$) and the $confidence$. The radius is generated by sampling from a normal distribution whose mean is $\mu = (k \cdot 0.8 - SumPre)/(k - NoPre)$ and standard deviation is $\sigma = \mu/confidence$ (the confidence will be set to 1.96 for a 95% confidence that the radius will lie in $(\mu - \sigma, \mu + \sigma)$), this will be repeated if the sample is negative. This

generation of radius is such that the pseudo-expectation is 0.8 (which was chosen simply by observing previous ranges which gave optimal cuts), and that if previously small radiuses were chosen the distribution is skewed so that a larger radiuses are more likely to be chosen next and vice versa.

All the partitions obtained by the higher order Fielder partition method can now be obtained by this alternative algorithm, however we have not encountered this in our analysis. Taking this algorithm for the d_F metric and analysing IEEE 118-bus test case for $k = 3$ again for example, we find that after ten thousand iterations of this algorithm the optimal solution is found 0.22% of the time. For the $\hat{d}_F$ metric the optimal solution is found 0.26% of the time. Despite the inconsistencies of these algorithms they are showing some obvious benefit because computation increases linearly with k, where as with the computation time of higher order Fiedler vector partitions increase with a relation n^k.

Analysis of Higher Order Spectral Partitioning $\rho(3)$ for GB Network

Remark 3.42. *For the GB network of 790 vertices, we witness the first occurrence of the alternative higher order spectral partitioning method out performing the higher order Fiedler partitioning method. To compute $\rho_G(3)$ for this network takes 4.99 hours, and for the higher order spectral partitioning method with d_F takes approximately 13 seconds to calculate all distances and subsequent calculations taking 0.70 seconds. The higher order Fiedler partition method gives you $\rho_G(3) = 0.0126$ and the minimum obtained from higher order spectral partition with d_F metric is $\rho_G(3) = 0.0125$ (this is the difference of eight vectors ownership swapping islands) this is taken over one thousand iterations this is found 0.3% of the time. If we use the $\hat{d}_F$ to measure all the shortest path distances takes 25 minutes and 9 seconds to calculate, and subsequent calculations taking an average of 1.26 seconds to compute. The same minimum $\rho_G(3)$ is obtained as with the d_F metric 0.1% of the time. These results mean that after 998 iteration of the alternative higher order spectral partitioning algorithm with the d_F metric which takes 11 minutes and 52 seconds, we can be 95% confident that we have an improved partition, for the $\hat{d}_F$ metric this takes 60 minutes and 6 seconds to be 95% sure that we have an improved partition.*

Below is an illustration of the higher order spectral partitioning method with varied

radiuses out-performing the higher order Fiedler method.

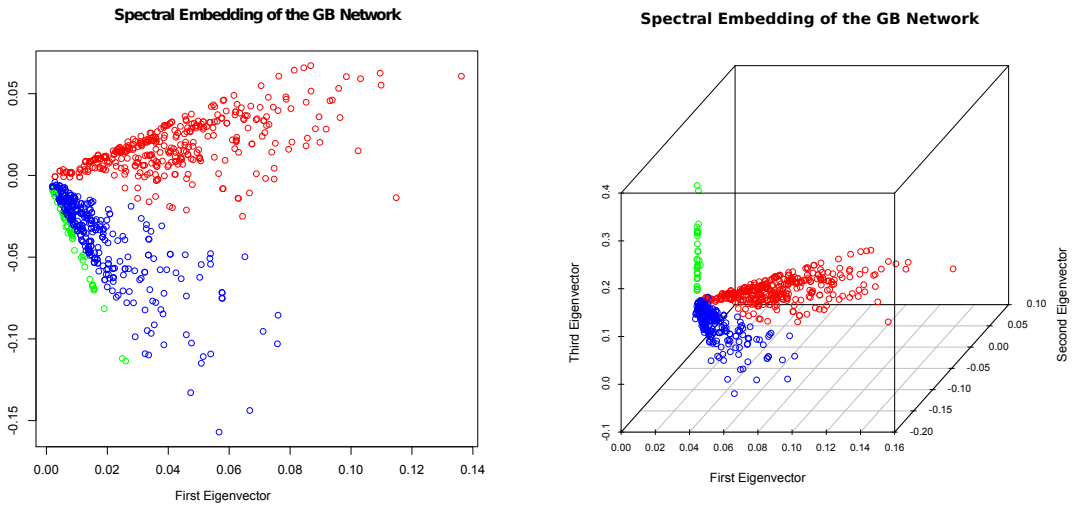

Figure 3-13: The graph on the left hand side below illustrates the three subsets obtained by the higher order Fiedler method and the graph on the right hand side illustrates the partition obtained by the higher order spectral partitioning algorithm with varied ball radiuses.

Results of Algorithms where Theorem 3.27 is Applicable

The algorithms are constructed in such away that the vertices are embedded in a particular metric space, which takes place in Step 0, but also the distance between any pair of vertices is calculated so that there is an $n \times n$ chart of distances to refer to, this makes the code more efficient and repeated calculations are avoided. The time that it takes to calculate this distance chart is given in the table as "Time to embed in metric space", after this initial computation to complete the algorithm iterates one thousand times, the average time of a subsequent iteration of the algorithm is headed in the table as "calculation time", the average higher order isoparametric ratio achieved in an iteration is headed in the table as "Average isoparametric ratio" and the column headed "Theorem's claim" is the bound that is put on the probability of at least a 1/2 of of resulting isoparametric ratio of a partitioned subset by Theorem 3.27.

Table 3.3: IEEE 39-bus test case for the d_F metric

No. of subsets	Average isoparametric ratio	Time to embed in metric space	Calculation time	Theorem's claim
$k = 2$	3.99%	0.0278 sec	0.001 sec	$0.140 + (18.4725)$
$k = 3$	46.65%	0.0295 sec	0.0011 sec	$0.3167 + (114.0181)$
$k = 4$	59.79%	0.0435 sec	0.0013 sec	$0.8829 + (649.2004)$

Table 3.4: IEEE 39-bus test case for the $\hat{d}_F$ metric

No. of subsets	Average isoparametric ratio	Time to embed in metric space	Calculation time	Theorem's claim
$k = 2$	17.55%	0.2139 sec	0.0014 sec	$0.140 + O\left(\frac{h^2}{4}(18.4725)\right)$
$k = 3$	45.72%	0.2224 sec	0.0017 sec	$0.3167 + O\left(\frac{h^2}{9}(114.0181)\right)$
$k = 4$	60.45%	0.2098 sec	0.0018 sec	$0.8829 + O\left(\frac{h^2}{16}(649.2004)\right)$

Remark 3.43. *The claim here is not actually in theorem 3.27 but if (3.10) were taken forward in a similar way to how (3.9) was taken forward in theorem 3.27 the following claim could be made.*

The graph minors of IEEE 39-bus test case have not been calculated but it is clear to see that in both the 39-bus and 118-bus test cases that genus is zero and thus the bound (3.11) of theorem 3.27 does not apply.

Table 3.5: IEEE 118-bus test case for the d_F metric

No. of subsets	Average isoparametric ratio	Time to embed in metric space	Calculation time	Theorem's claim
$k = 2$	19.17%	0.2408 sec	0.0040 sec	$0.1114 + (14.6921)$
$k = 3$	40.63%	0.2327 sec	0.0056 sec	$0.7809 + (281.1176)$
$k = 4$	63.66%	0.2434 sec	0.0067 sec	$2.6660 + (1960.3205)$

Table 3.6: IEEE 118-bus test case for the $\hat{d}_F$ metric

No. of subsets	Average isoparametric ratio	Time to embed in metric space	Calculation time	Theorem's claim
$k=2$	20.59%	3.9453 sec	0.0065 sec	$0.1114 + O\left(\frac{h^2}{4}(14.6921)\right)$
$k=3$	42.86%	4.0530 sec	0.0081 sec	$0.7809 + O\left(\frac{h^2}{9}(281.1176)\right)$
$k=4$	64.38%	4.0152 sec	0.0070 sec	$2.6660 + O\left(\frac{h^2}{16}(1960.3205)\right)$

Table 3.7: GB network for the d_F metric

No. of subsets	Average isoparametric ratio	Time to embed in metric space	Calculation time	Theorem's claim
$k=2$	14.94%	14.0853 sec	0.1859 sec	$0.0663 + (8.7519)$
$k=3$	23.97%	13.3267 sec	0.2243 sec	$0.4360 + (156.9453)$

Table 3.8: GB network for the $\hat{d}_F$ metric

No. of subsets	Average isoparametric ratio	Time to embed in metric space	Calculation time	Theorem's claim
$k=2$	17.02%	862.8272 sec	0.0257 sec	$0.0663 + O\left(\frac{h^2}{4}(8.7519)\right)$
$k=3$	29.60%	1508.7453 sec	0.1335 sec	$0.4360 + O\left(\frac{h^2}{9}(156.9453)\right)$

Remark 3.44. *We see here that many of the theoretical claims are redundant as they are in fact larger than one, this is a reflection of the fact that this type of analysis is not applicable to these sort of network partitions.*

3.5 Evolving Set Processes

There are other algorithms in the literature which find subsets with a small parameter $\frac{\partial(S)}{w(S)}$ called conductance and referred to as $\phi(S)$ here for unweighted graphs. The conductance parameter resembles the Cheeger constant, definition 2.5, indeed the same definition for Conductance which is the ratio between the size of a boundary of a subset and its volume, the difference from the Cheeger constant being that there is no restriction of $w(S) \leq w(V)/2$ which means that the conductance will always be less

than or equal to the the Cheeger constant. We will find that these algorithms and their theoretical framework can be generalised to weighted graphs.

These algorithms main mechanism is called a volume biased evolving set process (ESP) devised by Diaconis and Fill in [48], which iteratively updates a vertex and subset pair (v, S). The first step of this algorithm Step 0 is to select an arbitrary starting vertex $v \in V$, the first vertex and subset pair is $(v, \{v\})$, the next vertex is chosen via a standard random walk using the weights of the edges so that the probability of moving to an adjacent vertex u is $b(v,u)/d(v)$. Next step is to update the subset $\{v\}$, if we take a measure on the vertices as follow,

$$q(x,y) = \begin{cases} b(x,y)/(2d(x)) & \text{if } \{x,y\} \in E, \\ 1/2 & \text{if } x = y \\ 0 & \text{otherwise.} \end{cases}$$

We form possible subsets from this measure q by taking our subset to be a set of vertices that has measure q higher that a set value $\tilde{q} \in (0,1)$. To satisfy a restriction that each one of these subsets must contains u we have to set $\tilde{q}$ less than $b(u,v)/(2d(v))$, then for a uniform choose of $\tilde{q}$ in the interval $(0, b(u,v)/(2d(v))$ we have a subset which contains vertex u.

We then recalibrate the probability kernels for the transition of $\{v\}$ to a subsets S' which is $K(v, S')$ to include a volume bias

$$\hat{K}(v, S') = \frac{Vol(S')}{Vol(S)} K(v, S').$$

Completing one iteration can be done by giving the second vertex subset pair as (u, S').

R. Andersen and Y. Peres in [2] construct an algorithm `EvoPartition` which iterate this volume bias ESP which terminates after $T \in \mathbb{N}$ iteration and outputs a subset S. This algorithm takes as an input a vertex $v \in V$ and a target conductance $\tilde{\phi}$.

Theorem 3.45. *`EvoPartition` performing $T \in \mathbb{N}$ iterations of the volume bias ESP.*

If $A \subseteq V$ is a set of vertices that satisfies $h(A) \leq h$ and $w(A) \leq (2/3)w(V)$, then there is a subset $A' \subseteq A$ with volume at least $w(A)/2$ such that whenever $v \in A'$, with probability at least $1/2$ the output set S satisfies all of the following:

(a) $\phi(S) = O(\phi^{1/2} \log^{1/2} |V|)$,

(b) $w(S) \leq (3/4)w(V)$,

(c) $w(S \cap A) \geq (9/10)w(S)$.

D. Spielman and S. Teng devised a similar algorithm `Partition` in [56] with a similar theoretical framework, this mainly focused on finding small cuts in very large sets whilst minimising the computational complexity. With a couple of tweaks we applied this algorithm to the IEEE 39-bus test case and found the minimal $\phi = 0.01$ cut in 5.2690 seconds, and when applied to the IEEE 118-bus test case we found a cut of $h = 0.0224$ in 97.3225 seconds.

Chapter 4

Hierarchical Spectral Clustering

Here we present a novel approach to spectral clustering algorithms within the context of electrical networks these are hierarchical spectral clustering algorithms. The previous algorithms in Chapters 2 and 3, have all used spectral information to give a partition of a graph into k subgraphs. The hierarchical spectral clustering algorithms will provide not only a partitioning into a pre-specified number of (k) subsets, but use the spectral information to give a partitioning scheme. This hierarchical partitioning scheme will inform partitions into any numbers of subsets and inform how subsets can be further clustered thus revealing the internal interconnectivity structure of the network. The results presented here have been published in [52].

Prior to this chapter we have only dealt with taking partitions with the objective of minimise the disruption caused to the electrical flow in the network, we have done this by weighting the Laplacian with the power flows within transmission lines. However the Laplacian can be weighed with any electrical measure of a transmission line. In this chapter we introduce the notion of weighting the Laplacian with the admittance measure of a transmission line (using the DC power model this can be approximated to be the inverse of the reactance) this measure can be thought of as the capacity of a line to carry electrical flow. Using the admittance measure the objective of these techniques will be to produce partitions with minimal loss of electrical capacity of the network.

The admittance is a static measure of a transition line, as opposed to the power flow which is of course dynamic. The technique presented in this chapter will have

further scope for implementation for the Laplacian weighted with the admittance than the Laplacian weighted with the power flows. A hierarchical scheme informed by the initial admittances produces clusters can then inform further sub-clustering routines, with the static measure of admittance these sub-cluster routines will be valid, with the dynamic measure of power flow a sub-routine from the initial power flows will no longer be valid as the power flows will have changed since the initial clustering.

4.1 Algorithm and Results

4.1.1 Hierarchical Spectral Clustering Algorithm

This approach does leave some uncertainty as to what spectral information to use. Previously we used the first k eigenvectors of the normalised Laplacian to embed the graph in k dimensions and partition into k subsets. Here we need to make a choice of how many eigenvectors of the normalised Laplacian to use and thus how many dimensions to embed a graph into, that will give an optimal scheme for partitioning the graph into any number of subsets.

Embedding Dimension: Algorithm Step 0

The first step of this algorithm is to determine the dimension we will embed the graph $G(V, E)$ into. As was mentioned before, a particular convention can be used to make this determination. Denoting eigenvalues of the normalised Laplacian operator as $\lambda_1, \lambda_2, \ldots, \lambda_n$, we calculate the relative gaps in the spectrum as follows,

$$\gamma_i = \frac{\lambda_{i+1} - \lambda_i}{\lambda_i}. \tag{4.1}$$

We take the embedding dimension to be the value i which gives γ_i to be one of the highest amongst the $n-1$ values, we will call this dimension k. Justification for doing this can be seen in appendix A.1.1, the justifications here revolves around perturbation theory. This choice will also depend on how many subsets we would like to form from the final schema. For example in the IEEE 118−bus test case, our relative eigen-gaps are illustrated below.

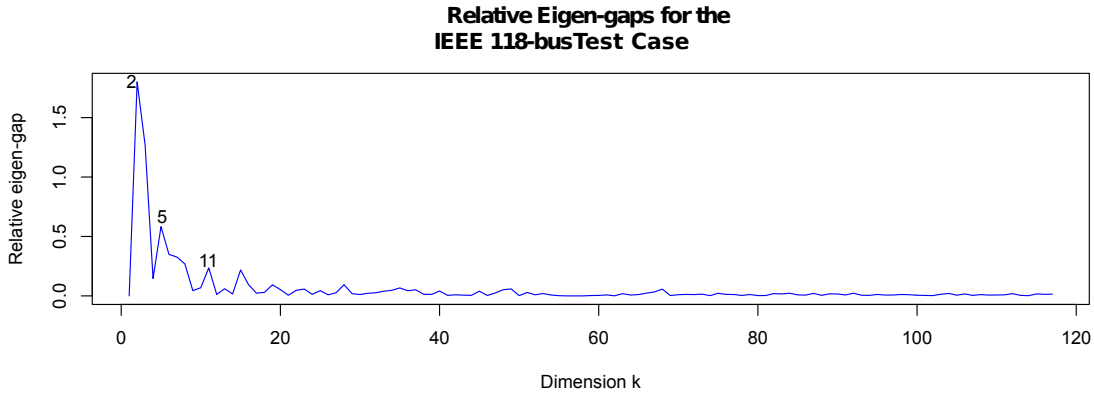

Figure 4-1:

At dimension two there is the highest spectral gap, but this will only be sufficient information to form partitions into two subsets (according to our previous theoretical framework) so 5 or 11 may be better options. This is more of a heuristic (or ad-hoc) method than one with a concise mathematical justification, but support for the approach can be seen in appendix A.1.1.

Embedding and Metric: Algorithm Step 1

This is the same as **Step 0** in section 3.2.1, here we determine the embedding and the metric, which is either Euclidean metric d_F or the shortest path metric $\hat{d}_F$.

Forming Dendrogram: Algorithm Step 2

This is the final step of the algorithm, where the schema for partitioning into any number of subgraphs is found, this is in the form of a dendrogram.

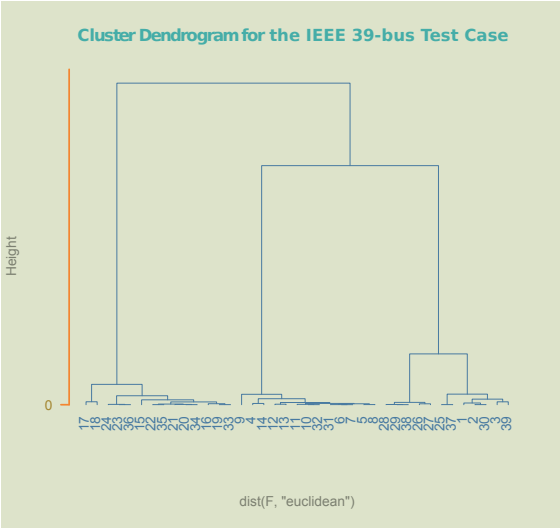

Figure 4-2: Dendrogram of the spectral 3 embedding of the system weighted by power flows.

This schema will give a partition for a given height as illustrated in figure 4-3, in this dendrogram the Blue, Green, Yellow and Red subsets of the IEEE 39-bus test case from the previous chapter (refer to figure 3-8) are shown.

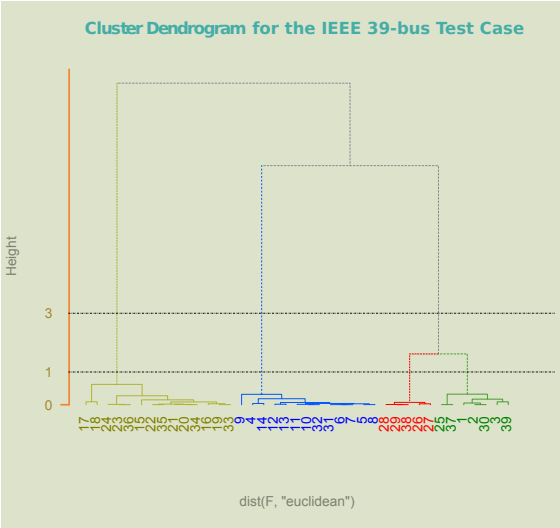

Figure 4-3: Dendrogram of the spectral 3 embedding of the system weighted by power flows. The Blue, Green, Yellow and Red islands are recovered at height 1, while cutting at height 3 suggests merging the Green and Red islands for a good 3-partition (cf. Fig. 1 and Table II). Long vertical lines in a dendrogram reveal a good clustering at that level.

The hight measure in the figure 4-3 (1 and 3) is a y coordinate measure, when given as an input to the dendrogram, the dendrogram will then give a partition. The partition is formed from the height input and can be seen by taking all nodes that are linked together by the branches of the dendrogram that are below the height. Crucially when forming a partition from a dendrogram all branches above the height are ignored, and the sets of vertices that are connected through the remaining branches are the clusters of the partition.

The process represented in the dendrogram is known as agglomerative clustering, this can be understood if we look at the results of the schema for height zero (where we would essentially ignore all branches of the dendrogram) and how this result changes for increased values of height when more branches connecting the vertices of the dendrogram are considered. When the height is equal to zero all connections between vertices in the dendrogram structure are ignored as all branches are ignored the vertices are all clusters themselves and are illustrated in dendrograms as the leaves of the dendrogram tree. If one were to continuously increase the high from zero one would first witness the single vertex clusters joining to from clusters of two vertices (these can be seen in the dendrogram structure as bridge shapes at the base of the structure), still increasing the height these clusters would in turn agglomerate with other clusters forming clusters of three or four vertices. As the height increases the n single vertex clusters agglomerate and form larger and larger clusters until the whole graph is joined.

The way that the height measure is taken will dictate the process of agglomeration (which appears as the horizontal branches of the dendrogram), there are several different ways which this can be done, the methods which gave the best experimental results was *'Ward's minimum variance method'* [67] and *'Single'*. When using the 'Single' method the construction of the dendrogram structure can be conceptualised in the following way for the height continuously increasing from zero; at height zero the resulting set of clusters of the dendrogram are the n single vertex clusters, when the hight is increased the first agglomeration occurs between vertices the have the minimum Euclidean distance between them, this agglomeration happens once the height is equal to than this distance. The way that distance between clusters is measured with 'Single' is the same as with definition 3.20 (the minimum distance between any vertex in one cluster and any vertex in the other cluster), when the height is increased

further more agglomeration occurs when the height is equal to the minimum distance between any pair of clusters at which point these clusters are agglomerated. For the method 'Single' the height in this way is the upper bound of any distance between clusters, but to appreciate the dendrogram's construction this height must be increase continuously from zero. When the method 'Ward' is used to construct a dendrogram this means that the variances of all clusters is measured in a similar way to how the distance as in definition 3.20 was measured in the construction of the dendrogram using the 'Single' method. For height zero all clusters must have zero variance in their vertex coordinates, which means that the clusters the dendrogram would give is the n single vertex clusters. The variance of any two pairs of the n vertices would be non-zero, the pair of vertices that give the minimum variance out of these $n(n-1)/2$ possible pairs will be the first agglomeration of the dendrogram structure once the height is equal to this variance. When the heigh is increased further more agglomeration occurs when a pair of clusters exist which are such that if their vertices were considered in one set the variance of the coordinates of the vertices of that set would be less an the height, then that pair of clusters will agglomerate. For both the 'Single and 'Ward methods we have outlined the starting point of the dendrogram construction and the point at which agglomeration occurs, this is all that is needed to appreciate the whole construction which for height zero give clusters all vertices into n single vertex clusters up to giving the whole graph as one cluster for large height. The 'Ward' method can only be used for Euclidean metric thus only for d_F and not $\hat{d}_F$. The 'Single method can be used with $\hat{d}_F$ as opposed to the Euclidean metric.

4.1.2 Results

We have applied our algorithm to the IEEE 39-bus and 118-bus test cases, and the GB network for *power flows*. Illustrated in this table are some of the more successful results.

Table 4.1: Results from systems

	Method	Dimension	$k =$	$\rho_G(k)$	Metric	Time
39-bus	Single	5	4	4.51%	$\hat{d}_F$	0.1410 sec
118-bus	Single	8	6	9.29%	d_F	0.3593 sec
GB	Ward	16	11	6.46%	d_F	8.1564 sec

For the 39-bus test case as we saw in the previous chapter the higher order Fiedler partitioning method finds $\rho_G(4) = 0.0451$ and an **Alternative Algorithm** proposed in section 3.4 will have a non-zero probability of finding this partition. However for dimension 5 and for the $\hat{d}_F$ metric the hierarchical spectral clustering algorithm finds this many times faster.

4.2 Hierarchical Spectral Clustering with Admittances and Comparisons with Evolutionary Algorithm

When using the admittance to weight the graph Laplacian our hierarchical spectral clustering algorithm (SC) has a similar philosophy to [4], in that they both use a static distance measure to inform partitions, the main difference being that in [4] electrical distances are used, where as in our approach spectral information of the graph Laplacian weighted by the admittances is uses to give a distance. [16] builds on [4] to give testable partitioning algorithm, this means that when we use our algorithm as a partitioning tool we can compare results with those given in [16]. We do this for a 3-way partition of the IEEE 118-bus test case and a 5-way partition of a Polish network which consists of 2,383 buses (1,733 buses after removing leaf-nodes). The algorithm in [16] is a evolutionary algorithm (EA) meaning that it has a fitness score associated with a partition which is its quality measure, we will be comparing our quality measures (the isoparametric ratios of subsets) and the fitness scores for resulting partitions of both algorithms. For the IEEE 118-bus test case we set $k = 3$ in our spectral clustering and for the Polish network we set $k = 4$ in our spectral clustering (referred to as SC in the table).

Table 4.2: Results from systems

	Fitness	Ratio 1	Ratio 2	Ratio 3	Ratio 4	Ratio 5
118-bus EA	0.2822	3.95%	2.54%	1.28%	- -	- -
118-bus SC	0.2729	3.52%	2.17%	0.99%	- -	- -
Polish EA	0.2271	5.53%	5.12%	3.45%	2.33%	2.05%
Polish SC	0.2189	4.00%	2.47%	2.18%	1.41%	1.08%

For the IEEE 118-bus test case and for the Polish network, as could be expected our quality measure of the isoparametric ratios is better for the our spectral clustering than those achieved by the EA, and the fitness measure is better for the EA than that achieved by the our spectral clustering. The measures are all very similar, and the resulting partitions for the IEEE 118-bus test case are in fact the same for both algorithms apart from four vertices.

There is a strong correlation between the electrical distance used in the EA and the d_F distance used in our spectral clustering. This along with the fact that the fitness score tries to maximise inter connectivity within subsets, minimise connectivity between subsets and at the same time balance the subset sizes. This is essentially the same objectives as we have for our spectral clustering, expressed by minimised the isoparametric ratios.

4.3 Further

The novelty of this approach is its ability to further sub-cluster the structure of an electrical network beyond its initial partitioning, this is in large part the reason for the choice of the hierarchical clustering methodology. Beyond preventative islanding as an application of the algorithm, another possible application could be as a visualisation tool. In this case a systems operator could identify in an instant, by observing the dendrogram, which clusters of nodes form stable islands. This application could be valuable in circumstances where intervention is required.

There is potential for the algorithm to be improved further, using tuning techniques similar to those seen in [66]. Here the partition produced by the algorithm is treated as a suggestion and further process is performed. This processing is a trail and error

technique, that identifies nodes, which lie at the periphery of some islands and potentially have a certain amount of ambiguity as to which islands they belong to (according to the embedding). Such a node could alternatively belong to a neighbouring island, this presents an alternative clustering that would be tested. In this way the partition can be tuned and potentially improved.

Chapter 5

Two-Step Clustering

Thus far our justification for the utility of spectral clustering techniques for power system islanding has been that they minimise the disruption to power flow in the network. We have argued that the minimisation of power flow disruption should take president over power flow imbalance, but there are many more considerations that could be taken when islanding a power system such as: generator coherency, thermal limits of transmission lines, voltage stability, transient stability, etc.

Thus far we have also ignored the oscillatory nature of the electrical flow by taking the DC approximation of AC flow. As discussed in chapter 2 section A.3 generators are essentially rotating magnets surrounded by coils, and thus produce an alternating current, the phase angle difference between these generators will determine how power dissipates though the system. For a system to be stable the generators have to be synchronised and are engineered to be, however when failures occur these generators can fall out of sync making the system unstable. There is a measure for how *coherent* a pair of generators are, if a pair of generators would tend to rotate in sync together in a system then they have a high measure of coherency, if a pairs of generators would tend to drift and to rotate out of sync with one another then they have a low measure of coherency. To add this dynamic element of *generator coherency* to partitioning algorithms L Ding, F Gonzalez-Longatt et al in [18] devised a two-step spectral clustering algorithm. In the first step of their algorithm a weight of the coherency is given between all pairs of generators with the objective of grouping pairs of generators with high coherency and separating pairs of generators with low coherency. In the second step to partition

the rest of the system the same considerations are taken as before, namely the power flows and the minimisation of the power flow disruption, however the final partitions is restricted by the generator groupings established in the first step which must be present in the final partition.

5.1 Algorithm and Results

5.1.1 Two-step Spectral Clustering Algorithm

Forming Coherent Generators Groups: Step 0

We take as an input: the full admittances (which is the inverse of the impedance see A.6) for every edge Ad whose entries are imaginary numbers, the phase angle differences of the generators $\delta_1, \delta_2, \ldots, \delta_g$ and the voltage potentials of the generators $V_1, V_2, \ldots, V_g$ (where g is the number of generators). We then identify the generator vertices V_G and reorder so that the information of the generator vertices is given in the last rows and columns of Ad. Ad can be now given as

$$Ad = \begin{pmatrix} Ad_a & Ad_b \\ Ad_c & Ad_d \end{pmatrix}.$$

We form the generator coherency matrix with the following equation (see [53, p. 214]).

$$B' = abs(imag(Ad_d + Ad_c(Ad_a)^{-1}Ad_b)).$$

We then take the off diagonal entries of our Laplacian in this first step to be,

$$[\mathcal{L}_D]_{ij} = -|V_i| \cdot |V_j| B'_{ij} \cos(\delta_i - \delta_j)$$

these are in fact the synchronising coefficient. To complete this as a Laplacian take the diagonal entries to be $[L_D]_{ii} = -\sum_{j=1}^{n} L_{Dij}$.

We then take the the inertia coefficients of each generator $H_1, H_2, \ldots H_g$ (this is a measure of the physical inertia of the rotating magnet) so the matrix $M = diag\{1/(2H_1), 1/(2H_2), \ldots, 1/(2H_g)\}$.

With the first two nontrivial eigenvectors from the system $ML_D = \lambda v$ of this un-

normalised Laplacian we embed into $\mathbb{R}^2$, and then partition using k-medoids algorithm to give the coherent groupings of generators V_{G_1} and V_{G_2} (consisting of g_1 and g_2 generators respectively).

Partitioning the Rest of the Graph: Step 1

In this step we will partition the rest of the graph whilst preserving the coherent generator groups. The following matrix will essentially enforce the coherent generator grouping in the first step to persist in any subsequent partition formed. Illustrating this here for $k = 2$ so two generator groups are formed in step one, with sizes of g_1 and g_2 generators this can be generalised to k group see [63].

Note that for this to work we would need to relabel the vertices to the first g_1 vertices are those of the first generator group V_{G_1} and the next g_2 vertices are those of the second generator group V_{G_2}.

$$U = \begin{pmatrix} 1_{g_1} & 1_{g_1} & 0_{g_1\times(n-g)} \\ 1_{g_2} & -1_{g_2} & 0_{g_2\times(n-g)} \\ 1_{n-g} & 0_{n-g} & I_{(n-g)\times(n-g)} \end{pmatrix}.$$

Within this matrix 1_l, 0_l are one vectors of length l and zero vectors of length l respecively. $0_{l_1\times l_2}$ are zero matrices of dimension $l_1 \times l_2$ and $I_{(n-g)\times(n-g)}$ is a $(n-g)\times(n-g)$ identity matrix.

As in previous chapter with the Laplacian weighted with the power flow we take the first two nontrivial eigenvectors, here we do this for the system $U^T\mathcal{L}Uv = \lambda U^T DUv$ we use these eigenvectors Uv_1 and $Uv_2 \in \mathbb{R}^n$ to form an embedding of V in $\mathbb{R}^2$. U essentially reduces the dimension of the system from n to $n-g+2$ where the generator sets are each considered as one node. When forming the embedding in $\mathbb{R}^n$ using Uv_1 and Uv_2 as the generator sets are considered as one node, the nodes of each generator sets embedded to the same coordinatein $\mathbb{R}^n$. K-mediods algorithm is then performed on this embedding giving the final partition $V_1, V_2 \subset V$.

5.1.2 Results of Two-step Spectral Clustering

The objectives of the two-step spectral partitioning algorithms objective as stated in [18] is as follows: for the generator groupings,

$$\min_{V_{G_1}, V_{G_2} \subset V_G} \sum_{v_i \in V_{G_1}} \sum_{v_j \in V_{G_2}} \left(\frac{\partial P_{ij}}{\partial \delta_{ij}} \cdot \left(\frac{1}{H_i} + \frac{1}{H_j} \right) \right), \tag{5.1}$$

and for the partition of the rest of the graph

$$\min_{V_1, V_2 \subset V} \sum_{v_i \in V_1, v_j \in V_2} |P_{ij}|. \tag{5.2}$$

It becomes apparent when running this algorithm for the IEEE 39-bus test case that the persistence of the generator groupings established in the first step of the algorithm are not guaranteed in the final partition. The use of the matrix U effectively projects the solutions space of the second step from n dimensions to $n - g + 2$ where the vertices of generator groups V_{G_1} and V_{G_2} are embedded to the same coordinate there is no guarantee that these coordinates will be separated by the implementation of k-mediods. It would become less of an issue for larger systems but for the IEEE 39-bus test case the generator groupings persist 66.3% of the time, however there are ways to penalise more heavily the grouping of the generator groups in this step (see [63]).

In the table below we have the results of this in the form of the two objective measures of [18] (5.1) and (5.2), also the isoparametric constant (our quality measure of previous chapters), an analogous isoparametric measure for the generator groupings and the average time take to run the simulation.

Table 5.1: Results for Two-step Spectral Clustering of IEEE 39-bus test case

	(5.1)	(5.2)	Generator ratio	Partition ratio	Average time
39-bus	2.3134	646.7976	61.90%	15.69%	0.0116 sec

The Generator ratio isoperimetric ratio is particularly large because partitions are formed that group the generator at bus 39 by itself giving a ratio of one but a small measure in (5.1).

5.1.3 Alternative Two-step Algorithm

Here we will propose an alternative algorithm to the one presented in 5.1.1, this algorithm will differ in that k-medoids will not be used to partition the embedded vertices, instead a Fiedler vector implementation will be made. In effect a Fiedler vector step should go beyond k-medoids as it explores all possible partitions resulting from an embedding of just the first nontrivial eigenvector and take to best one according to an isoparametric quality measure. From the theoretical framework shown in chapter 2 there should be no extra benefit from including the spectral information of the second non trivial eigenvector when bisection the graph.

In this algorithm we also polarise embedding coordinates of the two generator set in the second step. With the current construction the first generator group has a positive coordinate 0.24 and second generator group has a negative coordinate -0.24; if we instead place them at 1 and -1 respecively this effectively guarantees the separation of the generator groupings. The results are shown below.

Table 5.2: Results for Alternative Two-step Spectral Clustering of IEEE 39-bus test case

	(5.1)	(5.2)	Generator ratio	Partition ratio	Average time
39-bus	2.3825	482.9382	23.11%	8.86%	0.0250

Here we see that the (5.1) measure for the generator grouping is similar but not quite as optimal as the previous algorithm. The generator isoparametric ratio is considerable smaller. The partitioning as a whole is improved for L. Ding and Gonzalez-Longatt's measure (5.2) and our isoparametric ratio measure has almost halved.

This algorithm has the added benefit of being deterministic and having the theoretical framework of Chapter 2 behind it. It does however require more that twice the computation time.

Chapter 6

Connes Metric

In this Chapter we begin an investigation of a different way of characterising the metric structure of a space, which is equipped with a particular differentiation operator. This uses a key idea of Connes, which is central to his noncommutative geometry. However, there are very few specific examples of computation of the Connes metric, and this investigation provides a potential source of examples for applications of this metric. The Connes metric on a space is a metric that is determined by a differential constraint on the operator algebra of that space. We will see here that the Connes metric can be related to more familiar classical metrics, commencing this chapter by looking at classical metrics and then finding instances where classical metrics coincide with the Connes metric.

We will introduce two constructions of the discrete Connes metric. One approach is by Davies in [17] and the other by Requardt in [51]. This will lead onto the computation of the Connes metric later in chapter 7, which has not been explicitly solved in the literature, the computation of the Connes metric for general graphs is a subtle and nontrivial problem. We believe that the Connes metric will have significance in electrical networks, to reinforce this conviction, we also introduce a metric specifically devised to show distance in electrical networks (the resistance metric) and show similarities between the metric for particular forms. Also to find a strong relationship between Thevenin's impedance and the Connes metric.

6.1 Classical Metrics

In classical geometry the path distance between two points (or coordinates) is defined by the length of the shortest path between those points, where a path is defined on a space X, as a simple curve that can be given as a continuous function from a parameter space to X.

For any two points $p, q \in X$

$$d_I(p,q) = \inf\{L(\gamma) : \gamma \text{ continuous curve in } X \text{ between } p \text{ and } q\}. \tag{6.1}$$

While defining the distance in this way conveys the right intuition, it is not easy to compute of distance between any two points. To construct a viable computational scheme, one needs to link the global information in (6.1) with the local properties of the space.

Before we introduce another classical metric we must define the norm on a space X of a vector $v \in X$ this is $\|v\| = \langle v, v\rangle_X^{1/2}$.

$$d_S(p,q) = \sup_{f \in C^\infty(X)} \{|f(p) - f(q)| \big| \|\nabla(f(x))\|_X \leq 1 \text{ for all } x \in X\}, \tag{6.2}$$

where $\|\nabla(f(x))\|_X = (\langle \nabla(f(x)), \nabla(f(x))\rangle_X)^{1/2}$.

As motivation for our later discussion, let us check that the two metrics (6.1) and (6.2) agree on $\mathbb{R}^n$.

In the following lemma the $\|\cdot\|_\infty$ norm is given as follows

$$\|\nabla(f)\|_\infty = \left(\sup_{w \in \mathbb{R}^n} \langle \nabla_w(f), \nabla_w(f)\rangle\right)^{1/2}$$

where ∇_w is,

$$\nabla_w(f) = \left(\frac{\partial f}{\partial x_1}(w), \frac{\partial f}{\partial x_2}(w), \ldots, \frac{\partial f}{\partial x_n}(w)\right).$$

Lemma 6.1. *If there is a uniform Lipschitz constant for f in $\mathbb{R}^n$ then $\nabla(f)$ is uniformly bounded.*

Proof. Given that the function f is Lipschitz $\forall x, y \in \mathbb{R}^n$ (where $x = (x_1, x_2, \ldots, x_n)$

and $y = (y_1, y_2, \ldots, y_n)$) there exists constant $C \in \mathbb{R}$ such that,

$$\|f(x) - f(y)\|_{\ell^2} \leq C\|x - y\|_{\ell^2}.$$

If we take $y(t) = (x_1 + t, x_2, \ldots, x_n)$ and using the Lipschitz condition of f we have,

$$\begin{aligned} \Big|\frac{|f(x) - f(y(t))|}{t}\Big| &\leq C \\ \lim_{t\to 0}\Big|\frac{f(x) - f(y(t))}{t}\Big| &\leq C \\ \therefore \Big|\frac{\partial f(x)}{\partial x_1}\Big| &\leq C. \end{aligned}$$

The same procedure can show this bound for partial derivatives of any dimension thus we have the following,

$$\|\nabla_x(f)\| = \left(\sum_{j=1}^{n} |\partial_j(f(x))|^2\right)^{1/2} \leq \sqrt{n}C.$$

As this is for all $x \in \mathbb{R}^n$ we have,

$$\|\nabla(f)\|_\infty = \left(\sup_{w\in\mathbb{R}^n} \|\nabla_w f\|^2\right)^{1/2} \leq \sqrt{n}C.$$

Completing the proof.

□

Theorem 6.2. *Let a be a Lipschitz function which is continuous on $\mathbb{R}^n$ and smooth on $\mathbb{R}^n$ except on a finite set of point $p_1, p_2, \ldots, p_r \in \mathbb{R}^n$. Then a can be approximated uniformly by a smooth function which is also Lipschitz and with the same constant as a.*

Proof. Let $p \in \{p_1, p_2, \ldots, p_r\}$ be a point where not all derivatives of a exist.

Using the Stone-Weierstrass theorem A.9 here there exists a sequence of functions $f_i \in C^\infty(\mathbb{R}^n)$ where $f_i \to a$ uniformly on a ball $\bar{B}_R(p)$ (for $R > 0$ this is a compact subset of $\mathbb{R}^n$) and $\forall \epsilon > 0$ there exists $N \in \mathbb{N}$ such that $\forall i > N$ and $\forall x \in \bar{B}_R(p)$ we have,

$$|f_i(x) - a(x)| \leq \epsilon.$$

Say that we take the radius r to be larger enough so that the ball $\bar{B}_R(p)$ includes all points where a is not smooth ($\{p_1, p_2, \ldots, p_r\} \subset \bar{B}_R(p)$). Then $\forall\, x, y \in \bar{B}_R(p)$,

$$|f_i(x) - f_i(y)| \leq |f_i(x) - a(x)| + |a(x) - a(y)| + |a(y) - f_i(y)| \leq 2\epsilon + C|x - y|, \quad (6.3)$$

for large enough N (taking the Lipschitz constant for a to be $C \in \mathbb{R}$ here). As ϵ can be as small as you like we have that (6.3)

$$\implies |f_i(x) - f_i(y)| \leq C|x - y|.$$

□

Remark 6.3. *Note here that in the previous proof for the sequence of functions f_i to be a smooth uniform approximation of a on $\mathbb{R}^n$, we take f_i to be equal to a on $\bar{B}_R \subset \mathbb{R}^n$ and a is such that it is smooth on the boundary of B_R.*

We will also assume that at the boundary of $\bar{B}_R \subset \mathbb{R}^n$ the function We will also assume that for all points in $\mathbb{R}^n$ where a is not smooth ($\forall p \in \{p_1, p_2, \ldots, p_r\}$) and for all $i \in \mathbb{N}$, we have

$$\|\nabla(f_i)(p)\| \leq \sup_{x \in \mathbb{R}^n \setminus \{p_1, \ldots, p_r\}} \|\nabla_x(a)\|. \quad (6.4)$$

Theorem 6.4. *For any $p, q \in \mathbb{R}^n$*

$$d_I(p, q) = d_S(p, q).$$

Proof. In the case of $\mathbb{R}^n$ it is given that the shortest distance between any two points $p, q \in \mathbb{R}^n$ is along a straight line and is equal to the Euclidean distance (which we will refer to as d) $d_S(p, q) = d(p, q) = \|p - q\|$ with the standard $\ell^2(\mathbb{R}^n)$ norm.

$a : \mathbb{R}^n \to \mathbb{R}$ is Lipschitz if there exists a constant $C \in \mathbb{R}$ such that for any points $x, y \in \mathbb{R}^n$ we have $C \in \mathbb{R}$ where $|a(x) - a(y)| \leq Cd(x, y) = C\|x - y\|$. In accordance with (6.2) $a \in C^\infty(\mathbb{R}^n)$, where $\gamma : [0, 1] \to \mathbb{R}^n$ is a smooth curve.

$\gamma(0) = p$, $\gamma(1) = q$.

$$\begin{aligned} a(p) - a(q) &= a(\gamma(0)) - a(\gamma(1)) \\ &= \int_0^1 \frac{d}{dt} a(\gamma(t)) dt = \int_0^1 \langle \underbrace{\nabla_{\gamma(t)} a}_{(\nabla_{\gamma(t)} a)^T}, \gamma'(t) \rangle dt. \end{aligned}$$

Using the chain rule $Da(\gamma(t)) = (Da)(\gamma(t)) \circ (D\gamma)(t)$.

$$\begin{aligned} |a(p) - a(q)| &= \Big| \int_0^1 \langle \nabla_{\gamma(t)}(a), \gamma'(t) \rangle dt \Big| \\ &\leq \int_0^1 |\langle \nabla_{\gamma(t)}(a), \gamma'(t) \rangle| dt \\ &\underbrace{\leq}_{Cauchy-Schwartz} \int_0^1 \|\nabla_{\gamma(t)}(a)\| \|\gamma'(t)\| dt \qquad (6.5) \\ &\leq \|\nabla(a)\|_\infty \int_0^1 \|\gamma'(t)\| dt \qquad (6.6) \\ &= \|\nabla(a)\|_\infty l(\gamma). \qquad (6.7) \end{aligned}$$

Note in (6.7) $l(\gamma)$ is equal to the length of the line γ. (6.5) implies (6.6) here because $\|\nabla(a)\|_\infty = \left(\sup_{x \in \mathbb{R}^n} \underbrace{\langle \nabla_x(a), \nabla_x(a) \rangle^{1/2}}_{\|\nabla_x(a)\|} \right)$.

We know that the Euclidean distance (which we will call d) is equal to the shortest path metric so:

$$d(p, q) = \inf\{l(\gamma) | \gamma \text{ is a continuous curve connecting } p \text{ and } q\},$$

and from (6.7) we have

$$|a(p) - a(q)| \leq \|\nabla(a)\|_\infty l(\gamma).$$

So for $\|\nabla(a)\|_\infty \leq 1$ (a constraint of a in (6.2)), we have that $|a(p) - a(q)| \leq l(\gamma)\ \forall \gamma$ for continuous curve $\implies |a(p) - a(q)| \leq d(p, q)$ as $d(p, q) = l(\gamma)$ when γ is a straight line between p and q.

So

$$\sup_{\forall a \in C^\infty(\mathbb{R}^n)} \{|a(p) - a(q)| \Big| a \in C^\infty(\mathbb{R}^n), \|\nabla(a)\|_\infty \leq 1\} \leq d(p, q). \qquad (6.8)$$

Now take $p \in \mathbb{R}^n$, $a_p(x) = \|p - x\|$. This is C^1 except at $p \in \mathbb{R}^n$

$$a_p(x) = \left(\sum_{i=1}^{n} |x_i - p_i|^2 \right)^{1/2}.$$

However the function $a_p : \mathbb{R}^n \to \mathbb{R}$ isn't a valid candidate according to (6.2) as the function must be a smooth function on $\mathbb{R}^n$. The function is Lipschitz (with a Lipschitz constant $C = 1$), which can be shown as follows $\forall\ x, y \in \mathbb{R}^n$

$$|a_p(x) - a_p(y)| = |\|x\| - \|y\|| \leq \|x - y\| = d(x, y).$$

We can use theorem 6.2 on a to show that this can be uniformly approximated by a sequence of functions f_i that are smooth and is Lipschitz with the same Lipschitz constant. Using Lemma 6.1 we know also that $\|\nabla(f_i)\|_\infty$ is finite.

As we assume (6.4) we have $\lim_{i\to\infty} \|\nabla(f_i)\|_\infty = 1$.

$$\begin{aligned}
\sup_{\forall a \in C^\infty(\mathbb{R}^n)} \left\{ |a(p) - a(q)| \middle| a \in C^\infty(\mathbb{R}^n), a \text{ is Lipschitz, } \|\nabla(a)\| \leq 1 \right\} & \\
\underbrace{\geq}_{\text{for } \lim_{i\to\infty} f_i = a} & \big| \|p - p\| - \|q - p\| \big| \\
= \|q - p\| & \\
= d(p, q). & \qquad (6.9)
\end{aligned}$$

From (6.8) and (6.9) we have

$$\sup \left\{ |a(p) - a(q)| \middle| a \in C^\infty(\mathbb{R}^n), a \text{ is Lipschitz}, \|\nabla(a)\| \leq 1 \right\} = d(p, q).$$

□

6.2 Operator Framework

The idea that Connes introduced in his book on noncommutative geometry [15], was to have an analogous distance to the supremum metric (6.2) but where the constraint is an operator constraint not a differential constraint.

Definition 6.5. ***(Operator norms)*** *For a Hilbert space $\mathcal{H}$ (refer to appendix A.2) the norm of an operator on $\mathcal{H}$ given by $P : \mathcal{H} \to \mathcal{H}$,*

$$\|P\|_{Op} = \sup_{C \in \mathcal{H}, \|C\|=1} \{\|P(C)\|_{\mathcal{H}}\}.$$

To use a metric analogous to the supremum metric in classical geometry (6.2), we have to devise an analogy for $\|\Delta(f(x))\| \leq 1$ for all $x \in X$. This will be $\|[D, \pi(f)]\|_{Op} \leq 1$, where the square brackets indicate a commutator and $\pi(f)$ is the operator of pointwise multiplication by f so that $(\pi(f)(\psi))(x) = f(x) \cdot \psi(x)$. To evaluate the operator norm $\|[D, \pi(f)]\|_{Op}$, we have to know how this acts as a operator so for any $\psi \in \mathcal{H}$

$$[D, \pi(f)](\psi) = D\pi(f)(\psi) - \pi(f)D(\psi) = D(f)(\psi) + \pi(f)D(\psi) - \pi(f)D(\psi) = D\pi(f)(\psi). \tag{6.10}$$

Thus the operator norm,

$$\|[D, \pi(f)]\|_{Op} = \sup_{\forall \psi \in \mathcal{H}} \|D\pi(f)(\psi)\|.$$

6.2.1 Spectral Triple

To introduce the Connes metric first we have to define a spectral triple. Forming a spectral triple is equivalent to creating a representation of an algebra $\mathscr{A}$, in the pair $(\mathcal{H}, F)$ (where $\mathcal{H}$ is a Hilbert space and F is a self adjoint operator (refer to appendix A.3) acting on $\mathcal{H}$).

Definition 6.6. ***(C*-algebra)*** *If $\mathscr{A}$ is a Banach involution algebra, the norm and the involution must also satisfy for all $A \in \mathscr{A}$, $\|A^*A\| = \|A\|^2$, $\mathscr{A}$ is a C^*-algebra.*

This can be otherwise stated in the following axioms;

For all A and B in $\mathscr{A}$,

1. $\|AB\| \leq \|A\| \cdot \|B\|$.
2. $(AB)^* = B^*A^*$.
3. $\|A\| = \|A^*\|$.
4. $\|A^*A\| = \|A\|^2$.

Example 6.7. *The algebra $\mathscr{A}$ of all bounded operators on $\ell^2(V)$ is a C^*-algebra.*

Definition 6.8. ***(Resolvent of an Operator)*** *The resolvent of an operator $A : \mathcal{H} \to \mathcal{H}$ is given by $R(z; A) = (A - zI)^{-1}$: if there exists a value $z \in \mathbb{Z}$ such that this resolvent exists, is a bounded linear operator, is defined on a dense subset of $\mathcal{H}$ and is a compact operator (refer to appendix definitions A.4, A.5, A.6 and A.7).*

Definition 6.9. ***(Spectral Triple)*** *A spectral triple $(\mathscr{B}, \mathcal{H}, D)$ is given by a C^*-algebra $\mathscr{B}$ which can be represented as an algebra of operators on a Hilbert space $\mathcal{H}$ and a self adjoint operator D with compact resolvent such that a commutators $[D, \pi(a)]$ are bounded operators for all $a \in \mathcal{H}$.*

Here is a simple example to show that using the Connes metric can uncover the Euclidean metric distance.

Example 6.10. *Take $D = \frac{\partial}{\partial s}$, the operator of differentiation acting on the space $C^\infty(\mathbb{R})$ smooth functions on the real line.*

Consider a function $f \in C^\infty(\mathbb{R})$ as a linear operator on $C^\infty(\mathbb{R})$, where the action is given by point-wise multiplication, once this is established we can form the commutator $[D, \pi(f)] = D \cdot \pi(f) - \pi(f) \cdot D$, this itself is an operator on $C^\infty(\mathbb{R})$. For every $g \in C^\infty(\mathbb{R})$ we have from (6.10) that

$$[D, \pi(f)]g = \pi\left(\frac{\partial f}{\partial s}\right) g.$$

Hence the commutator $[D, f]$ acts as the operator of point-wise multiplication by $\frac{\partial f}{\partial s}$.

In this case the Connes metric maybe defined as follows. For all $p, q \in \mathbb{R}$,

$$d_c(p, q) = \sup\{|f(p) - f(q)| \big| f \in C^\infty(\mathbb{R}), \|[D, f]\|_{Op} \leq 1\}.$$

Note that by mean value theorem

$$|f(p) - f(q)| = f'(c)|p - q|$$

for some $c \in (p, q)$.

By our previous calculation, $[D, \pi(f)] = \pi(\frac{\partial f}{\partial s})$ and $\|[D, \pi(f)]\| = \|\pi(\frac{\partial f}{\partial s})\|_{Op} = \|\frac{\partial f}{\partial s}\|_\infty$, the ℓ^∞-norm.

Hence the condition that $\|[D, f]\| \leq 1$*, implies that* $|\frac{\partial f}{\partial s}(c)| \leq 1$ *and so* $|f(p)-f(q)| \leq |p-q|$ *for all* $f \in C^\infty(\mathbb{R})$ *such that* $\|[d, f]\| \leq 1$*. This implies that*

$$d_c(p, q) \leq |p - q|.$$

But note that function $f(x) = x$ *also satisfies Connes condition and* $\|\frac{\partial f}{\partial s}\|_\infty = 1$*. Hence the supremum in the definition of the Connes metric is attained and*

$$d_c(p, q) = |p - q|.$$

6.3 Discrete Connes Metric

We are now going to adapt Connes general definition to the special case of graphs. To successfully define a Connes metric on this space we need to define a spectral triple, there is no unique way of doing this.

We shall describe two approaches of constructing a discrete version of the Connes metric, both are devised by Davies in [17]. In [17] Davies focuses on one of these two constructions, defining three different forms of the discrete Connes metric and uses them to provide tighter bounds on the heat kernel (functions which determine how heat dissipates through a system). Davies forms these tighter bounds by first proving a number of estimates for the Connes metric, in terms of more established graph metrics, see later. It is Requardt in [51] that uses the other construction and attempts to calculate the Connes metric for some simple constructions.

Both of these approaches are equivalent, but each contributes different insights. We will review both of these approaches here.

6.3.1 Davies' Discrete Connes Metric

Our goal here is to construct a Connes metric on the space V of graph vertices. We will do this by defining a suitable operator algebra for operators which act on real valued functions on V.

After the follow three definition we will be able to define Davies' Hilbert space $\mathcal{H}$ for his version of the spectral triple. First we need a definition of the trace.

Definition 6.11. ***Separable Hilbert Space*** *A Separable Hilbert space is a Hilbert space that have a countable orthogonal basis.*

Definition 6.12. ***(Trace)*** *Given any orthogonal basis $\{e_k\}_k$ of a separable Hilbert space $\mathcal{H}$, the trace of a bounded linear operator A is as follows,*

$$trace(A) = \sum_k \langle Ae_k, e_k \rangle.$$

$(\mathscr{A}, \tau)$ this is the algebra of bounded operators on $\ell^2(V)$ and τ is the usual trace. The following definition illustrates how we will take a norm of an operator.

Definition 6.13. *For the linear bounded operator $T : \ell^2(V) \to \ell^2(V)$ where $\ell^2(V)$ is a separable Hilbert space and $p \in [1, \infty)$ the Schatten p-norm is defined to be,*

$$\|T\|_p = \left(\sum_{i \geq 1} s_i(T)^p \right)^{1/p}, \tag{6.11}$$

where $s_i(T)$ are the square roots of eigenvalues of the symmetric positive definite $T^*T : \ell^2(V) \to \ell^2(V)$.

Remark 6.14. *Recall from the spectral theory that the spectrum of a compact operator consists of a sequence of eigenvalues which converging to zero.*

Definition 6.15. ***(L^p)*** *The space of operators L^p is a noncommutative L^p spaces that are associated $(\mathscr{A}, \tau)$ where τ is the usual trace,*

$$L^p = \{T \in \mathscr{A} \big| \sum_{n \geq 0} s_n(T)^p < \infty\}$$

(which is the same as the Schatten p-norm in (6.11)). For the norm of any operator $T \in L^p$,

$$\|T\|_p = (trace(|T|^p))^{1/p}.$$

For Davies Hilbert space $\mathcal{H}$ we will take $p = 2$ this means we have a Schatten 2-norm defined in definition 6.13. This is also called a Hilbert-Schmidt and can be

expessed as follows,

$$\|T\|_2^2 = (\text{trace}(|T|^2)) = (\text{trace}(|T^*T|)) = \sum_{i=1}^{n} \langle T^*Te_i, e_i\rangle = \sum_{i=1}^{n} \langle Te_i, Te_i\rangle = \sum_{i=1}^{n} \|Te_i\|_2^2. \tag{6.12}$$

Definition 6.16. *The innerproduct for any two operators T and $U \in \mathcal{H} = L^2$*

$$\langle T, U\rangle_{L^2} = trace\,(TU^*)\,.$$

Remark 6.17. *Definition 6.15 in fact defines the pth Schatten class.*

Note that in notation we will take $\ell^p(\mathscr{A})$ to be L^p.

We want now to introduce Davies $\mathscr{B}$ the C^*-algebra of the spectral triple that can be represented as operators on the Hilbert space, we will first go through two more definitions.

Definition 6.18. ***(Diagonal Operators)*** *Let δ_i be a Dirac delta function defined by*

$$\delta_i(k) = \begin{cases} 1 & \text{if } i = k \in V, \\ 0 & \text{otherwise.} \end{cases}$$

Then a diagonal operator B is defined by the property,

$$\langle B\delta_i, \delta_j\rangle = 0$$

if $i \neq j$.

Definition 6.19. ***(Representation π)*** *The operator of pointwise multiplication by a function $f \in \ell^2(V)$ can be represented by a diagonal operator as follows,*

$$\pi(f)(\delta_i) = f(i)(\delta_i).$$

The $\mathscr{B}$ space for Davies is $\ell^\infty(V)$ and the representation as defined above in 6.19 is it representation in the Hilbert Space $\mathcal{H}$. We will consider $\mathscr{B} = \ell^\infty(V)$ and $\mathscr{B} \subset \mathscr{A}$ in an interchangeable way.

Remark 6.20. *When representation the elements of $\mathscr{B}$ with π we have that $\mathscr{B} \subset \mathscr{A}$.*

We can also say that the representation of functions in $\ell^p(V)$ with π are in $\mathscr{B} \cap L^p$, as $\|f\|_{\ell^p} = \|\pi(f)\|_p$ ($\|\cdot\|_p$ being an operator norm as in definition 6.15).

As an aside in the next two remarks we will see the duality between the space of function $\ell^p(V)$ and the space of operators L^p.

Remark 6.21. *There is a correspondence between the space of oparators L^p (Davies Hilbert space for $p = 2$) and the space of functions $\ell^p(V)$, which can we shown as follows.*

$$\ell^p(V) = \{f : V \to \mathbb{C} \big| \sum_{v \in V} |f(v)|^p < \infty\}.$$

If we use the representation π representation $\pi : \ell^p(V) \longmapsto \pi(f) \in \mathscr{B} \cap L^p$ to calculate the L^p norm as in definition 6.15 first we need to find $s_v(\pi(f))$ as in definitions 6.13 and 6.15. Then using that $|\pi(f)|^2 = \pi(f)^*\pi(f) = \pi(\pi(\bar{f})f)$, $s_v(\pi(f)) = (\overline{f(v)}f(v))^{1/2} = |f(v)|$ we conclude $\underbrace{\sum_{v \in V} S_v(\pi(f))^p}_{\|\pi(f)\|_p^p} = \underbrace{\sum_{v \in V} |f(v)|^p}_{\|f\|_p^p} < \infty.$

Remark 6.22. *The inner product between functions f and $g \in \ell^2(V)$,*

$$\langle \pi(f), \pi(g) \rangle_{L^2} = tr(\pi(f)^*\pi(g)) = \langle f, g \rangle_{\ell^2}.$$

So we will take our space of functions $\ell^2(V)$ to be equivalent to the space of operators $\mathscr{B} \cap L^2$.

We will now define how Davies adjoint D operator the last element need to define Davies construction of a spectral triple.

To eventually prove that Davies' Dirac operator is indeed a Dirac type operator, we need to show that if we apply the operator and then its adjoint D^*D, this will result in the the Laplacian on $\mathscr{B}$ (as defined in Chung [14]). As we wish to generalise for infinite networks in this construction thus we will define the Laplacian operator in a slightly different way than in chapter 2.

Definition 6.23. ***(Laplacian Matrix and Operator)*** *The laplacian matrix of a weighted graph G with no loops or multiple edges taking d_v to be the degree of a vertex*

$v \in V$ (as defined in 2.2) is

$$\mathcal{L}(u,v) = \begin{cases} -b(u,v) & \text{if } e = (u,v) \in E, \\ d_v & \text{if } u = v \\ 0 & \text{otherwise.} \end{cases}$$

This can equivalently be defined as an operator, on the space of real valued function on the set of vertices $f : V \to \mathbb{R}$,

$$\mathcal{L}(f)(v) = \sum_{v \sim u} b(u,v)(f(v) - f(u)).$$

The notation $\sum_{v\sim u}$ is a summation over the set of all vertices which are adjacent to v.

We will now define an analogue of a differentiation operator, for which we need first a real symmetric matrix defined as follows.

$$B(i,j) = \begin{cases} (b(i,j)/2)^{1/2} & \text{if } e = (i,j) \in E, \\ 0 & \text{otherwise.} \end{cases} \tag{6.13}$$

Where $b(e)$ is the weight associated with the edge $e \in E$ as in definition 2.1 the particular choice for the weighting will become apparent later.

Lemma 6.24. *For a function $f \in \ell^\infty(V)$ the Dirac operator D on the operator of pointwise multiplication of $\pi(f) \in \mathscr{B}$ is defined as follows.*

$$D(\pi(f)) = \iota[B, \pi f] \tag{6.14}$$

here ι is taken to be an imaginary unit of $\mathbb{C}$.

Proof. For a function $f \in \ell^\infty(V)$ we will have $D(\pi(f))$, to investigate what this operator

is, we will look at the i,jth enry of $D(\pi(f))$,

$$\begin{aligned}\langle D\pi(f))\delta_i,\delta_j\rangle_{\ell^2(V)} &= (D\pi(f))_{i,j}\\ &= (\iota[B,\pi(f)])_{i,j}\\ &= \iota(B\pi(f)-\pi(f)B)_{i,j}\\ &= \iota\left(\sqrt{\frac{b(j,i)}{2}}f(i)-\sqrt{\frac{b(j,i)}{2}}f(j)\right)\\ &= \iota\sqrt{\frac{b(j,i)}{2}}(f(i)-f(j)).\end{aligned} \tag{6.15}$$

And the i,jth entry of $D^*(\pi(f))$

$$\begin{aligned}\langle D^*\pi(f))\delta_i,\delta_j\rangle_{\ell^2(V)} &= (D^*\pi(f))_{i,j}\\ &= (\iota[B^*,\pi(f)])_{i,j}\\ &= \iota(B^*\pi(f)-\pi(f)B^*)_{i,j}\\ &= \iota\left(\sqrt{\frac{b(i,j)}{2}}f(i)-\sqrt{\frac{b(i,j)}{2}}f(j)\right)\\ &= \iota\sqrt{\frac{b(i,j)}{2}}(f(i)-f(j)).\end{aligned} \tag{6.16}$$

As the weighting between vertices is only non-zero if they are adjacent, we can see that we can only have non-zero entries at the i,jth entry in this matrix when the edge (i,j) exists. So in effect the operator D takes us from an action of a function on vertices to an action of a function on edges, also the diagonal entries are zero.

To show that D is indeed a Dirac operator we observe the i,jth entry of

$$\frac{1}{2}\left(\underbrace{D^*(D\pi(f))}_{1}+\underbrace{D(D^*\pi(f))}_{2}\right) \tag{6.17}$$

on $\mathcal{H}$. We will break this down into two parts as indicated above, *1* is as follows, (the operator $D^*(\pi(f)) = \iota[B^*,\pi f]$) we will be using the result from (6.15) in this

calculation,

$$\begin{aligned}
[D^*(D\pi(f))]_{ij} &= \iota(B^*(D\pi(f)) - (D\pi(f))B^*)_{ij} \\
&= \sum_{k=1}^{n} \iota\left(B^*_{ik} \cdot \iota \cdot \sqrt{\frac{b(j,k)}{2}}(f(k) - f(j))\right) - \sum_{k=1}^{n} \iota\left(\iota \cdot \sqrt{\frac{b(k,i)}{2}} \cdot (f(i) - f(k))B^*_{kj}\right) \\
&= -\sum_{k=1}^{n}\left(B_{ki} \cdot \sqrt{\frac{b(j,k)}{2}}(f(k) - f(j))\right) - \sum_{k=1}^{n}\left(\sqrt{\frac{b(k,i)}{2}}(f(i) - f(k))B_{jk}\right) \\
&= -\sum_{k=1}^{n}\left(\sqrt{\frac{b(k,i)}{2}} \cdot \sqrt{\frac{b(j,k)}{2}}(f(k) - f(j))\right) - \sum_{k=1}^{n}\left(\sqrt{\frac{b(k,i)}{2}}(f(i) - f(k))\sqrt{\frac{b(j,k)}{2}}\right).
\end{aligned} \tag{6.18}$$

And similarly for *2*,

$$\begin{aligned}
[D(D^*\pi(f))]_{ij} &= \iota(B(D^*\pi(f)) - (D^*\pi(f))B)_{ij} \\
&= \sum_{k=1}^{n} \iota\left(B_{ik} \cdot \iota \cdot \sqrt{\frac{b(k,j)}{2}}(f(k) - f(j))\right) - \sum_{k=1}^{n} \iota\left(\iota \cdot \sqrt{\frac{b(i,k)}{2}} \cdot (f(i) - f(k))B_{kj}\right) \\
&= -\sum_{k=1}^{n}\left(B_{ik} \cdot \sqrt{\frac{b(k,j)}{2}}(f(k) - f(j))\right) - \sum_{k=1}^{n}\left(\sqrt{\frac{b(i,k)}{2}}(f(i) - f(k))B_{kj}\right) \\
&= -\sum_{k=1}^{n}\left(\sqrt{\frac{b(i,k)}{2}} \cdot \sqrt{\frac{b(k,j)}{2}}(f(k) - f(j))\right) - \sum_{k=1}^{n}\left(\sqrt{\frac{b(i,k)}{2}}(f(i) - f(k))\sqrt{\frac{b(k,j)}{2}}\right).
\end{aligned} \tag{6.19}$$

1 in (6.18) and *2* are equal in as B is symmetric (6.19) to together to form (6.17) we have,

$$-\frac{1}{2}\mathcal{L}(f)(i) - \frac{1}{2}\mathcal{L}(f)(j).$$

We are interested in what this is on $\mathscr{B}$ which only has diagonal entries, thus we take $i = j$ here,

$$\frac{1}{2}[D^*(D\pi(f))]_{i,i} + \frac{1}{2}[D(D^*\pi(f))]_{i,i} = -\mathcal{L}(f)(i). \tag{6.20}$$

Completing the proof. □

Remark 6.25. *The Dirac operator is in fact a local derivative this can be seen by showing that the Leibniz rule holds which is that,*

$$D(\pi(f)\pi(g)) = D(\pi(f))\pi(g) + \pi(f)D(\pi(g)). \tag{6.21}$$

Expanding the LHS of (6.21),

$$LHS = \iota[B, \pi(\pi(f)g)] = \iota B\pi(\pi(f)g) - \iota\pi(\pi(f)g)B.$$

And the RHS of (6.21),

$$\begin{aligned} RHS =& \iota[B, \pi f]\pi(g) + \pi(f)\cdot\iota[B, \pi g] \\ &= (\iota B(\pi f) - \iota(\pi f)B)\pi(g) + \pi(f)(\iota B(\pi g) - \iota(\pi g)B) \\ &= \iota B(\pi f)\pi(g) - \iota(\pi f)B\pi(g) + \pi(f)\iota B\pi(g) - \pi(f)\iota(\pi g)B \\ &= \iota B(\pi(f)g) - \iota(\pi(f)g)B. \end{aligned}$$

We now have Davies' complete spectral triple $(\mathscr{B}, L^2, D)$ and we can introduce the Connes metric.

Definition 6.26. ***(First Connes Metric)*** *Let $x, y \in V$ be two vertices. Then the first Connes metric is defined by*

$$d_{c_1}(x, y) = \sup_{f\in\ell^\infty(V)} \{|f(x) - f(y)| : \|[D, \pi f]\|_{Op} \leq 1\}. \tag{6.22}$$

Theorem 6.27. *For $f \in \ell^\infty(V)$,*

$$\|[D, \pi f]\|_{Op} = \|[B, f]\|_{Op} \tag{6.23}$$

(B is as defined in (6.13)) the left hand side is an operator norm on L^2 and the right hand side is an operator norm on $\ell^2(V)$.

Proof. For $C \in L^2$ and $\|C\|_{L^2} = 1$ we can take C as a basis element of L^2 and we will set $C = \delta_{ij}$. The operator δ_{ij} is such that $\langle\delta_{ij}\delta_l, \delta_k\rangle_{\ell^2} = 1$ if and only if $l = j$ and $k = i$ otherwise this is zero.

$$\begin{aligned} [D, \pi f](C) &= (D\cdot(\pi f))(C) - (\pi f\cdot D)(C) \\ &= \iota[B, \pi(f)(C)] - \pi(f)\iota[B, C] \\ &= \iota B\pi(f)(C) - \iota\pi(f)(C)B - \pi(f)\iota BC + \pi(f)\iota CB \\ &= \iota B\pi(f)(C) - \iota\pi(f)BC. \end{aligned} \tag{6.24}$$

Setting $C = \delta_{ij}$ we will have $\pi(f)\delta_{ij} = f(i) \cdot \delta_{ij}$, continuing the calculation (6.24),

$$\iota B(f(i) \cdot \delta_{ij}) - \iota\pi(f)B\delta_{ij} = \iota(f(i) \cdot B\delta_{ij} - \pi(f)B\delta_{ij}). \tag{6.25}$$

$\langle B\delta_{ij}\delta_l, \delta_k\rangle$ is only nonzero when $k = j$ and l is adjacent to i, in this case we have $\langle B\delta_{ij}\delta_l, \delta_k\rangle = \sqrt{b(i,l)/2}$ so for the L^2 norm of (6.25) is

$$\sum_{\forall i\sim l} \frac{b(i,l)}{2}(f(i) - f(l))^2 \tag{6.26}$$

here we have a result for what is on the left hand side of (6.23) for all basis elements. We will take a similar approach for the right hand side of (6.23),

$$\|[B, f]g\|_{\ell^2(V)} = \|(Bf)g - f(Bg)\|_{\ell^2(V)} \underbrace{=}_{\text{for } g=\delta_i} \sum_{\forall i\sim j} \frac{b(i,l)}{2}(f(j) - f(i))^2. \tag{6.27}$$

So we have from (6.26)

$$\|[D, \pi f]\|_{Op} = \sup_{\forall i\in V} \sum_{\forall i\sim l} \frac{b(i,l)}{2}(f(i) - f(l))^2,$$

and from (6.27)

$$\|[B, f]\|_{Op} = \sup_{\forall i\in V} \sum_{\forall i\sim j} \frac{b(i,l)}{2}(f(j) - f(i))^2.$$

Thus both the right a left hand sides of (6.23) are equal. □

Note that in the following proposition, there will be an arbitrary orientation assigned to all of the edges. This calculation shows that the two operators are in fact identical, and so the Proposition follows. The notation ie will be used to indicate the tail vertex of the edges e and je will be used to indicate the head or leading vertex of the edge.

Corollary 6.28. *The following two conditions are equivalent*

$$\|[B, \pi f]\|_{Op} \leq 1 \iff \forall x \in V,\ \frac{1}{2}\sum_{ie=x} b(e)|f(ie) - f(je)|^2 \leq 1. \tag{6.28}$$

Definition 6.29. ***(Second Connes Metric)*** *Let us introduce the space of $\mathcal{E}$ of*

bounded functions which satisfy the following conditions:

$$\mathcal{E} = \{f \big| f \in \ell^\infty(V) \text{ and } \forall x \in V, \frac{1}{2}\sum_{ie=x} b(e)|f(ie) - f(je)|^2 \leq 1\}. \tag{6.29}$$

Using Corollary 6.28 we are able to define the following version of Connes metric:

$$d_{c_2}(x,y) = \sup\{|f(x) - f(y)| \big| f \in \mathcal{E}\}. \tag{6.30}$$

As we want to show some comparisons with more traditional metrics we will define these here.

Definition 6.30. *($\Gamma(x,y)$) For every $x, y \in V$ let $\Gamma(x,y)$ be the set of all paths connecting x and y.*

Definition 6.31. *(d_0) For every $x, y \in V$ the combinatorial graph distance is given by:*

$$d_0(x,y) = \inf\{n(\gamma) \big| \gamma \in \Gamma(x,y)\}.$$

Where $n(\gamma)$ is the number of edges in the path γ.

The weighted graph distance metric is by definition This is a weighted graph distance metric

$$d_1(x,y) = \inf_{\gamma\in\Gamma}\Big\{\sum_{e\in\gamma} b(e)^{-1/2} \big| \gamma \in \Gamma(x,y)\Big\}. \tag{6.31}$$

Lemma 6.32. *For all $x, y \in V$ the following inequality holds*

$$d_{c_1}(x,y) \leq \sqrt{2} d_1(x,y).$$

Proof. In the definition of d_{c_1} (Definition 6.26) the constraint on the function which gives this metric ($f \in \ell^\infty(V)$) is $\|[D, \pi f]\|_{Op} \leq 1$, from proposition 6.28 we have that $\forall z \in V$, $\frac{1}{2}\sum_{ie=z} b(e)|f(ie) - f(je)|^2 \leq 1$, which clearly implies that for all $e \in E$ and for all $f \in \ell^\infty(V)$,

$$|B(ie,je)(f(je)) - B(je,ie)(f(ie))| = B(ie,je)|f(je) - f(ie)| \leq \sqrt{2}.$$

$\implies$ for each $e \in E$ we have,

$$|f(je) - f(ie)| \leq (2/b(e))^{1/2}. \tag{6.32}$$

For x and $y \in V$ let the path identified in the minimisation process which is part of the definition of d_1 (in 6.31) be $\gamma = (e_1, e_2, \ldots, e_p)$ where $i(e_1) = x$ and $j(e_p) = y$, we have that,

$$|f(x) - f(y)| \leq \sum_{r=1}^{p} |f(i(e_r)) - f(j(e_r))| \leq \sum_{r=1}^{p} \left(\frac{2}{b(e_r)}\right)^{1/2}.$$

The second inequality is a result of used (6.32) on every edge of the path γ, the proof is now complete given the definition of d_1.

$$|f(x) - f(y)| \leq \sqrt{2} \cdot d_1(x, y).$$

Now if we take the supremum of all $f \in \ell^\infty(V)$ as with the Connes metric formulation we have,

$$d_{c_1}(x, y) \leq \sqrt{2} d_1(x, y).$$

□

6.3.2 Requardt's Discrete Connes Metric

In [51] Requardt has proposed an alternative way of expressing the Connes metric, with a different construction of the spectral triple. To do this, we will first need some change in notation.

Requardt's Functions

In the next two definitions we give the orthogonal basis elements of two different Hilbert spaces $\mathcal{H}_0$ and $\mathcal{H}_1^a$ which are spaces of functions on vertices and of antisymmetric function on edges respectively. We will assume that there is some standard numbering of the vertices.

Definition 6.33. ***(The basis elements for $\mathcal{H}_0$)*** *For all $i \in V$ we have a basis element $n_i \in \mathcal{H}_0$.*

$$n_i(j) = \begin{cases} 1 & \text{if } i = j, \\ 0 & \text{otherwise.} \end{cases}$$

This is the set of basis functions that span the space of functions on vertices. So $f \in \mathcal{H}_0$ *can be expressed as* $f := \sum_{i \in V} f_i n_i$.

Definition 6.34. ***(The basis elements of*** $\mathcal{H}_1^a$***)*** *For all* $i, j \in V$ *where* i *is adjacent to* j*, we have the basis element* $d_{ij} \in \mathcal{H}_1$.

$$d_{ij}(k,l) = \begin{cases} 1 & \text{if } (k,l) = (i,j), \\ 0 & \text{otherwise.} \end{cases}$$

If a function $g \in \mathcal{H}_1^a \implies g := \sum_{(i,j) \in E} g_{ij} d_{ij}$ with $g_{ij} = -g_{ji}$ we will be interested in the Hilbert space $\mathcal{H}_1^a \subset \mathcal{H}_1$ of antisymmetric functions on the set of edges only.

This same function g could be expressed using a slightly more compact form, which exploits the antisymmetry of the function g. If we define $h_{ij} = d_{ij} - d_{ji}$, then we can express g as follows $g := \sum_{\{i,j\} \in E} g_{ij} h_{ij}$ where we sum over all unordered pairs.

Hilbert Spaces for Edges and Vertices

For functions $f, f' \in \mathcal{H}_0$ given by $f := \sum_{i \in V} f_i n_i$ and $f' := \sum_{i \in V} f'_i n_i$, their inner product on the space is,

$$\langle f, f' \rangle_{\mathcal{H}_0} = \sum_{i \in V} f_i \overline{f'_i}.$$

This Hilbert space is in fact $\ell^2(V)$. For functions $g, g' \in \mathcal{H}_1^a$ given by $g := \sum_{(i,j) \in E} g_{ij} d_{ij}$ and $g' := \sum_{(i,j) \in E} g'_{ij} d_{ij}$, their inner product on the space is,

$$\langle g, g' \rangle_{\mathcal{H}_1^a} = \sum_{(i,j) \in E} g_{ij} \overline{g'_{ij}}.$$

This Hilbert space is in fact $\ell^2(E, 1/2)$.

Requardt's Differential Operators

We will now introduce a Dirac operator which will combine two differential operators d and its adjoint d^*.

The discrete differentiation operator $d : \mathcal{H}_0 \to \mathcal{H}_1^a$ is defined by,

$$df = d\left(\sum_{i\in V} f_i n_i\right) = \sum_{(i,j)\in E} b(i,j)^{1/2}(f_j - f_i)d_{ij} = \sum_{\{i,j\}\in E} b(i,j)^{1/2}(f_j - f_i)h_{ij}.$$

Notice here that we are giving the difference operator a similar weights that found in matrix B in (6.13) with Davies construction but without an inverse $\sqrt{2}$ factor.

Proposition 6.35. *The adjoint of this is $d^* : \mathcal{H}_1^a \to \mathcal{H}_0$, acts on a functions of the form $g : E \to \mathbb{R}$,*

$$d^*g = d^* \sum_{(i,j)\in E} g_{ij}d_{ij} = \sum_{i\in V}\sum_{i\sim j} b(i,j)^{1/2} g_{ij}(n_j - n_i) = 2\sum_{i\in V}\sum_{i\sim j} b(i,j)^{1/2} g_{ij} n_i.$$

Proof. For a function $f \in \mathcal{H}_0$,

$$df = \sum_{(i,j)\in E} b(i,j)^{1/2}(f_j - f_i)d_{ij},$$

now applying d^* to this

$$\begin{aligned} d^*(df) &= d^*\left(\sum_{(i,j)\in E} b(i,j)^{1/2}(f_j - f_i)d_{ij}\right) \\ &= \sum_{(i,j)\in E} b(i,j)(f_i - f_j)(n_j - n_i) \\ &= 2\sum_{i\in V}(d_i f_i - \sum_{i\sim j} b(i,j)f_j)n_i), \\ &= 2\Delta f \end{aligned} \tag{6.33}$$

where d_i is the degree of vertex $i \in V$.

□

Requardt's Hilbert space

To create the required operator, we first take the orthogonal direct sum to define the Hilbert space

$$\mathcal{H} = \mathcal{H}_0 \bigoplus \mathcal{H}_1^a. \tag{6.34}$$

This is the orthogonal sum of the two previously defined Hilbert spaces will give us our Hilbert space.

Natural Representation of Function Algebra $\mathscr{B}$

Requardt's C$^*-$algebra $\mathscr{B}$ is the same as for Davies' $\mathscr{B} = \ell^\infty(V)$. The description of the action of these functions on the Hilbert space (6.34) is equivalent to the representation (π) of function in $\mathscr{B}$. As Requardt's Hilbert space is a direct sum of $\mathcal{H}_0$ and $\mathcal{H}_1^a$ by describing the action of $\mathscr{B}$ on these spaces separately we can description the action on $\mathcal{H}$ as a whole.

Between functions in $f \in \ell^\infty(V) = \mathscr{B}$ and $f' \in \mathcal{H}_0$ there is a pointwise multiplication.

$$f \cdot \sum_{i \in V} f'_i n_i = \sum_{i \in V} f_i f'_i n_i. \tag{6.35}$$

Between functions in $f \in \ell^\infty(V) = \mathscr{B}$ and $g \in \mathcal{H}_1^a$ there is a pointwise multiplication.

$$f \cdot \sum_{(i,j) \in E} g_{ij} d_{ij} = \sum_{(i,j) \in E} f_i g_{ij} d_{ij}. \tag{6.36}$$

These equation being about the following module structure that determines how this functions in Requardt's $\mathscr{B}$ can be represented on $\mathcal{H}_0 \bigoplus \mathcal{H}_1^a$. For $f \in \mathscr{B}$ and $f' \in \mathcal{H}_0 \bigoplus \mathcal{H}_1^a$ where $f'^0 \in \mathcal{H}_0$ is the vertex component of f' and $f'^1 \in \mathcal{H}_1^a$ is the edge component of f',

$$(f) \begin{pmatrix} f'^0 \\ f'^1 \end{pmatrix} = \begin{pmatrix} f \sum_{i \in V} {f'^0}_i n_i \\ f \sum_{ij} {f'^1}_{ij} d_{ij} \end{pmatrix} = \begin{pmatrix} \sum_{i \in V} f_i {f'^0}_i n_i \\ \sum_{ij} f_i {f'^1}_{ij} d_{ij} \end{pmatrix}.$$

Note that the sum over ij here is equivalent to the sum over $(i,j) \in E$.

The following equation shows a right $\ell^\infty(V)-$module structure of $\ell^2(E, 1/2)$ over $\mathcal{H}_0$,

$$\sum_{i\ j} g_{ij} d_{ij} \cdot f := \sum_{i\ j} g_{ij} f_j \cdot d_{ij} \tag{6.37}$$

This will also be useful for later calculations.

Dirac Operator and Calculation of $[D, f]$

With this notation in hand we can define the operator D on H by the following formula:

$$D = \begin{bmatrix} 0 & d^* \\ d & 0 \end{bmatrix}.$$

Remark 6.36. *The square of D is the Laplacian on $\mathcal{H}_0 \bigoplus \mathcal{H}_1^a$.*

$$DD^* = \begin{bmatrix} 0 & d^* \\ d & 0 \end{bmatrix} \begin{bmatrix} 0 & d^* \\ d & 0 \end{bmatrix} = \begin{bmatrix} d^*d & 0 \\ 0 & dd^* \end{bmatrix} = \begin{bmatrix} 2\Delta & 0 \\ 0 & 2\Delta \end{bmatrix}.$$

The d^*d is two times the Laplacian that we are familiar with (the Laplacian on the functions of the form $f : V \to \mathbb{R}$ refer to (6.33)). dd^* can be thought of as the equivalent operator resembling the Laplacian on $\mathcal{H}_1^a$.

We will now analysis the constraint condition on the Connes metric, as given in definition 6.26 but for Requardt's construction.

Proposition 6.37. *For any function $f \in \mathscr{B}$*

$$[D, f] = \begin{bmatrix} 0 & [d^*, f]|^{10} \\ [d, f]|^{01} & 0 \end{bmatrix} \tag{6.38}$$

this operator $[D, f] : \mathcal{H} \to \mathcal{H}$.

Proof. Expanding the right hand side of (6.38) as a operator on $\mathcal{H}$, note that the $F|_{\mathcal{H}}$ notation after an operator (F) means that this operator $F : \mathcal{H} \to \mathcal{H}$.

The $|^{10}$ notation after $[d^*, f]$ indicates that $[d^*, f] : \mathcal{H}_1 \to \mathcal{H}_0$ and $|^{01}$ notation after $[d, f]$ indices that $[d, f] : \mathcal{H}_0 \to \mathcal{H}_1$.

For a function $f' \in \mathcal{H}_0$,

$$[d, f]f' = df f' - f df'$$

which can be broken into two parts as follows,

$$df f' = d\left(\sum_{i \in V} f_i n_i \sum_{i \in V} {f'}_i n_i\right) = d\left(\sum_{i \in V} f_i {f'}_i n_i\right) = \sum_{(i,j) \in E} b(i,j)^{1/2}(f_j {f'}_j - f_i {f'}_i) d_{ij}$$

and

$$(fd)f' = \sum_{i\in V} f_i n_i \sum_{i\sim j} b(i,j)^{1/2}({f'}_j - {f'}_i)d_{ij} = \sum_{(i,j)\in E} b(i,j)^{1/2} f_i({f'}_j - {f'}_i)d_{ij}.$$

The summation $\sum_{i\sim j}$ is the sum over the set of vertices adjacent to i, this also utilises the module structure shown in (6.36). Bringing these results together

$$\begin{aligned}[d,f]f' &= \sum_{(i,j)\in E} b(i,j)^{1/2}(f_j{f'}_j - f_i{f'}_i)d_{ij} - \sum_{(i,j)\in E} b(i,j)^{1/2} f_i({f'}_j - {f'}_i)d_{ij} \\ &= \sum_{(i,j)\in E} b(i,j)^{1/2}(f_j - f_i){f'}_j d_{ij}.\end{aligned} \tag{6.39}$$

For $g' \in \mathcal{H}_1^a$,

$$[d^*, f]g' = d^* f g' - f d^* g'$$

which can again be broken down into two parts as follows,

$$\begin{aligned}d^*(f\cdot g') &= d^*\left(\sum_{i\in V} f_i n_i \cdot \sum_{(i,j)\in E} g'_{ij} d_{ij}\right) \\ &= d^*\left(\sum_{(i,j)\in E} f_i g'_{ij} d_{ij}\right) \\ &= \left(\sum_{(i,j)\in E} b(i,j)^{1/2} f_i g'_{ij}(n_i - n_j)\right)\end{aligned}$$

and

$$\begin{aligned}f\cdot d^*(g') &= \sum_{i\in V} f_i n_i \cdot d^*\left(\sum_{(i,j)\in E} g'_{ij} d_{ij}\right) \\ &= \sum_{i\in V} f_i n_i \cdot \left(\sum_{(i,j)\in E} b(i,j)^{1/2} g'_{ij}(n_i - n_j)\right) \\ &= \sum_{(i,j)\in E} b(i,j)^{1/2} g'_{ij}(f_i n_i - f_j n_j).\end{aligned}$$

Bring these results together we have,

$$\begin{aligned}[d^*, f]g' &= \left(\sum_{(i,j)\in E} b(i,j)^{1/2} f_i g'_{ij}(n_i - n_j)\right) - \left(\sum_{(i,j)\in E} b(i,j)^{1/2} g'_{ij}(f_i n_i - f_j n_j)\right) \\ &= \left(\sum_{(i,j)\in E} b(i,j)^{1/2} g'_{ij}(f_i n_i - f_i n_j)\right) - \left(\sum_{(i,j)\in E} b(i,j)^{1/2} g'_{ij}(f_i n_i - f_j n_j)\right) \\ &= \sum_{(i,j)\in E} b(i,j)^{1/2} g'_{ij}(f_j - f_i) n_j. \end{aligned} \tag{6.40}$$

This means that the operator,

$$\begin{bmatrix} \mathbf{0} & [d^*, f] \\ [d, f] & \mathbf{0} \end{bmatrix} \Bigg|_{\mathcal{H}}.$$

□

Requardt's Connes Metric

Now as we have defined Requardt's version of the spectral triple we can define his version of the discrete Connes metric.

Definition 6.38. *For all vertices $x, y \in V$,*

$$d_{c_3}(x, y) = \sup_{f\in\mathscr{B}} \{|f(x) - f(y)| : \|[D, f]\|_{Op} \leq 1\}. \tag{6.41}$$

The norm here is an operator norm for operator in $\mathcal{H}$.

The implication of the following theorem is that the two metrics d_{c_2} and d_{c_3} are essentially the same apart from a scale difference of $1/\sqrt{2}$. Thus the constraint condition in (6.41) is equivalent to the constraint condition in (6.29).

Theorem 6.39. *For all vertices $x, y \in V$,*

$$d_{c_3}(x, y) = d_{c_2}(x, y)/\sqrt{2}.$$

Proof. For the constraint of d_{c_3} is $\|[D, f]\|_{Op} \leq 1$ where the operator norm is on $\mathcal{H}$, the proof will proceed by showing that this constraint can be presented in a similar way to the constraint of d_{c_2} in (6.29).

From (6.38) the constraint of d_{c_3} can be interpreted as,

$$\left\| \begin{bmatrix} 0 & [d^*, f]|^{10} \\ [d, f]|^{01} & 0 \end{bmatrix} \right\|_{Op} = \sup_{\substack{\forall z \in \mathcal{H} \\ \text{and} \|z\|_{\mathcal{H}}=1}} \left\| \begin{bmatrix} 0 & [d^*, f]|^{10} \\ [d, f]|^{01} & 0 \end{bmatrix} z \right\|_{\mathcal{H}} \leq 1.$$

$z \in \mathcal{H}$ has a vertex and edge part, so we can say $z = (z^0, z^1)^\top$ then this can be rewritten as

$$\sup_{\substack{\forall z \in \mathcal{H} \\ \text{and} \|z^0\|^2_{\mathcal{H}_0} + \|z^1\|^2_{\mathcal{H}_1^a}=1}} \left\| \begin{bmatrix} [d^*, f]|^{10} z^1 \\ [d, f]|^{01} z^0 \end{bmatrix} \right\|_{\mathcal{H}} \leq 1. \tag{6.42}$$

The two optimisation problems

$$\sup_{\substack{\forall z^0 \in \mathcal{H}_0 \\ \text{and} \|z^0\|_{\mathcal{H}_0}=1}} \|[d, f]|^{01} z^0\|_{\mathcal{H}_1^a} \tag{6.43}$$

and

$$\sup_{\substack{\forall z^1 \in \mathcal{H}_1^a \\ \text{and} \|z^1\|_{\mathcal{H}_1^a}=1}} \|[d^*, f]|^{10} z^1\|_{\mathcal{H}_0} \tag{6.44}$$

are similar. As we can see when expanding (6.43) we have (using the same working in (6.39))

$$\sup_{\substack{\forall z^0 \in \mathcal{H}_0 \\ \text{and} \|z^0\|_{\mathcal{H}_0}=1}} \left\| \sum_{(i,j) \in E} b(i,j)^{1/2} z_j^0 (f_j - f_i) d_{ij} \right\|_{\mathcal{H}_1^a} = \sum_{(i,j) \in E} b(i,j) (z_j^0)^2 (f_j - f_i)(\bar{f}_j - \bar{f}_i) \tag{6.45}$$

and expanding (6.43) (using the same working in (6.40))

$$\sup_{\substack{\forall z^1 \in \mathcal{H}_1^a \\ \text{and} \|z^1\|_{\mathcal{H}_1^a}=1}} \left\| \sum_{(i,j) \in E} b(i,j)^{1/2} z_{ij}^1 (f_j - f_i) n_j \right\|_{\mathcal{H}_0} = \sum_{(i,j) \in E} b(i,j) (z_{ij}^1)^2 (f_j - f_i)(\bar{f}_j - \bar{f}_i). \tag{6.46}$$

We can see here that the optimisation problem (6.45) will alway be larger. This can be seen when we consider basis elements of $\mathcal{H}_0$ for (6.45) we get,

$$\sum_{i \sim j} b(i,j)(f_j - f_i)(\bar{f}_j - \bar{f}_i)$$

for $z_j^0 = 1$, and when we consider basis elements of $\mathcal{H}_1^a$ for (6.44) we get,

$$b(i,j)(f_j - f_i)(\bar{f}_j - \bar{f}_i)$$

for $z_{ij}^1 = 1$. Thus the earlier constraint (6.42) will be equivalent to

$$\sup_{\substack{\forall z^0 \in \mathcal{H}_0 \\ \text{and} \|z^0\|_{\mathcal{H}_0}=1}} \|[d,f]|^{01} z^0\|_{\mathcal{H}_1^a} \leq 1 \iff \forall i \in V \sum_{i \sim j} b(i,j)|(f_j - f_i)|^2 \leq 1.$$

The constraint for the d_{c_2} metric in (6.30) is

$$\forall i \in V \sum_{i \sim j} b(i,j)|(f_j - f_i)|^2 \leq 2 \iff \forall i \in V \sum_{i \sim j} b(i,j) \left| \left(\frac{f_j}{\sqrt{2}} - \frac{f_i}{\sqrt{2}} \right) \right|^2 \leq 1.$$

As the constrinats for both Connes metrics are the same apart from the $1/\sqrt{2}$ factor, the resulting Connes metric of d_{c_2} will thus be smaller by a factor of $1/\sqrt{2}$.

□

6.3.3 Resistance Metric

The basic idea of resistance metrics can be described as follows and is in [33, p. 55]. If one amp of electricity is put into vertex x and one amp of electricity is drawn from vertex y, the voltage drop that is present between x and y is equal to the resistance metric between x and y.

Before we introduce this Resistance metric we must define some terms. In what follows, the vertex set V can be finite or infinite, and similarly for the edge set E.

Definition 6.40. *For voltage potential function $v : V \to \mathbb{R}$ (which give a voltage potential at ever vertex $i \in V$), the space $Dom(\mathcal{E})$ is the space of v that result in a finite total energy for the whole network, which is the summation of the energy flowing across all lines in the network where energy is as defined as in A.18. So for $v \in Dom(\mathcal{E})$ similarly to equation (6.29),*

$$\mathcal{E}(v) = \frac{1}{2} \sum_{\forall (i,j) \in E} b(i,j)(v(i) - v(j))^2 < \infty. \tag{6.47}$$

where $b(i,j)$ is the inverse of the resistance between vertices i and j.

The resistance metric can be expressed in several ways, we have chosen one that we think resembles the Connes metric the most.

Definition 6.41. ***(Resistance metric)*** *The resistance metric $\mathcal{R}$ between vertices vertices x and $y \in V$ is given as follows,*

$$\mathcal{R}(x, y) = \sup\{|v(x) - v(y)|^2 : \mathcal{E}(v) \leq 1\}$$

where $v : V \to \mathbb{R}$ gives the a possible voltage potential at every vertex.

This can be interpreted as the maximum square differences between the voltage potential at vertex x and at vertex y, with the condition that the total energy flowing in the network is bounded by 1.

This is similar to the Connes metric, both have as conditions bounds on the energy and both are related to the voltage potential differences. However the bound on the energy in the Connes metric applies to the energy flowing adjacent to every single vertex independently as follows $\forall i \in V \sum_{i \sim j} b(i, j)|(f_j - f_i)|^2$, where as with the resistance metric the bound on the energy is global ($\mathcal{E}(v) \leq 1$). The other more obvious difference is the resistance metric is give by the square of the voltage potential difference and the Connes metric is give by the scalar of the difference.

In the next chapter we will see more applications of the Connes metric to electrical power networks.

Chapter 7

Computation of the Connes Metric

Leading on from the previous chapter where we showed various constructions of the Connes metric, in this chapter we will attempt to find an effective way to compute the Connes metric for a general graph. There is no algorithm for computing such a metric, explicit computations that have been performed are limited to simple configurations such as the unweighted tree in [51]. We will follow a remark in [49] that the problem of computing the Connes metric can be restated as a convex optimisation problem. The subtlety and the challenge of this problem is in describing a seemingly local metric that is determined by global properties of a network. We will also note here that in this chapter we will just be dealing with unweighted graph, but this can easily be generalised to weighted graphs.

To frame this as a convex optimisation problem, we need to introduce some notions such as the Lagrangian formulation and the Karush Khun Tucker conditions. We are able to infer some general properties of a function that gives the Connes from these conditions, and to verify these properties we are able to prove these with a different approach. We then find a more compact algebraic way of expressing the Connes metric. We show a simple example of the use of this construction and we find the limitations of this. Finally we explain in full the physical interpretation of the Connes metric.

7.1 Convex Optimisation

The problem of computing the Connes metric can be interpreted as essentially a convex optimisation problem, for this to be the case we have to: have a convex objective and be optimising over a convex state space (terms which we will now define).

Definition 7.1. ***(Convex space)*** *A space X is convex if for any two elements $X_1, X_2 \in X$ and for any $t \in [0,1]$, we have that $tX_1 + (t-1)X_2 \in X$.*

Definition 7.2. ***(Convex Functions)*** *Let X be a convex vector space and let F be a real-valued function on X. We say that F is convex iff for every $X_1, X_2 \in X$ and for all $t \in [0,1]$,*

$$F(tX_1 + (t-1)X_2) \leq tF(X_1) + (t-1)F(X_2).$$

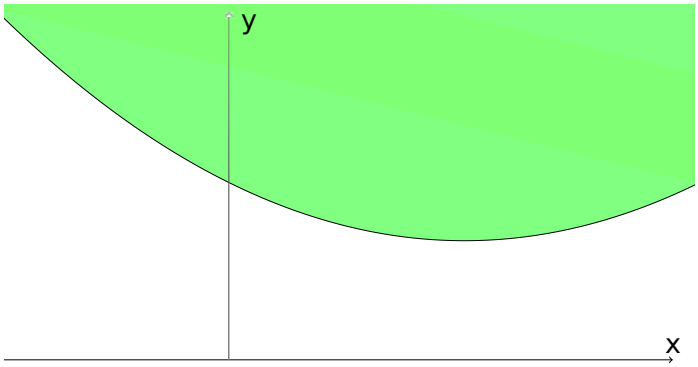

Figure 7-1: This is a polynomial function of second order with positive coefficients, for the vector space of $\mathbb{R}$ this function is a convex function.

Lemma 7.3. *For functions f and $f' \in \ell^\infty$ where $\forall z \in V$,*

$$\frac{1}{2}\sum_{ie=z} |f(ie) - f(je)|^2 \leq 1 \tag{7.1}$$

and $\frac{1}{2}\sum_{ie=z} |f'(ie) - f'(je)|^2 \leq 1$, we have that $\forall z \in V$

$$\sum_{j \in A(z)} (f'_z - f'_j)(f_z - f_j) \leq 2.$$

Proof.

$$\begin{aligned}
0 &\leq \sum_{j\in A(z)} \big((f'_z - f'_j) - (f_z - f_j)\big)^2 \\
&= \sum_{j\in A(z)} (f'_z - f'_j)^2 + \sum_{j\in A(z)} (f_z - f_j)^2 - 2\sum_{j\in A(z)} \big(f'_z - f'_j\big)(f_z - f_j) \\
&\underbrace{\leq}_{\text{condition in (7.1)}} 2 + 2 - 2\sum_{j\in A(z)} \big(f'_z - f'_j\big)(f_z - f_j) \\
&\text{which} \implies \sum_{j\in A(z)} \big(f'_z - f'_j\big)(f_z - f_j) \leq 2.
\end{aligned}$$

□

Lemma 7.4. ***(Connes Metric as Convex Optimisation Problem)*** *For the space,*

$$\mathcal{E} = \{f | f \in \ell^\infty(V) \text{ and } \forall z \in V, \frac{1}{2}\sum_{ie=z} |f(ie) - f(je)|^2 \leq 1\}. \tag{7.2}$$

the problem of computing the value of the metric

$$d_{c_2}(x,y) = \sup_{f\in\ell^\infty(V)} \{|f(x) - f(y)| \big| \|[D, \pi f]\|_\infty \leq 1\} = \sup\{|f(x) - f(y)| \big| f \in \mathcal{E}\}.$$

This is a convex optimisation problem as it is essentially the optimisation of a convex operator over a convex space.

Proof. We are given x, $y \in V$, $\ell^\infty(V)$ is a vector space and if we take $F : \ell^\infty(V) \to \mathbb{R}$ such that for $f \in \ell^\infty(V)$, $F(f) = |f(x) - f(y)|$. It can be shown that F is a convex function on the space $\ell^\infty(V)$, if we take any two functions f, $f' \in \ell^\infty(V)$, and for any $t \in [0,1]$,

$$\begin{aligned}
F(tf + (1-t)f') =& |(tf(x) + (1-t)f'(x)) - (tf(y) + (1-t)f'(y))| \\
=& |(tf(x) - tf(y) + (1-t)(f'(x) - f'(y))| \\
\leq& |(tf(x) - tf(y))| + |(1-t)(f'(x) - f'(y))| \\
=& t|f(x) - f(y)| + (1-t)|(f'(x) - f'(y))| \\
=& tF(f) + (1-t)F(f').
\end{aligned}$$

The next problem will be to prove that the space of functions $\mathcal{E}$ is a convex set of functions. The set of functions $\mathcal{E} = \{f \in \ell^\infty(V) | \forall z \in V, \sum_{j\in A(z)}(f_z - f_j)^2 \leq 2\}$ (we have reverted to subscript notation here where $f(i) = f_i$ also $A(z)$ will denote the set of all vertices that are adjacent to z). We need to show that for all two functions f and $f' \in \mathcal{E}$ we have that any intermediate point would also lies in the space $\mathcal{E}$, thus for any $t \in [0,1]$, $tf + (t-1)f' \in \mathcal{E}$ (will be all intermediate points between f and f').

$$\begin{aligned}
&\sum_{j\in A(z)} ((tf_z + (t-1)f'_z) - (tf_j + (t-1)f'_j))^2 \\
&\quad = \sum_{j\in A(z)} (t^2(f_z - f_j)^2 + (t-1)^2(f'_z - f'_j)^2 - 2t(t-1)(f_z - f_j)(f'_z - f'_j)) \\
&\quad = \underbrace{t^2 \sum_{j\in A(z)} (f_z - f_j)^2 + (t-1)^2 \sum_{j\in A(z)} (f'_z - f'_j)^2}_{\leq 2t^2 + 2(t-1)^2 = 2(2t^2 - 2t + 1)} + \underbrace{2t(1-t) \sum_{j\in A(z)} (f'_z - f'_j)(f_z - f_j)}_{\leq 4t(1-t) = 4t - 4t^2}.
\end{aligned} \tag{7.3}$$

What is in the first under brace is a direct consequence of the conditions in (7.2), what is in the second under brace follows indirectly from the conditions in (7.2). As an aside this can be shown as follows,

From (7.3) we have that,

$$\sum_{j\in A(z)} ((tf_z + (t-1)f'_z) - (tf_j + (t-1)f'_j))^2 \leq 2$$

So now it has been established that this is a convex space and thus that this is a convex optimisation problem. □

7.1.1 Restatement of the Connes Metric

The Connes metic of the previous section is restated here so that we can apply the machinery of convex optimisation. For this restatement a number of notational conventions will be used. As in the proof of Lemma 7.4 the set of adjacent vertices to a vertex $i \in V$ will be denoted $A(i) \subseteq V$. In the previous definitions of the Connes metrics it can be notices that for the function $f : V \to \mathbb{R}$, that will determine a particular Connes metric, it is the differences of this functions across adjacent edges that entirely determines the metric, a consequence of this is that if we add a constant function to

f the Connes metric will be the same, this can be seen most clearly in definition 6.29. So to reduce the size of functions in the state space there will be a value $K \geq 0$ and an index $a \in V \setminus \{x, y\}$ where for any function f in the state space will be equal to K at $a \in V$ ($f(a) = K$). Thus the following is equal to d_{c_2} in (6.30) in definition 6.29,

$$c(x,y) := \sup_{f \in \ell^\infty(V), f(a)=K} \left\{ |f(x) - f(y)| : \forall z \in V \sum_{j \in A(z)} (f(z) - f(j))^2 \leq 2 \right\}. \tag{7.4}$$

Note here that $f(a) = K$, for some $K \in \mathbb{R}$ which can be set to be equal to any value that we like, as the addition of a constant function have no effect on either the objective or the constraints.

For simplification of the notation, we will take $f_z = f(z)$ for all $z \in V$. As the constraints for the state space are even and the objective is even we can without loss of generality consider our objective without absolutes values and take $f_x > f_y$,

$$c(x,y) = \sup_{f \in \ell^\infty(V)} \left\{ f_x - f_y \middle|\ f_a = K,\ \forall z \in V : \sum_{j \in A(z)} (f_z - f_j)^2 \leq 2 \right\}. \tag{7.5}$$

Similarly this can be expressed as a minimisation of $-c(x, y)$,

$$-c(x,y) = \min_{f \in \ell^\infty(V)} \left\{ f_y - f_x \middle|\ f_a = K,\ \forall z \in V : \sum_{j \in A(z)} (f_z - f_j)^2 \leq 2 \right\}. \tag{7.6}$$

7.1.2 Karush-Kuhn-Tucker Conditions For Convex Problems

A standard optimisation problem over the vector space $\mathbb{R}^n$ [5], is given by an objective the objective function $F : \mathbb{R}^n \to \mathbb{R}$, inequality constraints function $g_i : \mathbb{R}^n \to \mathbb{R}$ and equality constraint functions $h_j : \mathbb{R}^n \to \mathbb{R}$ respectively. The problem can be stated as follows for $z \in \mathbb{R}^n$,

$$\begin{aligned} &\text{Minimize } F(z) \\ &\text{Subject to } g_i(z) \leq 0 \text{ for all } i \in \{1, 2, \ldots, m\} \\ &\text{Subject to } h_j(z) = 0 \text{ for all } j \in \{1, 2, \ldots, l\}. \end{aligned} \tag{7.7}$$

F, $g_1, \ldots, g_m$ and $h_1, \ldots, h_p$ have continuously partial derivatives. We will take the domain $\mathcal{D} = \bigcap_{i=1}^{m} \mathbf{dom}(g_i) \cap \bigcap_{j=1}^{p} \mathbf{dom}(h_j)$ where the constraints holds, to be a convex state space and the objective F to be convex operator. The basis idea of Lagrangian duality is to solve the optimisation problem (7.7) in one expression by adding to the objective function a weighted sum of the constraint expressions.

Definition 7.5. ***(Lagrangian)*** *The Lagrangian defined in relation to the optimisation problem above (7.7)* $\Lambda : \mathbb{R}^n \times \mathbb{R}^m \times \mathbb{R}^l \to \mathbb{R}$ *is as follows where* $z \in \mathbb{R}^n$, $\mu \in \mathbb{R}^m$ *and* $\lambda \in \mathbb{R}^l$,

$$\Lambda(z, \mu, \lambda) = F(z) + \sum_{i=1}^{m} \mu_i(g_i(z)) + \sum_{j=1}^{l} \lambda_j(h_j(z)). \tag{7.8}$$

Say that (7.8) is maximised over $(\mu, \lambda) \in \mathbb{R}^m \bigoplus \mathbb{R}^l$ with the condition that $\mu \succeq 0$ (meaning that for all j we have $\mu_j \geq 0$) and minimise over $z \in \mathbb{R}^n$. This way the Lagrangian multipliers can be thought of as administering a punishment for having unfeasible z where for some $i \in \{1, \ldots, m\}$ we have $g_i(z) > 0$ or for some $j \in \{1, \ldots, l\}$ we have $h_j(z) \neq 0$ in these circumstance maximising over (μ, λ) will give ∞. For this optimisation problem a set of rules (or conditions) must be meet which can be used to determine what indeed is the optimal point, these are called *The Karush-Kuhn-Tucker conditions*. So for a optimal point $(z^*, \mu^*, \lambda^*) \in \mathbb{R}^n \times \mathbb{R}^m \times \mathbb{R}^l$ the *The Karush-Kuhn-Tucker conditions* are as follows (refer to [5, p. 244]).

$$\begin{aligned}
h_j(z^*) &= 0 \qquad \forall j \in \{1, \ldots, l\}, && (7.9)\\
g_i(z^*) &\leq 0 \qquad \forall i \in \{1, \ldots, m\}, && (7.10)\\
\mu_i^* &\geq 0 \qquad \forall i \in \{1, \ldots, m\}, && (7.11)\\
\mu_i^* g_i(z^*) &= 0 \qquad \forall i \in \{1, \ldots, m\}, && (7.12)\\
\nabla(F(z^*)) + \sum_{i=1}^{m} \mu_i^* \nabla g_i(z^*) + \sum_{j=1}^{l} (\lambda_j^* \nabla(h_j(z^*))) &= 0. && (7.13)
\end{aligned}$$

The first two of these conditions (7.9) and (7.10) simply mean that the solution is feasible. The third condition (7.11) ensures that Λ is convex in $\mathbb{R}^n$. The last condition (7.13) says that the gradient of Λ (with respect to $\mathbb{R}^n$) is zero at (z^*, μ^*, λ^*), this is a

result of this being a convex optimisation problem.

$$\Lambda(z^*, \lambda^*, \mu^*) = F(z^*) + \sum_{i=1}^{m} \mu_i^* g_i(z^*) + \sum_{i=1}^{l} \lambda_i^* (h_i(z^*)) = F(z^*).$$

7.1.3 Application of the Karush-Kuhn-Tucker Conditions

First we will show that our optimisation problem (7.6) (the evaluation of the Connes metric) this can be presented in the same form as (7.7). Note there that functions $f : V \to \mathbb{R}$ can be conceptualised as a point in $\mathbb{R}^n$, as for any of the n vertices f gives a real value and so consists of n real values, a point in $\mathbb{R}^n$ will consist of n real values for each of the n dimensions.

$$\begin{aligned} &\text{Minimize } F(f) = f_y - f_x \\ &\text{Subject to } g_i(f) = \sum_{v \in A(i)} (f_i - f_v)^2 - 2 \leq 0 \text{ for all } i \in \{1, 2, \ldots, n\} \\ &\text{Subject to } h(f) = f_a - K = 0. \end{aligned} \tag{7.14}$$

We have a Lagrangian,

$$\Lambda(f, \mu, \lambda) = f_y - f_x + \sum_{z \in V} \mu_z \left(\sum_{j \in A(z)} (f_j - f_z)^2 - 2 \right) + \lambda(f_a - K). \tag{7.15}$$

When this is used in the optimisation problem function f will act to minimise this expression and the Lagrangian multiplier μ_z's and λ will act to maximise the Lagrangian. The gradient of the Lagrangian $\Lambda(z, \mu, \lambda)$ in (7.15) is equal to zero for an optimal function f.

It is the Karush-Kuhn-Tucker conditions which will hold for an optimal solution

(f^*, μ^*, λ^*) these are equivalent to (7.9) - (7.12).

$$
\begin{aligned}
f_a^* - K &= 0. && (7.16)\\
\sum_{j\in A(z)} (f_z^* - f_j^*)^2 - 2 &\leq 0 \qquad \forall z \in V, && (7.17)\\
\mu_z^* &\geq 0 \qquad \forall z \in V, && (7.18)\\
\mu_z^* \left(\sum_{j\in A(z)} (f_z^* - f_j^*)^2 - 2 \right) &= 0 \qquad \forall z \in V. && (7.19)\\
\lambda(f_a - K) &= 0, && (7.20)
\end{aligned}
$$

The inequality constraints here comes from the n constraints that we have at each vertex, the equality constraint is to establish a value for $K = f(a)$ for all functions.

As the gradient of the Lagrangian in (7.15) has to be a zero vector we can view this in component form so for every $k \in \{1, \dots n\}$, this is equivalent to (7.13),

$$
\begin{aligned}
&\frac{\partial}{\partial f_k}\Lambda(f^*, \mu^*, \lambda^*) = && (7.21)\\
&= \delta_{y,k} - \delta_{x,k} - 2\mu_k^* \sum_{j\in A(k)} (f_j^* - f_k^*) + 2 \sum_{j\in A(k)} \mu_j^*(f_k^* - f_j^*) + \lambda^*\delta_{a,k}\\
&= \delta_{y,k} - \delta_{x,k} + 2 \sum_{j\in A(k)} (\mu_k^* + \mu_j^*)(f_k^* - f_j^*) + \lambda^*\delta_{a,k}\\
&= 0.
\end{aligned}
$$

7.1.4 Properties of the Optimal Function

Using (7.16) - (7.21) we are able to infer certain properties for an optimal function f^* and for the optimal Lagrange multipliers μ_k^*. In fact we are able to infer directly the redundancy of λ from (7.16).

Here we will be using the following notions *binding* and *non-binding* constraints at vertices, when a binding constraint is present at $w \in V$ we have $\sum_{j\in A(w)}(f_w^* - f_j^*)^2 = 2$ (an equality in the associated constraint this is otherwise expressed as $g_w(f^*) = 0$), when there is a non-binding constraint present at $w \in V$ we have $\sum_{j\in A(w)}(f_w^* - f_j^*)^2 < 2$ (a strict inequality in the associated constraint is otherwise expressed as $g_w(f^*) < 0$). We will also be using *complementary slackness*, which is a property that is as result of (7.17) - (7.19) and the fact the the Lagrange multipliers μ_w^* act to maximise the

Lagrangian. We have

$$\text{if } \sum_{j\in A(k)} (f_k^* - f_j^*)^2 - 2 < 0 \implies \mu_k^* = 0, \tag{7.22}$$

$$\text{and if } \mu_k^* > 0 \implies \sum_{j\in A(k)} (f_k^* - f_j^*)^2 - 2 = 0. \tag{7.23}$$

The properties that we want to show for an optimal function $f^* : V \to \mathbb{R}$ and optimal Lagrange multipliers μ_k^* will be shown in the following Lemmas.

Lemma 7.6. ***(Properties 1 and 2)*** *The constraint $g_x(f^*)$ (from (7.7)) for an optimal function f^* is binding at $x \in V$; $g_x(f^*) = 0$, or at a neighbouring vertex $z \in A(x)$; $g_z(f^*) = 0$ where $f_x > f_z$, (or there is a binding constraint at both; $g_x(f^*) = 0$ and $g_z(f^*) = 0$ where $f_x > f_z$) (recall that $f_x > f_y$ we first established this in (7.5)).*

Similarly the constraint is binding at y; $g_y(f^*) = 0$, or at a neighbouring vertex $z \in A(y)$ where $f_y < f_z$; $g_z(f^*) = 0$, (or binding both; $g_y(f^*) = 0$ and $g_z(f^*) = 0$ where $f_y < f_z$).

Proof. In (7.21) we have

$$\delta_{y,k} - \delta_{x,k} + 2 \sum_{j\in A(k)} (\mu_k^* + \mu_j^*)(f_k^* - f_j^*) + \lambda^* \delta_{a,k} = 0$$

$$\text{for } x = k,\ \delta_{y,x} - 1 + 2 \sum_{j\in A(x)} (\mu_x^* + \mu_j^*)(f_x^* - f_j^*) + \lambda^* \delta_{a,x} = 0$$

$$\text{As } x \neq y \text{ and } x \neq a \text{ this implies } \sum_{z\in A(x)} (\mu_x^* + \mu_z^*)(f_x^* - f_z^*) = 1/2, \tag{7.24}$$

as the right hand side of (7.24) is a positive summation there must exists a positive term within the summation, thus there exists a vertex $z \in A(x)$ with

$$\mu_x^* + \mu_z^* > 0 \text{ and } f_x^* - f_z^* > 0. \tag{7.25}$$

From (7.25) we can thus say that $\mu_x^* > 0$ or $\mu_z^* > 0$ (or both), with the use of (7.17) - (7.19) and the notion of complementary slackness in (7.22) - (7.23), we can conclude that,

$$\sum_{j\in A(x)} (f_x^* - f_j^*)^2 = 2 \text{ or } \sum_{j\in A(z)} (f_z^* - f_j^*)^2 = 2 \text{ (or both)}.$$

That is the constraint is binding at x or at a neighbouring vertex $z \in A(x)$ (or both), and we have $f_x > f_z$. The proof follows in exactly the same way for y. □

Lemma 7.7. ***(Property 3)*** *For any $k \in V \setminus \{x, y, a\}$ where for an optimal function f^* the constraint is non-binding; $g_k(f^*) < 0$, if the following two properties hold.*

1. *There exists a vertex $z \in A(k)$ where the constraint is binding; $g_z(f^*) = 0$ and $0 < f_k^* - f_z^*$.*
2. *There exists a vertex $p \in A(k)\backslash\{z\}$ such that $f_k^* - f_p^* < 0$.*

There will be a binding constraint at $p \in V$; $g_p(f^*) = 0$.

Proof. $k \in V \setminus \{x, y, a\}$: here we have from (7.21)

$$\delta_{y,k} - \delta_{x,k} + 2 \sum_{j \in A(k)} (\mu_k^* + \mu_j^*)(f_k^* - f_j^*) + \lambda^* \delta_{a,k} = 0$$

$$\text{As } k \neq x,\ k \neq y \text{ and } x \neq a \text{ this implies } \sum_{j \in A(k)} (\mu_k^* + \mu_j^*)(f_k^* - f_j^*) = 0. \tag{7.26}$$

As we have a summation of terms to zero on the right hand side of (7.26), we have either of two possible scenarios: *one* we have

$$(\mu_k^* + \mu_j^*)(f_k^* - f_j^*) = 0 \text{ for all } j \in A(k) \tag{7.27}$$

or, *two* there exists a vertex $p \in A(k)$ where

$$(\mu_k^* + \mu_p^*)(f_k^* - f_p^*) < 0 < (\mu_k^* + \mu_z^*)(f_k^* - f_z^*). \tag{7.28}$$

Case *one* means that $(\mu_k^* + \mu_j^*)(f_k^* - f_j^*) = 0$ for all $j \in A(k)$: we cannot have $\mu_k^* + \mu_j^* \neq 0$ and $f_k - f_j \neq 0$ simultaneously. For $j = p$ or $j = z$ we have $f_k - f_j \neq 0$, means that $\mu_k^* + \mu_p^* = \mu_k^* + \mu_z^* = 0$ and this along with condition (7.18) implies $\mu_k^* = \mu_p^* = \mu_z^* = 0$, this does however contradict complementary slackness condition (7.23) for k as it is a binding constraint.

Case *two* as there is a non-binding constraint at k we have by complementary slackness condition (7.22) that $\mu_k^* = 0$ thus for (7.28) to hold true we must have $\mu_z^* > 0, \mu_p^* > 0$, and thus by complementary slackness condition (7.23) we have binding constraints at z and $p \in V$.

$$\sum_{j\in A(i)} (f_z^* - f_j^*)^2 = 2 \text{ and } \sum_{j\in A(i)} (f_k^* - f_j^*)^2 = 2.$$

□

What these properties mean for our Connes metric, is that the function f^* which determines the Connes metric distance between two vertices x and $y \in V$: in *properties 1 and 2* that fact that there will be a binding constraint in at least one of $x \cup A(x)$ and at least one binding constraint in $y \cup A(y)$, in *property 3* what we will tend to observe is f being largest at x and decreasing at vertices that are further away from x and closer to y on such a path, where this decrease can be seen, of vertices between x and y you will never observe three consecutive vertices with non-binding constraints. It is important to note however that the optimal function f^* found by this optimisation methodology is not necessarily unique.

We will prove these Lemmas with a different approach, without Karush-Kuhn-Tuckers conditions. The first step in all these proofs will be to negate the statement by considering a different function. $f^{*\prime}$ for which $f^{*\prime}(x) - f^{*\prime}(y) > f^*(x) - f^*(y)$ (a more optimal objective function) and which holds for all of the constraints, thus showing that the original function f^*, is not the optimal function hence does not giving the Connes metric.

Proof. Property 1 and 2

The negation of the statement is that for all $z \in A(x)$ where $f_x^* - f_z^* > 0$, $\sum_{j\in A(x)}(f_x^* - f_j^*)^2 < 2$ (a non-binding constraint at x) and $\sum_{j\in A(z)}(f_z^* - f_j^*)^2 < 2$ (a non-binding constraint for all $z \in A(x)$). In such a case we will propose that there exists a function,

$$f'^*(i) = \begin{cases} f^*(x) + \epsilon & \text{if } i = x, \\ f^*(i) & \text{otherwise.} \end{cases}$$

Where ϵ is such that there exists a vertex, $k \in \{A(x) \cup \{x\}\}$, where

$$\left(2 - \sum_{j\in A(k)} (f_k'^* - f_j'^*)^2\right) = 0 \text{ and } \forall z \in \{A(x)\cup\{x\}\backslash\{k\}\} \sum_{j\in A(z)} (f_z'^* - f_j'^*)^2 \leq 2. \quad (7.29)$$

An aside here to establish some notation: $\forall i \in \{A(x) \cup \{x\}\}$ we have $\delta_i = 2 -$

$\sum_{j\in A(i)}(f_i^* - f_j^*)^2$. If $k = x$ then,

$$\epsilon_x = -\frac{\sum_{j\in A(x)}(f_x^* - f_j^*)}{2d_x} + \sqrt{\frac{(\sum_{j\in A(x)}(f_x^* - f_j^*))^2}{4d_x^2} + \frac{\delta_x}{d_x}} > 0. \tag{7.30}$$

If $k \in \{A(x)\}$ then

$$\epsilon_k = -(f_x^* - f_k^*) + \sqrt{(f_x^* - f_k^*)^2 + \delta_k} > 0. \tag{7.31}$$

We search through the whole set $\{A(x) \cup \{x\}\}$ and take the smallest ϵ_i's to be ϵ. The function f'^* will bring about a Connes metric that is larger by a value of ϵ than the Connes metric if f^* were optimal, thus completing the contradiction and showing that f^* is not the optimal function. The constraints holds for all $k \in V$, on $\{A(x) \cup \{x\}\}$ as f'^* is formed so that (7.29) holds, and for the rest of V due to the fact that for $v \in V\backslash\{A(x) \cup \{x\}\}$ we have that $\sum_{i\in A(v)}(f_v'^* - f_i'^*)^2 = \sum_{i\in A(v)}(f_v - f_i)^2 \leq 2$.

□

7.2 Second Lagrangian Approach

Firstly in this section we want to restate the Connes metric and find a more compact algebraic way of expressing the constraints that are on the functions f. The matrix defined below will help us to do this.

Definition 7.8. ***(Matrix** M_i**)*** *Let $M_i \in \mathbb{R}^{n\times n}$. r_i denote the ith row of the adjacency matrix of a graph G, and $e_i = (0, \ldots, 0, 1, 0, \ldots, 0)$ the ith unit vector (and only has a non-zero entry of one at the ith coordinate), M_i is given by*

$$M_i = diag(r_i) - e_i^\top r_i. \tag{7.32}$$

Remark 7.9. *The matrix is such that $M_i^\top f$ is equal to the vector with $f_z - f_i$ at coordinate z if $z \in A(i)$, and 0 elsewhere.*

The right hand side of the constraint on the function f at vertex $i \in V$ can now be

expressed in a different way.

$$\sum_{z\in A(i)} (f_i - f_z)^2 = (M_i^\top f)^\top M_i^\top f = \|M_i^\top f\|_2^2. \tag{7.33}$$

Theorem 7.10. *For given λ's and ρ, we have*

$$c(x,y) = \inf_{\forall i\in V\ \underline{\lambda_i}\in\mathbb{R}^{|V|},\rho\in\mathbb{R}} \left\{ \rho K + \sqrt{2}\sum_{i\in V} \|\underline{\lambda_i}\|_2 \Big| \sum_{i\in V} M_i\underline{\lambda_i} = \underline{c(\rho)} \right\}. \tag{7.34}$$

Moreover, for the vectors $\underline{\lambda_i} \in \mathbb{R}^n$ $(i \in V)$ and $\rho \in \mathbb{R}$ for which the infimum in (7.34) is attained, we have the following:

1. *For $i \in V$ and $j \notin A(i)$ we have $\underline{\lambda_i}_j = 0$ (this will dramatically reduce the computation required).*

2. *$\underline{\lambda_i} \in \mathrm{Im}(M_i)$ $(i \in V)$. More precisely, we have that there exists a $\underline{\mu} \in F$ $(F = \ell^\infty(V))$ with $\mu_a = K$ such that*

$$\underline{\lambda_i} = -\frac{\|\underline{\lambda_i}\|_2}{\sqrt{2}} M_i\underline{\mu} \tag{7.35}$$

   for all $i \in V$.

Proof. By introducing additional variables, we can write the constraint $\sum_{z\in A(i)}(f_i - f_z)^2 \leq 2$ as $\|\underline{\xi_i}\|_2^2 - 2 \leq 0$, where $\underline{\xi_i} \in \mathbb{R}^n$ and

$$\underline{\xi_i}_j = \begin{cases} f_i - f_j & \text{if } i \sim j, \\ 0 & \text{otherwise.} \end{cases}$$

We can now state the negative of the Connes metric as in (7.6) as follows,

$$-c(x,y) = \min_{f,\underline{\xi_i}\in F\ f_a=K} \left\{ f_y - f_x \Big| \forall i \in V : \underline{\xi_i} = M_i^\top \underline{f},\ \|\underline{\xi_i}\|_2^2 - 2 \leq 0 \right\}. \tag{7.36}$$

This can be expressed in terms of a Lagrangian, if we take the equality constraint $f_a = K$ this can be expressed equivalently to the Karush-Kuhn-Tucker conditions (7.20) and (7.16) as $\rho(f_a - K) = 0$ and $(f_a - K) = 0$ with Lagrange multiplier $\rho \in \mathbb{R}$. For the n constraints $(\|\underline{\xi_i}\|_2^2 - 2) \leq 0$ we take the Lagrange multiplier $\mu_i \geq 0\ \forall i \in V$. The equality constraint $\underline{\xi_i} = M_i^\top \underline{f}$ this actually represents n equality constraints for

each $i \in V$ will be expressed as $\underline{\lambda_i}^\top(\underline{\xi_i} - M_i\underline{f})$ with Lagrange multiplier $\underline{\lambda_i} \in \mathbb{R}^n$. All of the Lagrange multipliers will act to maximise the expression while $\underline{f}$ and $\underline{\xi_i}$, $\forall\ i \in V$ will act to minimise the expression.

$$\begin{aligned}
-c(x,y) = \min_{\forall i \in V\ \underline{f}, \underline{\xi_i} \in F} \sup_{\substack{\underline{\lambda_i} \in F, \mu_i, \rho \in \mathbb{R} \\ \mu_i \geq 0}} \Bigg(& f_y - f_x + \\
& \sum_{i \in V} \underline{\lambda_i}^\top (\underline{\xi_i} - M_i^\top \underline{f}) + \sum_{i \in V} \mu_i (\|\underline{\xi_i}\|_2^2 - 2) + \rho(f_a - K) \Bigg) \\
\underbrace{=}_{\text{Separating variables}} & \sup_{\substack{\forall i \in V\ \underline{\lambda_i} \in F, \rho, \mu_i \in \mathbb{R} \\ \mu_i \geq 0}} \Bigg(\inf_{f \in F} \left(f_y - f_x - \sum_{i \in V} \underline{\lambda_i}^\top M_i^\top f + \rho(f_a - K) \right) \\
& + \inf_{\forall i \in V\ \underline{\xi_i} \in F} \left(\sum_{i \in V} \left(\underline{\lambda_i}^\top \underline{\xi_i} + \mu_i (\|\underline{\xi_i}\|_2^2 - 2) \right) \right) \Bigg)
\end{aligned} \tag{7.37}$$

Thus we can look at the infimum of the expression in the first set of brackets, which is only dependent upon f,

$$\begin{aligned}
& \inf_{\underline{f} \in F} \left(\underline{f}_y - \underline{f}_x - \sum_{i \in V} \underline{\lambda_i}^\top M_i^\top \underline{f} + \rho(\underline{f}_a - K) \right) \\
& \qquad = \inf_{\underline{f} \in F} \left(\underline{c(\rho)}^\top \underline{f} - \sum_{i \in V} \underline{\lambda_i}^\top M_i^\top \underline{f} - \rho K \right) > -\infty
\end{aligned}$$

the minimum will be reached in this expression if and only if

$$\underline{c(\rho)}^\top = \sum_{i \in V} \underline{\lambda_i}^\top M_i^\top.$$

Now if we look at the second bracket in the above expression (7.37), which is only dependent upon $\underline{\xi_i}$'s. Taking a differentiation of this term with respect to $\underline{\xi_i}$, we have that for an infimum,

$$\underline{\lambda_i} + 2\mu_i \underline{\xi_i} = 0.$$

Thus achieves its minimum for those $\underline{\xi_i}$'s with $\underline{\xi_i} = -\underline{\lambda_i} \cdot \frac{1}{2\mu_i}$ for all $i \in V$. Also, if $\mu_i = 0$, then the outer sup-term would lead to $\underline{\lambda_i} = \underline{0}$, for otherwise the second inf term

would achieve $-\infty$. When $\underline{\xi}_i = -\underline{\lambda_i} \cdot \frac{1}{2\mu_i}$ means that in the second bracket we have,

$$\underline{\lambda_i}^\top \underline{\xi_i} + \mu_i(\|\underline{\xi_i}\|_2^2 - 2) = \frac{-\|\underline{\lambda_i}\|_2^2}{2\mu_i} + \mu_i \left(\frac{\|\underline{\lambda_i}\|_2^2}{4\mu_i^2} - 2 \right) = \frac{-\|\underline{\lambda_i}\|_2^2}{4\mu_i} - 2\mu_i. \tag{7.38}$$

Therefore (7.37) becomes,

$$-c(x,y) = \sup_{\substack{\underline{\lambda_i} \in F, \rho, \mu_i \in \mathbb{R} \\ \mu_i \geq 0}} \Big\{ -\rho K - \sum_{\substack{i \in V \\ \mu_i > 0}} \left(\frac{\|\underline{\lambda_i}\|_2^2}{4\mu_i} + 2\mu_i \right) \Big| \\ \mu_i \geq 0, \sum_{i \in V} M_i \underline{\lambda_i} = \underline{c(\rho)}, \forall i : \mu_i = 0 \Rightarrow \underline{\lambda_i} = 0 \Big\} \tag{7.39}$$

or

$$-c(x,y) = \inf_{\substack{\underline{\lambda_i} \in F, \rho, \mu_i \in \mathbb{R} \\ \mu_i \geq 0}} \Big\{ \rho K + \sum_{\substack{i \in V \\ \mu_i > 0}} \left(\frac{\|\underline{\lambda_i}\|_2^2}{4\mu_i} + 2\mu_i \right) \Big| \\ \mu_i \geq 0, \sum_{i \in V} M_i \underline{\lambda_i} = \underline{c(\rho)}, \forall i : \mu_i = 0 \Rightarrow \underline{\lambda_i} = 0 \Big\} \tag{7.40}$$

Consider now a $\underline{\lambda_i} \neq \underline{0}$. The term $\frac{\|\underline{\lambda_i}\|_2^2}{4\mu_i} + 2\mu_i$ is minimised for μ_i with $\frac{\|\underline{\lambda_i}\|_2^2}{4\mu_i^2} = 2$, i.e. $\mu_i = \frac{\|\underline{\lambda_i}\|_2}{2\sqrt{2}} \neq 0$. For this μ_i, we have

$$\frac{\|\underline{\lambda_i}\|_2^2}{4\mu_i} + 2\mu_i = 2\sqrt{2}\frac{\|\underline{\lambda_i}\|_2}{4} + \frac{\|\underline{\lambda_i}\|_2}{\sqrt{2}} = \sqrt{2}\|\underline{\lambda_i}\|_2,$$

which leads to

$$c(x,y) = \inf_{\underline{\lambda_i} \in F, \rho \in \mathbb{R}} \left\{ \rho K + \sqrt{2} \sum_{i \in V} \|\underline{\lambda_i}\|_2 \Big| \sum_{i \in V} M_i \underline{\lambda_i} = \underline{c(\rho)} \right\}, \tag{7.41}$$

i.e. (7.34). Now let $\underline{\lambda_i} \in F$ $(i \in V)$ and $\rho \in \mathbb{R}$ be such that the infimum in (7.34) is attained. As $M_i^\top = \operatorname{diag}(r_i) - e_i r_i^\top$, we have $M_i^\top \underline{\lambda_i} = \operatorname{diag}(r_i)\underline{\lambda_i} - e_i r_i^\top \underline{\lambda_i}$. Thus,

$$(M_i \underline{\lambda_i})_k = \begin{cases} 0 & : \quad k \neq i, k \notin A(i) \\ -\sum_{z \in A(i)} \underline{\lambda_i}_z & : \quad k = i \\ \underline{\lambda_i}_k & : \quad k \in A(i). \end{cases} \tag{7.42}$$

Now, the objective $\rho K + \sqrt{2}\sum_{i \in V} \|\underline{\lambda_i}\|_2$ of (7.34) is strictly monotone increasing in all

values of $\underline{\lambda_i}_j > 0$ and is strictly monotone decreasing in all values of $\underline{\lambda_i}_j < 0$, those $\underline{\lambda_i}_j$ with $j \notin A(i)$ do not occur at the infimum, we thus have $\underline{\lambda_i}_j = 0$ for such i, j.

Next we consider the Karush-Kuhn-Tucker conditions for the convex optimisation problem (7.34). Denote by $\underline{\mu} \in F$ the Lagrange multipliers for the constraints and define the Lagrangian function, as usual, i.e.

$$L(\lambda, \rho, \mu) := \rho K + \sqrt{2} \sum_{i \in V} \|\underline{\lambda_i}\|_2 + \underline{\mu}^\top \left(\sum_{i \in V} M_i \underline{\lambda_i} - \underline{c(\rho)} \right).$$

Thus, the infimum of (7.34) is attained at (λ, ρ) if and only if there exists $\underline{\mu} \in F$ such that

$$\begin{aligned} \nabla_\lambda L(\lambda, \rho, \mu) &= 0, \\ \nabla_\rho L(\lambda, \rho, \mu) &= 0, \\ \sum_{i \in V} M_i \underline{\lambda_i} - \underline{c(\rho)} &= 0, \end{aligned}$$

which is equivalent to

$$\begin{aligned} \frac{\sqrt{2}}{\|\underline{\lambda_i}\|_2} \underline{\lambda_i} &= -M_i \underline{\mu}, \\ K &= \underline{\mu}_a, \\ \sum_{i \in V} M_i^\top \underline{\lambda_i} - \underline{c(\rho)} &= \underline{0}. \end{aligned}$$

□

This is an alternative expression for $c(x, y)$. With it, we can find *upper bounds* for c by plugging in feasible values for λ, μ, ρ into (7.39).

Remark 7.11. The Theorem above provides us with a way to compute $c(x, y)$ manually resp. with the help of Matlab, as follows:

1. Define the Matrix $A := [M_1, \ldots, M_{|V|}, -e_a]$, the vector $b := -e_x + e_y$, the vector of unknowns $x^\top := [\lambda_1^\top, \ldots, \lambda_{|V|}^\top, \rho]$, and the convex function $f(x) := \rho K + \sqrt{2} \sum_{i \in V} \|\underline{\lambda_i}\|_2$.

2. Note that computing c is equivalent to solving

$$\begin{aligned} \min \quad & f(x) \\ \text{subject to} \quad & Ax = b. \end{aligned}$$

Simple Examples 1

In this section we will go through a simple example and calculate the Connes metric distance between two vertices in a graph, using (7.34).

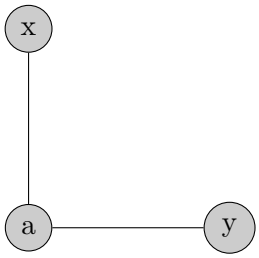

It is obvious here that if you were to simply choose a function $f : V \to \mathbb{R}$ that would give you the Connes metric, this function would be $f(x) = -1$, $f(a) = 0$ and $f(y) = 1$. So the constraint on the function will be binding at a and non-binding at x and y, this would bring about a Connes metric distance of 2 between vertices x and y.

We will now apply the Connes metric according to (7.34).

The adjacency matrix of this graph is,

$$\mathbf{A} = \begin{pmatrix} 0 & 1 & 0 \\ 1 & 0 & 1 \\ 0 & 1 & 0 \end{pmatrix}$$

According to (7.32),

$$\mathbf{M_x} = \begin{pmatrix} 0 & -1 & 0 \\ 0 & 1 & 0 \\ 0 & 0 & 0 \end{pmatrix}, \mathbf{M_a} = \begin{pmatrix} 1 & 0 & 0 \\ -1 & 0 & -1 \\ 0 & 0 & 1 \end{pmatrix}, \mathbf{M_y} = \begin{pmatrix} 0 & 0 & 0 \\ 0 & 1 & 0 \\ 0 & -1 & 0 \end{pmatrix}.$$

Putting these into the constraint in (7.34) "$\sum_{i \in V} M_i \underline{\lambda_i} = \underline{c(\rho)}$" will give us the three following simultaneous equations.

$$-\underline{\lambda_{x_2}} + \underline{\lambda_{a_1}} = -1 \tag{7.43}$$

$$\underline{\lambda}_{x_2} - \underline{\lambda}_{a_1} + \underline{\lambda}_{y_2} - \underline{\lambda}_{a_3} = \rho \tag{7.44}$$

$$-\underline{\lambda}_{y_2} + \underline{\lambda}_{a_3} = 1. \tag{7.45}$$

It is easy to see that these are not linearly independent $-(7.43) - (7.45)$ gives,

$$\underbrace{\underline{\lambda}_{x_2} - \underline{\lambda}_{a_1}}_{=-1 \text{ according to (7.43)}} + \underbrace{\underline{\lambda}_{y_2} - \underline{\lambda}_{a_3}}_{=1 \text{ according to (7.45)}} = 0.$$

But the left hand side of this is also equal to the left hand side of (7.44), thus this implies that $\rho = 0$.

So now in effect the set of equations is reduces from three to two, as (7.44) is redundant. All parameters (of the form $\underline{\lambda}_{i_j}$) that are not mentioned in equations (7.43) and (7.45), will be set equal to zero, as they will have no effect on the constraint and only serve to make our objective in theorem 7.10 $\sqrt{2}\sum_{i\in V} \|\underline{\lambda}_i\|_2$ larger.

$$\sqrt{2}\sum_{i\in V} \|\underline{\lambda}_i\|_2 = \sqrt{2}(|\underline{\lambda}_{x_2}| + \sqrt{\underline{\lambda}_{a_1}^{\,2} + \underline{\lambda}_{a_3}^{\,2}} + |\underline{\lambda}_{y_2}|),$$

substituting for $\underline{\lambda}_{x_2} = \underline{\lambda}_{a_1} + 1$ (take from rearranging (7.43)) and $\underline{\lambda}_{y_2} = \underline{\lambda}_{a_3} - 1$ (take from rearranging (7.45)), we have.

$$\sqrt{2}\sum_{i\in V} \|\underline{\lambda}_i\|_2 = \sqrt{2}(|\underline{\lambda}_{a_1} + 1| + \sqrt{\underline{\lambda}_{a_1}^{\,2} + \underline{\lambda}_{a_3}^{\,2}} + |\underline{\lambda}_{a_3} - 1|). \tag{7.46}$$

We will find the minimum of this by differentiation w.r.t. $\underline{\lambda}_{a_1}$ assuming that $\underline{\lambda}_{a_1} > -1$.

$$\frac{\partial}{\partial \underline{\lambda}_{a_1}}\left(\sqrt{2}\left(\underline{\lambda}_{a_1} + 1 + \sqrt{\underline{\lambda}_{a_1}^{\,2} + \underline{\lambda}_{a_3}^{\,2}} + |\underline{\lambda}_{a_3} - 1|\right)\right) = \left(\sqrt{2}\left(1 + \frac{\underline{\lambda}_{a_1}}{\sqrt{\underline{\lambda}_{a_1}^{\,2} + \underline{\lambda}_{a_3}^{\,2}}}\right)\right) > 0.$$

Assuming that $\underline{\lambda}_{a_1} < -1$

$$\frac{\partial}{\partial \underline{\lambda}_{a_1}}\left(\sqrt{2}\left(-\underline{\lambda}_{a_1} - 1 + \sqrt{\underline{\lambda}_{a_1}^{\,2} + \underline{\lambda}_{a_3}^{\,2}} + |\underline{\lambda}_{a_3} - 1|\right)\right) = \left(\sqrt{2}\left(-1 + \frac{\underline{\lambda}_{a_1}}{\sqrt{\underline{\lambda}_{a_1}^{\,2} + \underline{\lambda}_{a_3}^{\,2}}}\right)\right) < 0.$$

Thus at the minimum we must have $\underline{\lambda}_{a_1} = -1$.

Now setting $\underline{\lambda_{a_1}} = -1$ differentiating w.r.t. $\underline{\lambda_{a_3}}$ assuming that $\underline{\lambda_{a_3}} > 1$,

$$\frac{\partial}{\partial \underline{\lambda_{a_3}}} \left(\sqrt{2} \left(\sqrt{1 + \underline{\lambda_{a_3}}^2} + \underline{\lambda_{a_3}} - 1 \right) \right) = \left(\sqrt{2} \left(\frac{\underline{\lambda_{a_3}}}{\sqrt{1 + \underline{\lambda_{a_3}}^2}} + 1 \right) \right) > 0.$$

Assuming that $\underline{\lambda_{a_3}} < 1$,

$$\frac{\partial}{\partial \underline{\lambda_{a_3}}} \left(\sqrt{2} \left(\sqrt{1 + \underline{\lambda_{a_3}}^2} - \underline{\lambda_{a_3}} + 1 \right) \right) = \left(\sqrt{2} \left(\underbrace{\frac{\underline{\lambda_{a_3}}}{\sqrt{1 + \underline{\lambda_{a_3}}^2}}}_{<1} - 1 \right) \right) < 0.$$

So at the minimum is at $\underline{\lambda_{a_1}} = -1$ and $\underline{\lambda_{a_3}} = 1$. Substituting this back into the right hand side of (7.46), we have the Connes metric equal to,

$$\sqrt{2}(\sqrt{(1)^2 + (-1)^2}) = 2.$$

Which is the correct answer.

Simple Second Example 2

Here we will use our technique for measuring the Connes metric distance across a triangle.

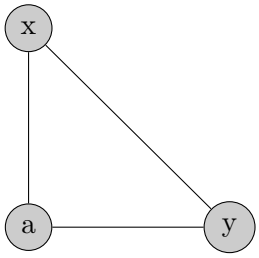

Say that $f : V \to \mathbb{R}$ is the function that gives the Connes metric between x and y in V, which is given as $f(x) - f(y) = c$. The difference of f has to be the same between x and y along all paths connecting x and y, meaning in this case a direct movement over an adjacent edge (which has a difference c), and of a path of two edges with an intermediate vertex a say that $f(x) - f(a) = b$ and $f(a) - f(y) = d$ then $c = b + d$. The constraints at x is that $c^2 + b^2 \leq 2$ implying $(b+d)^2 + b^2 = 2b^2 + 2bd + d^2 \leq 2$, similarly at y we have $b^2 + 2bd + 2d^2 \leq 2$ and the constraint at a is $b^2 + d^2 \leq 2$. Properties 1 and 2 tell

us that there must be a binding constraint somewhere, also there apparent symmetry of the triangle suggests that $b = d$ assuming this to be the case, the constraints can be expressed in one condition $5b^2 \leq 2$ and $c = 2b$ so to maximise c we need to maximise b, so we will thus have $b = \sqrt{2/5}$ and $c = 2\sqrt{2/5}$.

We will now apply our techniques to this.

The adjacency matrix,

$$\mathbf{A} = \begin{pmatrix} 0 & 1 & 1 \\ 1 & 0 & 1 \\ 1 & 1 & 0 \end{pmatrix}$$

According to (7.32),

$$\mathbf{M_x} = \begin{pmatrix} 0 & -1 & -1 \\ 0 & 1 & 0 \\ 0 & 0 & 1 \end{pmatrix}, \mathbf{M_a} = \begin{pmatrix} 1 & 0 & 0 \\ -1 & 0 & -1 \\ 0 & 0 & 1 \end{pmatrix}, \mathbf{M_y} = \begin{pmatrix} 1 & 0 & 0 \\ 0 & 1 & 0 \\ -1 & -1 & 0 \end{pmatrix}.$$

Putting these into the constraint in (7.34) "$\sum_{i \in V} M_i \underline{\lambda_i} = \underline{c(\rho)}$" will give us the three following simultaneous equations.

$$-\underline{\lambda_{x_2}} - \underline{\lambda_{x_3}} + \underline{\lambda_{a_1}} + \underline{\lambda_{y_1}} = -1 \tag{7.47}$$

$$\underline{\lambda_{x_2}} - \underline{\lambda_{a_1}} - \underline{\lambda_{a_3}} + \underline{\lambda_{y_2}} = \rho \tag{7.48}$$

$$\underline{\lambda_{x_3}} + \underline{\lambda_{a_3}} - \underline{\lambda_{y_1}} - \underline{\lambda_{y_2}} = 1. \tag{7.49}$$

A solution for this (found by implementing a MatLab code) is $\underline{\lambda_{x_2}} = 1/5$, $\underline{\lambda_{x_3}} = 2/5$, $\underline{\lambda_{y_1}} = -2/5$ and $\underline{\lambda_{y_2}} = -1/5$ where all other terms will be zero, which gives the Connes metric distance as expected $2\sqrt{2/5}$. This codes is also used to calculate the Connes metric between all pairs of vertices in the IEEE 39 and 188-bus test case.

7.3 Physical interpretation of the Connes metric

The Connes metric is of interest to us as it can have significant in an electrical sense, if we are to weight the edges of the graph in a certain way. Firstly we will see what the Connes metric could mean in a direct current network, in such a network we would have

voltage potentials at every vertex and every edge would have a resistance associated to it. The current flow in the network would be determined by the equation in A.16 (the potential voltage difference across an edge divided by the resistance). If we take the weight on the edges to be the inverse of the resistance, so that for edge $(i,j) \in E$ the weight $b(i,j) = 1/r(i,j)$ where $r(i,j)$ is the resistance inline (i,j), this is in the sense of Davies construction or Requardt's construction in section 6.3.1 or section 6.3.2 respectively. This will lead to a constraint such as can be seen in (6.28), where for all $v \in V$, $\sum_{v\sim w} b(v,w)(f(v)-f(w))^2 \leq 2$. If we were to conceptualise the function $f : V \to \mathbb{R}$ as the voltage potential function, then what the left hand side of this constraint would mean, would be the total power flow that vertex $v \in V$ is connected to in its adjacent edges. The physical interpretation of the Connes metric $c(x,y)$ would the be the maximum voltage potential difference between vertices x and y, where the total amount of power flow carried in the edges adjacent to each vertices in the graph is bounded above by 2.

If we want to interpret a meaning for the Connes in relation to alternating current we will take the DC (direct current) approximation of an AC (alternating current) as discussed in a subsection of section A.3. In equation (A.9) we have that under the DC approximation of the AC power flow the power in a line (i,j) is equal to the phase angle difference divided by the reactance X_{ij} in the line. If we are to weight the edges (in the sense of Davies or Requardt again), with the inverse of the reactance $1/X_{ij}$ and conceptualise the phase angles as being the function $f : V \to \mathbb{R}$, this will mean that the constraint is a bound not on the total power flow connected to each vertex, but to the total power flow times phase angle difference on every edge adjacent to each vertex. The physical interpretation of the Connes metric $c(x,y)$ for alternating current would be the maximum phase angle difference between vertices x and y, where the total power flow carries in adjacent edges to each vertex times by the phase angle differences on those edges, in the graph is bounded above by 2. Note that as the voltage magnitude of the alternating current will be normalised and taken as one in the DC approximation, this means that the Connes is proportional to a conceptualised phase angle difference, but not an actual phase angle difference that could be measured in degrees.

7.3.1 Connes on Electrical Networks

A metric one may expect to be similar to the Connes metric is Thevenin's impedance as this is also can be derived from the graph Laplacian. Thevenin's impedance when measure between buses i and j is a measure of the expected time of a random walk to travel from vertex i to vertex j and back again (the commute time), this is for edge weightings equal to the inverse of the reactance (as with the Connes metric). As mentioned this can also be derived from the pseudo inverse of the Laplacian $\mathcal{L}^{\dagger}$ the Thevenin's impedance between vertices i and j is $Vol(V)(e_i - e_j)'\mathcal{L}^{\dagger}_{ij}(e_i - e_j)$ [64, p.15]. The correlation between Thevenin's impedance and the Connes metric for all vertex pairs in the IEEE 39-bus test case is 0.8999 and for all pairs in the IEEE 118-bus test case we find a correlation of 0.9086.

The Connes metric between vertices x and y is found by considering all *critical* paths between x and y, all extraneous branches will be deemed irrelevant. Whereas for the Thevenin's impedance to be measured between vertices x and y all possible paths are considered.

Appendix A

Appendix

A.1 Mathematics

Definition A.1. ***(Inner Product)*** *An inner product space is a vector space V over a field of real $\mathbb{R}$ or complex numbers $\mathbb{C}$ with the inner product,*

$$\langle \cdot, \cdot \rangle : V \times V \to \mathbb{C}.$$

This inner produce map must satisfy the following three axioms $\forall x, y, z \in V$ and $C \in \mathbb{C}$.

Conjugate symmetry

$$\langle x, y \rangle = \overline{\langle y, x \rangle}.$$

Linearity of the first expression

$$\langle x + y, z \rangle = \langle x, z \rangle + \langle y, z \rangle$$
$$\langle Cx, z \rangle = C\langle x, z \rangle.$$

Positive definiteness

$$\langle x, x \rangle \geq 0.$$

and is equal to zeros only when $x = \underline{0}$.

Definition A.2. ***Hilbert Space*** *A Hilbert space is a real or complex valued complete inner product space. The space is complete in accordance with a distance measure that*

arising from the inner production as follows, for x and $y \in \mathcal{H}, d(x,y) = \|y-x\| = \sqrt{\langle y-x, y-x\rangle}$).

Definition A.3. ***(Adjoint Operator)*** *For a bounded linear operator on a Hilbert space $F : \mathcal{H} \to \mathcal{H}$, the adjoint of this operator $F^* : \mathcal{H} \to \mathcal{H}$ will satisfy $\forall x, y \in \mathcal{H}$*

$$\langle F(x), y\rangle = \langle x, F^*(y)\rangle.$$

Definition A.4. ***(Open Cover)***

$$C = \{U_\alpha : \alpha \in A\}$$

where A is a possible infinite family of indices and $\forall \alpha \in A$, U_α is an open set. C is an open cover of a topological space X if,

$$X \subset C.$$

Definition A.5. ***(Compact Space)*** *A compact space X is such that for any open cover $\{U_\alpha : \alpha \in A\}$ of X, where the index family A is infinite, there exists a subset of $\{U_\alpha : \alpha \in A\}$ which is still a cover[1] but consists of a finite set of U_α's [2].*

Definition A.6. ***(Relatively Compact Space)*** *A Relatively Compact subset is a subset of a topological space whose closure is compact.*

Definition A.7. ***(Compact Operator)*** *A compact operator is a linear operator T between Banach spaces X and Y, $T : X :\to Y$. Which is such that Image of any bounded sub set in X under T is relatively compact in Y.*

Theorem A.8. ***(Cauchy-Schwarz inequality)*** *For vertices x and y which are in an innerproduct space,*

$$|\langle x, y\rangle|^2 \leq \langle x, x\rangle \cdot \langle y, y\rangle.$$

Theorem A.9. ***(Stone-Weierstrass)*** *For a function $f : \mathbb{R}^n \to \mathbb{R}$ where $f \in C^\infty(\mathbb{R}^n)$ we can uniformly approximate f on a compact sub set of $\mathbb{R}^n$ by a polynomial.*

[1] This is a subcover of X for $\{U_\alpha : \alpha \in A\}$.
[2] This is a finite subcover of X for $\{U_\alpha : \alpha \in A\}$.

Lemma A.10. *For any embedding $F : V \to \mathbb{R}^h$, and for all u and $v \in V$, we have that $d_F(u,v)\|F(u)\| \leq 2\|F(u) - F(v)\|$.*

Proof. For any non-zero vectors $x, y \in \mathbb{R}^k$, we have

$$\|x\| \left\| \frac{x}{\|x\|} - \frac{y}{\|y\|} \right\| = \left\| x - \frac{\|x\|}{\|y\|} y \right\| \leq \|x - y\| + \left\| y - \frac{\|x\|}{\|y\|} y \right\| \leq 2\|x - y\|.$$

□

A.1.1 Justification of Spectral Clustering From Perturbation Theory

Perturbation studies the change in the eigenvalues and the eigenvectors of a Laplacian once some noise is introduced. Say $\mathcal{L}$ is our Laplacian (as in definition 6.23) of a graph G with power flows as the edge weights and will become $\tilde{\mathcal{L}} = \mathcal{L} + H$ once noise H is introduced. If $\tilde{\mathcal{L}}$ happens to be a Laplacian of a graph with power flows weighting the edges and has k connected components then the first k eigenvectors of $\tilde{\mathcal{L}}$ will be what is known as indicator vectors for respective clusters [3]. For $\tilde{\mathcal{L}}$ assuming the perturbation is not too large the first k eigenvectors of $\tilde{\mathcal{L}}$ will resemble the first k eigenvalues of $\mathcal{L}$ with some error.

The following theory by Davis and Kahan gives a way to measure such an error and to indicate the distance between eigenvector spaces, this is then estimated using H and the spectral gap.

Some brief preliminaries before the theorem, let $\|\cdot\|$ be the Frobenius norm or the two-norm for matrices (Hilbert-Schmidt) as in (6.12). For an interval $I \subset \mathbb{R}$ and a matrix A the term $\sigma_I(A)$ is the set of eigenvalues of A which are contained in I.

Theorem A.11. ***(Davis-Kahan)****[58] Let $A, H \in \mathbb{R}^{n\times n}$ be symmetric matrices and $S1 \subset \mathbb{R}$, take $\tilde{A} := A + H$. Take $V1$ and $\tilde{V}1$ to be the eigenspaces corresponding to all eigenvalues in $\sigma_{S1}(A)$ and $\sigma_{S1}(\tilde{A})$ respectively.*

$$\delta = \min\{|\lambda - s|; \lambda \text{ eigenvalue of } A, \lambda \notin S1, s \in S1\}. \tag{A.1}$$

Then the distance $d(V_1, \tilde{V}_1) := \|sin\Theta(V_1, \tilde{V}_1)\|$ between the two subspaces $V1$ and $\tilde{V}_1$ is

[3] This means that all the entries in the vector will be zero apart from entries that correspond to vertices of a cluster where we have constant values.

bounded by

$$d(V_1, \tilde{V}_1) \leq \frac{\|H\|}{\delta}. \tag{A.2}$$

The outcome of the theorem depends on the choice of the interval $S1$, we want to choose this interval so that the first k eigenvalues of A and the first k eigenvalues of $\tilde{A}$ lie in $S1$, so say that $S1 = [0, \lambda_k]$ this way $\delta = |\lambda_{k+1} - \lambda_k|$ the larger this is according to the theorem the closer V_1 and $\tilde{V}_1$ will be. The problem with fully utilising this theorem to help determine what dimension to embed into is with H.

A.2 Graph Theoretic Measures

Definition A.12. ***(Graph Minor)*** *A minor of a graph G, is a graph that can be obtained from G by applying a series of operations listed below;*

Edge Contraction*: this is where a selected edge and its vertices at either end* contracted *in form one vertex, where all of the other connections which were present at both vertices are now present at the resulting single vertex. Essentially this is the merging of two adjacent vertices.*

Deletions *Edges and isolated vertices can be deleted.*

Lemma A.13. ***(Proof of Result (3.13))*** *For all $x \in \mathbb{R}^k$,*

$$\mathbb{E}\left(\|\Gamma_{k,h}(x)\|^2\right) = \|x\|^2.$$

Proof.

$$\begin{aligned}
\mathbb{E}\left(\|\Gamma_{k,h}(x)\|^2\right) &= \mathbb{E}\left(h^{-1}\sum_{i=1}^{h}\langle g_i, x\rangle^2\right) \\
&= \mathbb{E}\left(h^{-1}\sum_{i=1}^{h}\Big(\sum_{j=1}^{k} g_{ij}\cdot x_j\Big)^2\right), \\
&= h^{-1}\sum_{i=1}^{h}\mathbb{E}\Big[\Big(\sum_{j=1}^{k}(g_{ij}\cdot x_j)\Big)^2\Big]
\end{aligned} \tag{A.3}$$

as all $g_{ij} \sim N(0,1)$ [4] this implies that $g_{ij}\cdot x_j \sim N(0, x_j^2)$ (following the rule of multiplication of of a normally distributed variable), then we have that $\sum_{j=1}^{k}(g_{ij}\cdot x_j) \sim$

[4] This means normally distributed with mean zero and variance one.

$N(0, \sum_{j=1}^{k} x_j^2) = N(0, \|x\|^2)$ (following the rules of addition of independent normally distributed variables). Using the following rule

$$\mathbb{E}(X^2) = Var(X) - (\mathbb{E}(X))^2,$$

for $X = \sum_{j=1}^{k}(g_{ij} \cdot x_j)$ we have that (A.3) is equal to,

$$h^{-1}\Big(\sum_{i=1}^{h} \underbrace{Var\Big(\sum_{j=1}^{k} g_{ij} \cdot x_j\Big)}_{=\|x\|^2} - \Big(\underbrace{\mathbb{E}\Big(\sum_{j=1}^{k} g_{ij} \cdot x_j\Big)}_{=0}\Big)^2\Big) = h^{-1}\sum_{i=1}^{h}\|x\|^2 = h^{-1}{\cdot}h\|x\|^2 = \|x\|^2.$$

□

A.3 Electricity

A.3.1 Basic electrical Measures

Definition A.14. ***(Electrical Charge)*** *Is the amount of electricity (proportional to the number of electrons).*

Definition A.15. ***(Voltage)*** *The voltage is measured at any position of the electrical potential energy as a unit's charge, were this unit to be placed at the position.*

An analogy can be made of voltage as the electrical pressure of even better electrical tension.

Theorem A.16. ***(Ohm's Law)*** *Ohm's law is that for a potential voltage difference across a conductor V and an electrical resistance of the conductor R, the current I is given as follows.*

$$I = \frac{V}{R}.$$

A.3.2 Generators

We will be making a number of assumptions of electrical networks before we apply our analysis. We will be simplifying the structure of electrical networks somewhat, as we will only be considering simple graphs, when in reality electrical networks are

an enormously complex assembly of transformers, transmission lines and generators of varying sorts: some hydro, some thermal and some wind-powered.

The kinetic energy in an electric generator is converted into electrical energy, this all happens in a component of the generator called the alternator, this is formed of an inner moving magnetised part, which can rotate and a static outer part, that is itself composed of electrical conductors in the form of coils. The kinetic energy which is converted into electrical energy is usually in the form of steam flowing from high pressure to lower pressure, but this energy could be harnesser form wind, water or a combustion engine, all resulting in a rotation of the inner magnetic part of the alternator.

On the outer part of the alternator the conducting metal coils are setup to capture the lines of magnetic flux, as the magnet rotates the static coils move relative to the magnet, resulting in the movement of the coils through the magnetic lines of flux. This manipulates a deep connection between magnetism and electricity discovered by Michael Faraday in 1831 - 32 and will result in an electrical flow in the conducting coils. This flow will result in an alternating current, as it is the rotating movement of the magnet that determines the current thus generating an oscillatory flow.

A.3.3 Alternating Current

To fully appreciate alternating current we must first define capacitance and inductance, which are properties of any electrical components. We have to also pay particular attention the the relation between current and voltage.

Definition A.17. ***(Conductance)*** *The conductance of an electrical component is,*

$$C = \frac{q}{V_d}. \tag{A.4}$$

Where a charge $+q$ is present at one side of the component and a charge of $-q$ is present at the opposite side of the component. V_d is the voltage potential difference across the component.

For descriptions of voltage or charge refer to Appendix A.15 and A.14 respectively.

The capacitance is a measure of the extent to which a component can store electricity.

If we take a purely capacitive circuit and observe simultaneously the current and the voltage. The current will lead the voltage by 90 °, as indicated below. The red curve is the voltage and the blue curve is the current.

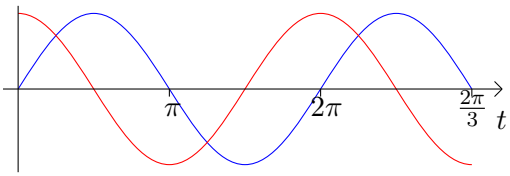

Figure A-1: Current and voltage for a purely capacitive circuit.

Definition A.18. ***(Electrical energy)*** *The electrical energy in a component is,*

$$I \cdot V = R \cdot V^2.$$

Where I is the current flowing in the component, V is the voltage potential difference across the component and R is the resistance across the component. The equality is a result of use ing Ohm's law A.16.

If we consider the energy transition for the circuit (which is proportional the $V \cdot I$ (voltage times current)). There is initially a positive transition of energy between $t = 0$ and $t = \pi/2$ but this become negative between $\pi/2$ and π. The energy will carry on oscillating in such a way. What this means is that any energy that is transferred is then taken back again, with no "real" energy transferal. With any real world electrical component there will be a degree of reactive power observed when current is passed through, the more that this can be reduced the better. Reactive power causes the transition of electrical energy from a source to a demand and then from the demand to the source, never being permanently transferred. Although here we have an idealised superconductive (zero resistance) circuit, the induced flow of the conductor will cause energy losses in real transmission lines in the form of heat which in turn increases the resistance, so these effects are largely undesirable.

Definition A.19. ***(Inductance)*** *Inductance (L) is a measure of the induced voltage V compared to the rate of chance of the current $\frac{dI}{dt}$.*

$$V = L \cdot \frac{dI}{dt}. \tag{A.5}$$

So the rate of change of the current can create a voltage, this voltage will always opposing this rate of change of the current that created it (so $L \leq 0$).

If we observe a purely inductive flow the current lags $90\,^\circ$ behind the voltage. The current and the voltage are observed simultaneously in the figure below, notice that the voltage is the same as in figure A-1.

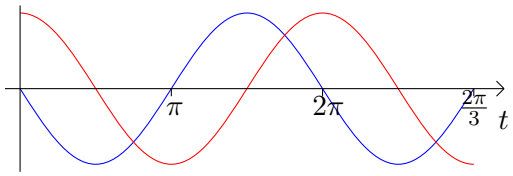

Figure A-2: Current and voltage for a purely inductive circuit.

A purely inductive circuit can be illustrated by a coil in a loop. We will now as before illustrate such a circuit at different times through a whole circle.

Notice here that the current flow is in the opposite direction from the purely capacitive circuit, so if both were to be present in a circuit they would cancel each other out, in other words inductive flow absorbs capacitive power flow. In electrical networks the undesirable reactive power is depleted locally by the installation of capacitors or inductors.

Engineers will give the power not as a real number but as a complex one.

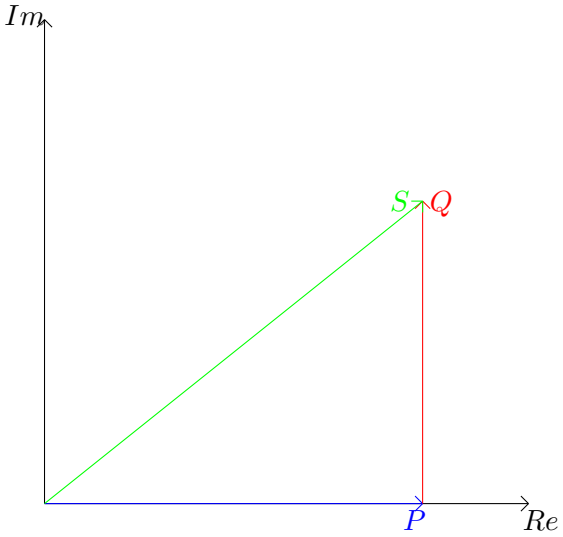

Figure A-3: Real and reactive power.

Here S is the complex power and the length of this is the apparent power. Q is

the reactive power and is given by the capacitance minus the inductance. P is the real power flow.

Generators AC current networks are engineered to all be producing voltages and currents that is the same frequency, so that they are stationary w.r.t each other. The formula for the alternating current in a line connecting vertices i and j is,

$$\bar{I} = \frac{\bar{V}_j - \bar{V}_i}{\bar{Z}_{ij}}.$$

The bar notation here indicates that we are referring to elements of the complex plane. $\bar{Z}_{ij}$ is the impedance and is given as

$$\bar{Z}_{ij} = R_{ij} + \iota X_{ij} \tag{A.6}$$

where R_{ij} is the resistance on line (i, j), X_{ij} is the reactance and ι is taken to be the unit imaginary number.

As opposed to the current and voltage the power is engineered to have direction. So if we consider instead the power flow on line (i, j) from vertex i (this is calculated by multiplying the voltage at i by the complex conjugate of the current along line (i, j)).

$$\begin{aligned} P_{ij} + \iota Q_{ij} =& \bar{V}_i \bar{I}^*_{ij} = \bar{V}_i \left(\frac{\bar{V}_j - \bar{V}_i}{\bar{Z}_{ij}} \right)^* \\ =& \frac{\bar{V}_i \bar{V}^*_j - V_i^2}{\bar{Z}_{ij}} \end{aligned} \tag{A.7}$$

here V_i is the scalar of $\bar{V}_i$ so $V_i = |\bar{V}_i|$.

A.3.4 DC Approximation of AC Power Flow

To achieve the DC approximation of (A.7), we want the power to be equal to the real power in each line. This is done firstly by considering the the reactance of each line to be much larger than the resistance, $X_{ij} >> R_{ij}$. Expanding (A.7) using the following form to express the complex numbers $V = |V|(\cos(\theta) + \iota \sin(\theta))$, where the angle θ is measured from a base vertex (so called slack node) and using the approximation we have,

$$\begin{aligned} P_{ij} + jQ_{ij} =& \frac{V_iV_j(\cos(\theta_i - \theta_j) + \iota V_iV_j \sin(\theta_i - \theta_j) - V_i^2}{R_{ij} + jX_{ij}} \\ \approx& \frac{V_iV_j \sin(\theta_i - \theta_j)}{X_{ij}} - \iota \frac{V_iV_j \cos(\theta_i - \theta_j) - V_i^2}{X_{ij}}. \end{aligned} \tag{A.8}$$

As well as approximating R_{ij} to be infinitesimal, there is also two more features of how the system will be engineered, that will allow for the DC approximation. The first one of these is that all of the voltage magnitudes are equal, hence $V_i = V_j$ in fact without loss of generality these will be canceled out of the equation by taking them to be of unit one. The second feature is that the phase angle differences are considered to be small, this is done so the at the system can maintain synchronicity, a result of this is that we can take $\sin(\theta_i - \theta_j) \approx \theta_i - \theta_j$. All of this means is that the imaginary part of (A.8) is infinitesimal, thus we are able to approximate the power to be just the real power,

$$P_{ij} + \iota Q_{ij} \approx \frac{(\theta_i - \theta_j)}{X_{ij}}. \tag{A.9}$$

This is called the DC approximation because what we have here resembles Ohm's Law for a DC line (refer to appendix A.16), where instead of voltage potential we have the phase angles θ and instead of current we have power and instead of resistance we have the reactance.

We shall be setting the Connes metric in terms of DC from this point forth, but through the approximation for AC power flow equivalent notions can be considered.

Bibliography

[1] Chira Achayuthakan, Chris J Dent, Janusz W Bialek, and Weerakorn Ongsakul. Electricity tracing in systems with and without circulating flows: Physical insights and mathematical proofs. *Power Systems, IEEE Transactions on*, 25(2):1078–1087, 2010.

[2] Reid Andersen and Yuval Peres. Finding sparse cuts locally using evolving sets. In *Proceedings of the 41st annual ACM symposium on Theory of computing*, STOC '09, pages 235–244, New York, NY, USA, 2009. ACM.

[3] Sanjeev Arora, Boaz Barak, and David Steurer. Subexponential algorithms for unique games and related problems. In *Foundations of Computer Science (FOCS), 2010 51st Annual IEEE Symposium on*, pages 563–572. IEEE, 2010.

[4] S Blumsack, P Hines, M Patel, C Barrows, and E Cotilla Sanchez. Defining power network zones from measures of electrical distance. In *Power & Energy Society General Meeting, 2009. PES'09. IEEE*, pages 1–8. IEEE, 2009.

[5] Stephen Poythress Boyd and Lieven Vandenberghe. *Convex optimization*. Cambridge university press, 2004.

[6] BA Carreras, DE Newman, I Dobson, and AB Poole. Evidence for self-organized criticality in electric power system blackouts. In *34th Hawaii International Conference on System Sciences, Maui, Hawaii*, 2001.

[7] Benjamin A Carreras, Vickie E Lynch, Ian Dobson, and David E Newman. Critical points and transitions in an electric power transmission model for cascading failure blackouts. *Chaos An Interdisciplinary Journal of Nonlinear Science*, 12(4):985, 2002.

[8] Benjamin A Carreras, Vickie E Lynch, Ian Dobson, and David E Newman. Complex dynamics of blackouts in power transmission systems. *Chaos: An Interdisciplinary Journal of Nonlinear Science*, 14(3):643–652, 2004.

[9] Benjamin A Carreras, Vickie E Lynch, ML Sachtjen, Ian Dobson, and David E Newman. Modeling blackout dynamics in power transmission networks with simple structure. In *hicss*, volume 1, page 2018, 2001.

[10] Rui Carvalho, Lubos Buzna, Flavio Bono, Eugenio Gutiérrez, Wolfram Just, and David Arrowsmith. Robustness of trans-european gas networks. *Physical review E*, 80(1):016106, 2009.

[11] Qiming Chen, Chuanwen Jiang, Wenzheng Qiu, and James D McCalley. Probability models for estimating the probabilities of cascading outages in high-voltage transmission network. *Power Systems, IEEE Transactions on*, 21(3):1423–1431, 2006.

[12] Joe H. Chow. Time-scale modeling of dynamic networks with applications to power systems. *Springer-Verlag*, 46, 1982.

[13] F. R. K. Chung and R. L. Graham. Quasi-random tournaments. *J. Graph Theory*, 15(2):173–198, May 1991.

[14] Fan Chung. *Spectral Graph Theory (CBMS Regional Conference Series in Mathematics, No. 92)*. American Mathematical Society, 1997.

[15] A. Connes. Compact metric spaces, fredholm modules, and hyperfiniteness. *Ergodic Theory and Dynamical Systems*, 9:207–220, 5 1989.

[16] Eduardo Cotilla-Sanchez, Paul DH Hines, Clayton Barrows, Seth Blumsack, and Mahendra Patel. Multi-attribute partitioning of power networks based on electrical distance. 2013.

[17] E. B. Davies. Analysis on graphs and noncommutative geometry. *J. Funct. Anal.*, 111(2):398–430, 1993.

[18] Lei Ding, F.M. Gonzalez-Longatt, P. Wall, and V. Terzija. Two-step spectral

clustering controlled islanding algorithm. *Power Systems, IEEE Transactions on*, 28(1):75–84, 2013.

[19] Ian Dobson. Where is the edge for cascading failure?: challenges and opportunities for quantifying blackout risk. In *Power Engineering Society General Meeting, 2007. IEEE*, pages 1–8. IEEE, 2007.

[20] Ian Dobson, Benjamin A Carreras, Vickie E Lynch, and David E Newman. Complex systems analysis of series of blackouts: Cascading failure, critical points, and self-organization. *Chaos: An Interdisciplinary Journal of Nonlinear Science*, 17(2):026103–026103, 2007.

[21] Ian Dobson, D Newman, Ben Carreras, and Vicki Lynch. An initial model for complex dynamics in electric power system blackouts. In *2013 46th Hawaii International Conference on System Sciences*, volume 2, pages 2017–2017. IEEE Computer Society, 2001.

[22] William E Donath and Alan J Hoffman. Lower bounds for the partitioning of graphs. *IBM Journal of Research and Development*, 17(5):420–425, 1973.

[23] Miroslav Fiedler. Algebraic connectivity of graphs. *Czechoslovak Mathematical Journal*, 23(2):298–305, 1973.

[24] Ronan Fitzmaurice, Andrew Keane, and Mark O'Malley. Effect of short-term risk-aversive dispatch on a complex system model for power systems. *Power Systems, IEEE Transactions on*, 26(1):460–469, 2011.

[25] Shayan Oveis Gharan and Luca Trevisan. Approximating the expansion profile and almost optimal local graph clustering. In *Foundations of Computer Science (FOCS), 2012 IEEE 53rd Annual Symposium on*, pages 187–196. IEEE, 2012.

[26] Stephen Guattery and Gary L Miller. On the quality of spectral separators. *SIAM Journal on Matrix Analysis and Applications*, 19(3):701–719, 1998.

[27] A. Gupta, R. Krauthgamer, and J.R. Lee. Bounded geometries, fractals, and low-distortion embeddings. In *Foundations of Computer Science, 2003. Proceedings. 44th Annual IEEE Symposium on*, pages 534–543, Oct 2003.

[28] Harvey Heinz Happ. *Piecewise methods and applications to power systems*. Wiley, 1980.

[29] J Hazra and AK Sinha. Identification of catastrophic failures in power systems using pattern recognition. In *Power India Conference, 2006 IEEE*, pages 7–pp. IEEE, 2006.

[30] VE Henner. A network separation scheme for emergency control. *International Journal of Electrical Power & Energy Systems*, 2(2):109–114, 1980.

[31] Paul Hines, Eduardo Cotilla-Sanchez, and Seth Blumsack. Do topological models provide good information about electricity infrastructure vulnerability? *Chaos: An Interdisciplinary Journal of Nonlinear Science*, 20(3):033122–033122, 2010.

[32] Ming Jin, Tarlochan S Sidhu, and Kai Sun. A new system splitting scheme based on the unified stability control framework. *Power Systems, IEEE Transactions on*, 22(1):433–441, 2007.

[33] Palle ET Jorgensen and Erin PJ Pearse. Operator theory of electrical resistance networks. *arXiv preprint arXiv:0806.3881*, 2008.

[34] Ravi Kannan, Santosh Vempala, and Adrian Vetta. On clusterings: Good, bad and spectral. *Journal of the ACM (JACM)*, 51(3):497–515, 2004.

[35] L Kocarev, N Zlatanov, and D Trajanov. Vulnerability of networks of interacting markov chains. *Physical and Engineering Sciences*, 368(1918):2205–2219, 2010.

[36] Gabriel Kron. *Diakoptics: the piecewise solution of large-scale systems*, volume 2. MacDonald, 1963.

[37] James R Lee and Assaf Naor. Extending lipschitz functions via random metric partitions. *Inventiones mathematicae*, 160(1):59–95, 2005.

[38] James R. Lee, Shayan Oveis Gharan, and Luca Trevisan. Multi-way spectral partitioning and higher-order cheeger inequalities. In *Proceedings of the 44th symposium on Theory of Computing*, STOC '12, pages 1117–1130, New York, NY, USA, 2012. ACM.

[39] Anand Louis, Prasad Raghavendra, Prasad Tetali, and Santosh Vempala. Many sparse cuts via higher eigenvalues. In *Proceedings of the 44th symposium on Theory of Computing*, pages 1131–1140. ACM, 2012.

[40] Jiří Matoušek. On embedding expanders into ℓ^p spaces. *Israel Journal of Mathematics*, 102(1):189–197, 1997.

[41] Arthur Mazer. *Electric power planning for regulated and deregulated markets*. Wiley. com, 2007.

[42] Igor Mishkovski, Mario Biey, and Ljupco Kocarev. Vulnerability of complex networks. *Communications in Nonlinear Science and Numerical Simulation*, 16(1):341–349, 2011.

[43] Bojan Mohar. *Some applications of Laplace eigenvalues of graphs*. Springer, 1997.

[44] R Moreno, MA Rios, and A Torres. Security schemes of power systems against blackouts. In *Bulk Power System Dynamics and Control (iREP)-VIII (iREP), 2010 iREP Symposium*, pages 1–6. IEEE, 2010.

[45] Assaf Naor. L_1 embeddings of the heisenberg group and fast estimation of graph isoperimetry. *arXiv preprint arXiv:1003.4261*, 2010.

[46] Andrew Y Ng, Michael I Jordan, Yair Weiss, et al. On spectral clustering: Analysis and an algorithm. *Advances in neural information processing systems*, 2:849–856, 2002.

[47] Ryan O'Donnell and David Witmer. Improved small-set expansion from higher eigenvalues. *CoRR, abs/1204.4688*, 152, 2012.

[48] J. A. Fill P. Diaconis. Strong stationary times via a new form of duality. *The Annals of Probability*, pages 1483–1522, 1990.

[49] Irina Petreska, Igor Tomovski, Eugenio Gutierrez, Ljupčo Kocarev, Flavio Bono, and Karmen Poljansek. Application of modal analysis in assessing attack vulnerability of complex networks. *Communications in Nonlinear Science and Numerical Simulation*, 15(4):1008–1018, 2010.

[50] Satish J Ranade, Ramchander Kolluru, and Joydeep Mitra. Identification of chains of events leading to catastrophic failures of power systems. In *Circuits and Systems, 2005. ISCAS 2005. IEEE International Symposium on*, pages 4187–4190. IEEE, 2005.

[51] M Requardt. Dirac operators and the calculation of the connes metric on arbitrary (infinite) graphs. *Journal of Physics A: Mathematical and General*, 35(3):759–779, 2002.

[52] Rubén J Sánchez-García, Max Fennelly, Seán Norris, Nick Wright, Graham Niblo, Jacek Brodzki, and Janusz W Bialek. Hierarchical spectral clustering of power grids. 2014.

[53] Peter W. Sauer. *Power system dynamics and stability*. Prentice Hall (Upper Saddle River, N.J.), 1998.

[54] Jianbo Shi and Jitendra Malik. Normalized cuts and image segmentation. *Pattern Analysis and Machine Intelligence, IEEE Transactions on*, 22(8):888–905, 2000.

[55] S Smale. On the mathematical foundations of electrical circuit theory. *Journal of Differential Geometry*, 7(1-2):193–210, 1972.

[56] Daniel A Spielman and Shang-Hua Teng. A local clustering algorithm for massive graphs and its application to nearly-linear time graph partitioning. *arXiv preprint arXiv:0809.3232*, 2008.

[57] David Steurer. *On the complexity of unique games and graph expansion*. PhD thesis, Citeseer, 2010.

[58] Gilbert W Stewart. Stochastic perturbation theory. *SIAM review*, 32(4):579–610, 1990.

[59] Mechthild Stoer and Frank Wagner. A simple min-cut algorithm. *Journal of the ACM (JACM)*, 44(4):585–591, 1997.

[60] Kai Sun, D-Z Zheng, and Qiang Lu. Searching for feasible splitting strategies of controlled system islanding. In *Generation, Transmission and Distribution, IEE Proceedings-*, volume 153, pages 89–98. IET, 2006.

[61] Kai Sun, Da-Zhong Zheng, and Qiang Lu. A simulation study of obdd-based proper splitting strategies for power systems under consideration of transient stability. *Power Systems, IEEE Transactions on*, 20(1):389–399, 2005.

[62] Márk Szenes, Zénó Farkas, and Gábor Papp. Modelling the dynamics and fragmentation of electric power systems. *na*, 2009.

[63] Bart De Moor Tijl De Bie, Johan Suykens. *Learning from General Label Constraints*. Springer Berlin Heidelberg, 2004.

[64] Ulrike Von Luxburg. A tutorial on spectral clustering. *Statistics and computing*, 17(4):395–416, 2007.

[65] CG Wang, BH Zhang, ZG Hao, J Shu, P Li, and ZQ Bo. A novel real-time searching method for power system splitting boundary. *Power Systems, IEEE Transactions on*, 25(4):1902–1909, 2010.

[66] Xiaoming Wang and Vijay Vittal. System islanding using minimal cutsets with minimum net flow. In *Power Systems Conference and Exposition, 2004. IEEE PES*, pages 379–384. IEEE, 2004.

[67] Joe H. Ward. Hierarchical grouping to optimize an objective function. *Journal of the American Statistical Association*, 58(301):236–244, 1963.

[68] M Woolf, Z Huang, and RJ Mondragón. Building catastrophes: networks designed to fail by avalanche-like breakdown. *New Journal of Physics*, 9(6):174, 2007.

[69] Nikola Zlatanov and Ljupco Kocarev. Random walks on networks: Cumulative distribution of cover time. *Physical Review E*, 80(4):041102, 2009.